Ref. Ares(2019)6800660 - 03/11/2019

# SOGNO

# D2.3 v1.0

# Validation of the techniques for grid awareness and their interfaces and services for grid awareness

The research leading to these results has received funding from the European Union's Horizon 2020 Research and Innovation Programme, under Grant Agreement no 774613.

| | |
|---|---|
| **Project Name** | SOGNO |
| **Contractual Delivery Date:** | 31.10.2019 |
| **Actual Delivery Date:** | 31.10.2019 |
| **Author(s):** | RWTH |
| **Work package:** | WP2– Advanced techniques for grid awareness |
| **Security:** | PU |
| **Nature:** | R |
| **Version:** | v1.0 |
| **Total number of pages:** | 87 |

**Abstract**
This document includes the description of the services developed in the SOGNO project for providing situational awareness to the distribution grid operators and support them in the management of the distributed energy resources available in the grid. The report details and validates the techniques of these services and contains an overview of the interfaces required in the Virtualized Substation to enable the coordinated operation of the services.

**Keyword list**
Distribution grid monitoring, State estimation, Power control, Power quality, Distributed generation, Distributed energy resources

**Disclaimer**
All information provided reflects the status of the SOGNO project at the time of writing and may be subject to change.

# Executive Summary

Improving the existing situational awareness allows grid operators to evaluate the real-time operating conditions of the system, to efficiently manage the network and to identify possible automation and control solutions and settings to be deployed for improving the grid performance. In the past situational awareness was not critical for operating a distribution system, due to the passive and relatively simple operation of these grids. Today, with the growing penetration of renewable generation and other distributed energy resources, the availability of situational awareness has become essential also at distribution level.

The objective of WP2 is the development of the hardware and software components needed to provide advanced situational awareness to distribution system operators by means of cost-effective solutions and virtualized substation intelligence. This report provides the description of the grid awareness services developed in the project, namely state estimation, power control and power quality evaluation service. The document provides a description of the concepts and models building the foundation of the algorithms running in these services, together with specific interfaces needed for the integration of the services in the cloud environment hosting the virtualized substation automation. The validation of each service in simulations or in a laboratory environment proves the feasibility and outlines the potential outcomes. The application of the monitoring and control services leads to a reduced amount of lost energy from renewables and enables a higher penetration of renewables without endangering system stability.

# Authors


| Partner | Name | e-mail |
|---|---|---|
| **RWTH (ACS)** | | |
| | Jonas Bielemeier | jonas.bielemeier@eonerc.rwth-aachen.de |
| | Marco Pau | mpau@eonerc.rwth-aachen.de |
| | Edoardo De Din | ededin@eonerc.rwth-aachen.de |
| **GH** | | |
| | Artur Löwen | aloewen@gridhound.de |
| | Khaled Tabbakh | ktabbakh@gridhound.de |
| **MAC** | | |
| | John O'Flaherty | j.oflaherty@mac.ie |
| | Connor O'Reilly | c.oreilly@mac.ie |
| **UNIBO** | | |
| | Alessandro Mingotti | alessandro.mingotti2@unibo.it |
| **ALTEA** | | |
| | Elisa Scala | escala@alteasolutions.com |
| | Andrea Nalli | analli@alteasolutions.com |

# Table of Contents


**1. Introduction ..... 7**

1.1 Related Project Work ..... 7

1.2 Objectives of the Report ..... 8

1.3 Outline of the Report ..... 8

1.4 How to Read this Document ..... 8

**2. Description of system awareness services ..... 9**

2.1 State estimation ..... 9

2.1.1 WLS-based state estimation approach ..... 10

2.1.1.1 WLS formulation ..... 10

2.1.2 Data-driven state estimation approach ..... 12

2.2 Power control ..... 13

2.2.1 Grid codes and state of the art power control ..... 13

2.2.2 Distributed consensus-based power control ..... 15

2.3 Power Quality Evaluation ..... 17

2.3.1 Power Quality Standards and Indices ..... 21

2.3.1.1 Power Quality Evaluation KPIs ..... 23

2.3.2 Power Quality Evaluation Added Value for DSOs ..... 23

2.3.2.1 Power Quality and Harmonics Issues ..... 24

2.3.2.2 Power Factor and Voltage Regulation ..... 31

2.3.2.3 Reactive Power and Compensation Solutions ..... 32

**3. Validation and KPI of system awareness services ..... 35**

3.1 State estimation ..... 35

3.1.1 Test grid and PMU placement ..... 35

3.1.2 Training phase of ANN estimator ..... 36

3.1.3 Testing phase of ANN estimator ..... 36

3.1.4 WLS estimator as reference case ..... 37

3.1.5 Results of ANN estimator ..... 37

3.1.6 Results of WLS estimator ..... 39

3.2 Power Control ..... 39
3.2.1 Selection and modification of test grid ..... 40
3.2.2 Implementation of reference control ..... 40
3.2.3 KPI definition and creation of test cases ..... 41
3.2.4 Test case results ..... 42
3.2.5 Summary of results ..... 49
3.3 Power Quality Evaluation ..... 54
3.3.1 APMU Characterisation Tests ..... 54
3.3.2 LV APMU Results ..... 55
3.3.2.1 Observations on test conditions of the test protocol ..... 56
3.3.2.2 LV APMU test results and conclusions ..... 56
3.3.3 MV APMU Results ..... 57
3.3.3.1 Tests of primary voltage measurements with step-up transformer ..... 58
3.3.3.2 Tests of current measurement accuracy with step-down transformer ..... 58
3.3.3.3 Tests of measurement accuracies with LPIT simulator ..... 59
3.3.3.4 MV APMU Conclusions ..... 61
**4. Documentation of the Application Programming Interface ..... 62**
4.1 The Interfaces ..... 63
4.1.1 Measuring Devices and Power Quality Service ..... 64
4.1.2 Converters ..... 64
4.1.3 Switches ..... 64
4.1.4 State Estimation ..... 64
4.1.5 Power Control ..... 65
**5. Conclusions ..... 66**
**6. List of Tables ..... 67**
**7. List of Figures ..... 68**
**8. Bibliography ..... 70**
**9. List of Abbreviations ..... 73**

**ANNEX ..... 74**

A1 – Exemplary files for the JSON Message sent by the services and the CIM files used . 74

A1.1 - Example for the JSON Message from the measuring devices with power quality service results ..... 74

A1.2 - Example for the JSON message from the switches ..... 76

A1.3 - Example for the JSON Message from the state estimator ..... 76

A1.4 - Example for the JSON Message from the power control service ..... 78

A1.5 - Example for a CIM file ..... 79

A2 – SE Validation grid data ..... 81

A3 – Power Quality Evaluation service outputs ..... 81

A3.1 – PQE outputs ..... 81

A3.2 – APMU sample script example ..... 82

A3.3 – LV AMPU Test Results ..... 84

A4 – Medium Voltage Test Results ..... 86

A4.1 - Accuracy Vs Test Voltage, Test Frequency 50 Hz ..... 86

A4.2 - Accuracy Vs Test Current, Test Frequency 50 Hz ..... 86

A4.3 - Overcurrent response, Test Frequency 50 Hz ..... 86

A4.4 - Overvoltage response, Test Frequency 50 Hz ..... 86

A4.5 - Apparent and Active Power (Resistive Load) ..... 87

A4.6 - Accuracy Vs Temperature (Current) ..... 87

A4.7 - Accuracy Vs Temperature (Voltage) ..... 87

# 1. Introduction

The project *Service Oriented Grid for the Network of the Future (SOGNO)* is funded by the Work Program H2020-LCE-2017-SGS. It has officially started in January 2018.

## 1.1 Related Project Work

This report is based on the work done in the tasks T2.1, T2.2, T2.4 and T2.5 of Work Package WP2. The first two tasks (T2.1 and T2.2) deal with the design of the main techniques for grid awareness. In particular, T2.1 focuses on the State Estimation service, which is the service allowing the real-time monitoring of the operating conditions of the distribution system, while T2.2 develops the techniques for the management of the power electronic components associated to the distributed generation (Power Control service), providing control and awareness of the behavior of the system with a large share of renewable energy sources. These tasks were partly covered in preceding deliverable D2.2 and are detailed with respect to their final implementation in this report. Task 2.4 encompasses the validation of the services based on simulations and laboratory tests that are used to prove the feasibility and identify key performance indicators directly and individually tailored to the services. Task T2.5 contains the development of low-cost measurement units needed to enable both state estimation and power control. The Advanced Power Measurement Units (APMUs) designed in SOGNO also allow monitoring different power quality parameters, as part of the Power Quality Evaluation service, offering an additional degree of situational awareness for the distribution system operators regarding the quality of the power supply in the grid. The accuracy of the power quality evaluation is determined in laboratory tests with calibrated equipment. Finally, T2.5 also includes the definition of the interfaces needed to integrate the above-mentioned grid awareness services in the cloud platform.

Figure 1 shows the overall structure of SOGNO. The grid awareness services designed in WP2, together with the specifications on required interfaces, are aligned with the architecture of the Virtualized Substation (ViSA) as developed in WP4. Lastly, the solution is deployed in the respective field trials (WP5).

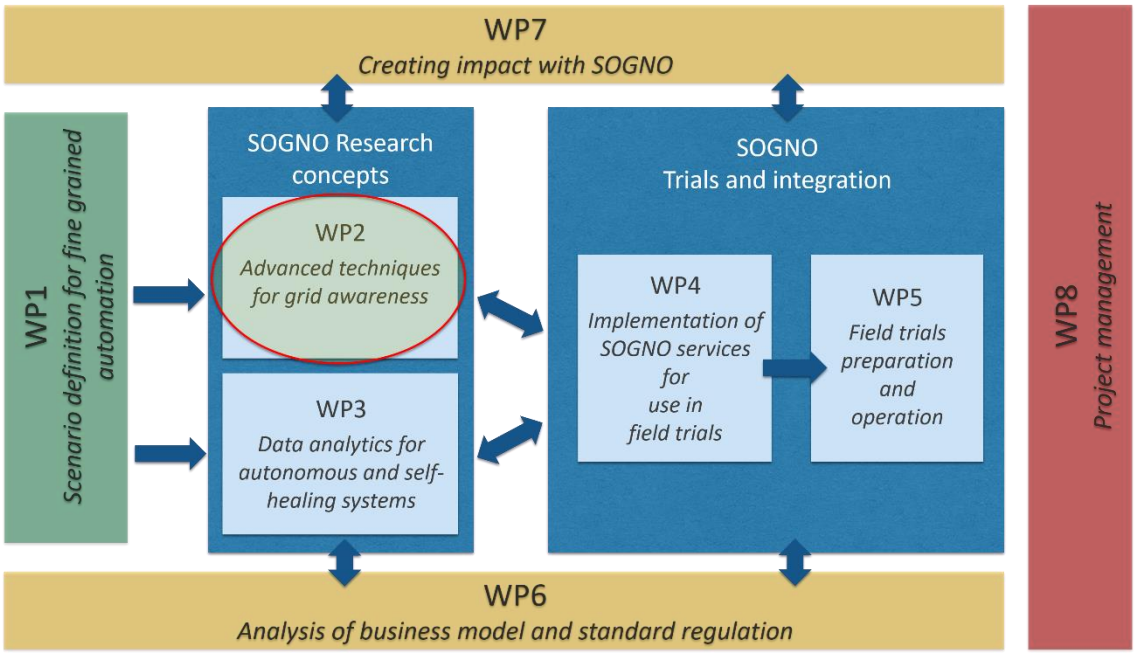


**Figure 1: Overview of SOGNO activities.**

## 1.2 Objectives of the Report

This report covers two main objectives: First, presenting the algorithms and their validations used in grid awareness services developed in the project (namely State Estimation, Power Control and Power Quality Evaluation) and secondly, specifying interfaces needed to enable to operate these services on the cloud platform hosting the Virtualized Substation (ViSA).

The presentation of the grid awareness services will not only focus on the description of technical details relevant for the design of the service itself, but also on main challenges in the distribution grid and the state of the art approaches. In this context, the SOGNO solutions are validated with respect to their theoretical claims.

## 1.3 Outline of the Report

The report consists of three main parts covering the service design, the service validation and the description of the service interfaces. The first part (Chapter 2) introduces three services developed for grid awareness, namely State Estimation, Power Control, and Power Quality Evaluation. Chapter 2 provides an update of the previous deliverable D2.2 regarding the details on the mathematical framework behind the algorithms and other technical aspects. The second part (Chapter 3) provides a validation of the developed services by means of simulations and laboratory test procedures. Finally, the last part (Chapter 4) contains the scheme of the interfaces required for integrating the services in the Virtualized Substation, including interface functions for the three services among each other and to other relevant components in the field or in the cloud.

## 1.4 How to Read this Document

This report can be read as a standalone document. However, other deliverables can be helpful to get a better view of the concepts advanced in the SOGNO project and to have more details on the grid awareness services. In particular, other deliverables closely related to this one are:

- D1.1 – Scenario & architectures for stable & secure grid (M12): This deliverable provides a description of power system scenarios investigated in the project for current and future distribution grids.
- D2.1 – Detailed description of 5G-based ICT concepts for supporting grid awareness (M22): This deliverable discusses the role of 5G communications for fostering the deployment of the grid awareness services presented in this deliverable.
- D2.2 – Description of initial interfaces & services for grid awareness (M12): This deliverable presents a first iteration of the designed grid awareness services and the corresponding interfaces.

# 2. Description of system awareness services

This chapter presents the services developed in the SOGNO project for providing system awareness to the Distribution System Operators (DSOs). These services are:

- State Estimation (SE)
- Power Control (PC)
- Power Quality Evaluation (PQE)

The descriptions are an extension or modification to the preliminary description of the services in deliverable D2.2. Unchanged parts of the algorithms are not elaborated in detail again and the reader is referred to D2.2. The ICT requirements and considerations for the communication in full rollout may be found in deliverable D1.1 and D2.1 respectively. For each service, this chapter provides the main objectives and the technical details related to the models or mathematical basics of the underlying algorithms. Moreover, the sections feature use cases and current state of the art practices.

## 2.1 State estimation

The State Estimation (SE) service aims at providing to the DSOs the visibility of the current operating conditions of the grid. It relies on the collection of measurements from the grid, which are then suitably processed in order to infer the most likely status of the grid compliant with the available measurement data. While being implemented already for several years in the control centers of transmission systems, the application of SE at the distribution level of the electric grid is still very limited, and most of the distribution grids are today still unmonitored or poorly monitored networks. Nevertheless, due to fundamental changes in act in the distribution grid (presence of reverse power flows, risk of overvoltage events, possible overloads of the grid assets, etc.), SE is now being more and more required in the management systems of the DSOs both to achieve simple system awareness and to trigger possible other management and control functions aimed at improving the grid performance.

While the underlying concepts behind the SE theory are similar for both transmission and distribution systems, the adopted algorithms and their implementation significantly differ due to the major differences between transmission and distribution grid characteristics. A first, important difference is the three-phase unbalanced nature of the distribution networks. This leads to the need of referring to the three-phase equations of the system and, accordingly, to the design of three-phase algorithms, which are computationally more expensive than the corresponding single-phase equivalent solutions. A second relevant difference between the two voltage levels is given by the size of the grid. From a topological perspective, distribution grids are composed of a much higher number of lines and nodes, making the distribution grid model larger and more complex than general transmission models. Once more, this automatically turns into additional computational demand for the distribution system SE algorithms. Last but not least, distribution grids significantly differ from transmission level systems due to the availability of meters and monitoring devices. In fact, since no strict monitoring requirements were existing for the last generation distribution systems, very few measurements are usually available to feed the SE algorithms. This poses a severe challenge for the achievement of sufficiently accurate results for the SE output. This issue is generally faced by introducing so-called pseudo-measurements, namely forecast measurements derived either from historical and statistical data, or from other assumptions defined thanks to the operators' experience. In the worst scenario, if forecast measurements cannot be reasonably defined, the nominal data of the power connection at the point of common coupling of the customer can be considered to set limits for the power consumption or injection at the node (see Figure 2).

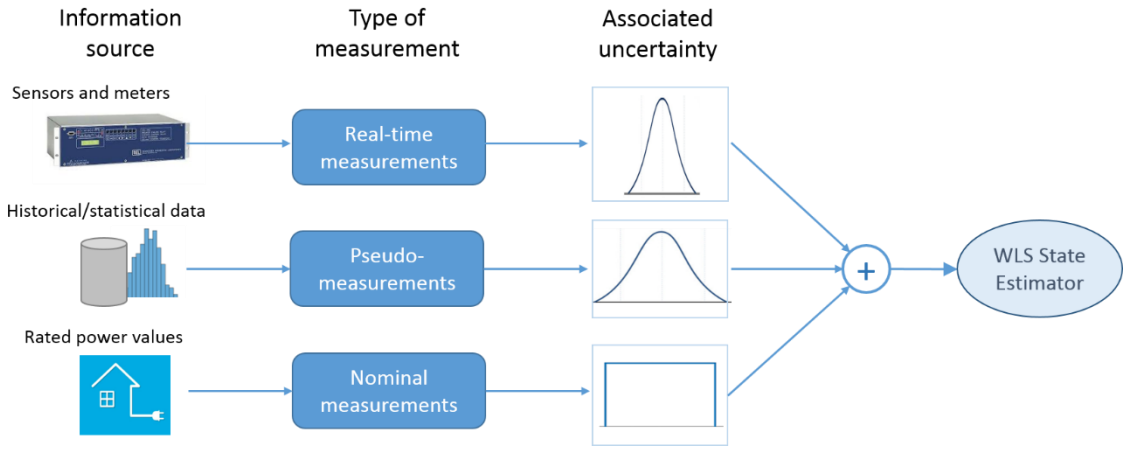


**Figure 2: Overview of input measurements to the WLS estimator**

Due to the above-mentioned characteristics of the distribution grid, the main targets to pursue in the design of the distribution system SE algorithms are: computational efficiency and maximization of the output accuracy given the set of input measurements. To fulfill these requirements, during the SOGNO project, two different SE solutions have been investigated. The first one is a classical solution, based on the well-known Weighted Least Squares approach. The reason to consider this type of algorithm is that it is based on a mature mathematical formulation and, under the general uncertainty conditions associated to the measurements, it is known to be a maximum likelihood estimator (namely an estimator capable of giving the best estimation accuracy achievable through the available set of input measurements). The second SE solution is a more innovative algorithm based on the use of Artificial Neural Networks (ANN). Such a solution is designed to cope with the limited availability of measurements in the grid and it aims at giving good accuracy results while minimizing the computational effort required to generate the output.

In the following of this Section, a brief review of the WLS and ANN approaches used for the design of the SOGNO SE service is given (as already described in D2.2). In Section 3, the validation of these algorithms at proof of concept level is provided, comparing the results given by both the WLS and he ANN estimator for the same sample benchmark grid.

### 2.1.1 WLS-based state estimation approach

#### 2.1.1.1 WLS formulation

The SE approach presented in this section is based on one of the most commonly used techniques to perform state estimation, namely the Weighted Least Squares (WLS) method [1]. The WLS-based SE technique applies the following measurement model:

$$\boldsymbol{z} = \boldsymbol{h}(\boldsymbol{x}) + \boldsymbol{e} \tag{1}$$

where $\boldsymbol{z}$ is the vector containing the measurements at a given instant of time, $\boldsymbol{x}$ is the vector of the variables representing the state of the electric grid, $\boldsymbol{h}(\boldsymbol{x})$ is the set of measurement functions expressing each measurement in $\boldsymbol{z}$ in terms of the state variables used in $\boldsymbol{x}$, and $\boldsymbol{e}$ is the vector of the errors associated with the measurements in $\boldsymbol{z}$.

In State Estimation for transmission systems, the state variables representing the electrical system are typically the voltage magnitudes and phase-angles at the different nodes of the grid. However, it is possible to use different parameters in the state vector, such as rectangular voltages [2] or branch currents either in polar or rectangular coordinates [3], [4], [5], and these alternatives offer specific advantages for distribution system SE. In the design of the SOGNO SE service, a formulation based on rectangular voltages has been chosen, since this allows to have

a computationally more efficient algorithm (since many of the measurement functions in eq. (1) can be linearized), an algorithm that is suitable for both radial and meshed grids, and an implementation that can flexibly and easily adapt to possible modification of the grid topology (through the simple modification of few terms within the distribution grid admittance matrix).

Based on the model in eq. (1), the objective of the WLS method is to minimize the following weighted sum of the measurement errors:

$$J = min\left(\sum_{i=1}^{m} w_i[z_i - h_i(x)]\right) \quad (2)$$

where $m$ is the number of measurements in the vector $\boldsymbol{z}$, and $w_i$ is the weight associated to the *i*-th measurement. Note that, to maximize the accuracy of the WLS method, the weight has to be chosen as the inverse of the overall measurement variance, which has to be derived from the uncertainty characteristics of the components present in the measurement chain such as sensors and measurement units.

Converting the minimization in (2) into a matrix form, the WLS objective function can be written as:

$$J = [\boldsymbol{z} - \boldsymbol{h}(\boldsymbol{x})]^T \boldsymbol{W} [\boldsymbol{z} - \boldsymbol{h}(\boldsymbol{x})] \quad (3)$$

where $\boldsymbol{W}$ is a weighting matrix having the weights $w_i$ in the elements of its diagonal. Under the assumption that the measurement errors are statistically independent, the other elements of the weighting matrix are equal to zero and, therefore, $\boldsymbol{W}$ is a diagonal matrix.

The WLS minimization can be performed using the iterative Gauss-Newton method, which leads to the following equation system solved at each iteration $k$:

$$\boldsymbol{G} \cdot \Delta \boldsymbol{x} = \boldsymbol{H}^T \boldsymbol{W} \left(\boldsymbol{z} - \boldsymbol{h}(\boldsymbol{x_{k-1}})\right) \quad (4)$$

where $\boldsymbol{x_{k-1}}$ is the state vector estimated at the iteration $k-1$, $\Delta \boldsymbol{x} = \boldsymbol{x_k} - \boldsymbol{x_{k-1}}$ is the vector computed to update the estimation of the state vector $\boldsymbol{x}$, $\boldsymbol{H}$ is the Jacobian matrix having the derivatives of the measurement functions $\boldsymbol{h}(\boldsymbol{x})$ with respect to the state variables in $\boldsymbol{x}$, and $\boldsymbol{G} = \boldsymbol{H}^T \boldsymbol{W} \boldsymbol{H}$ is the so-called Gain matrix. It is worth noting that, with the chosen formulation of the SE algorithm in rectangular voltage coordinates, many Jacobian sub-matrices (those related to linear measurement functions) are constant and thus they can be defined only once at the initialization of the SE algorithm (thus lowering the computational burden and allowing saving time).

Due to the fact that some measurement functions can still be non-linear, the equation system in (4) has to be solved iteratively until a certain convergence criterion is satisfied. Usually, the convergence criterion is set as:

$$max(|\Delta \boldsymbol{x}|) < \varepsilon \quad (5)$$

where $\varepsilon$ is a convergence threshold arbitrarily chosen (for example, a typical value for polar voltage based state estimators is $\varepsilon = 10^{-6}$). Note that the smaller the convergence threshold, the larger the number of iterations required by the WLS algorithm to converge and, consequently, the larger the execution time of the algorithm.

After the convergence of the iterative procedure, the last computed value of the state vector $\boldsymbol{x}$ represents the final estimation of the state of the grid. According to the made choice of the SE state vector, the final state of the grid will be thus expressed in terms of real and imaginary voltages at each node. However, it is worth noting that the obtained system state allows retrieving any other electrical quantity of the grid (namely powers and currents either consumed/injected at the nodes or flowing through the grid lines) using the power system equations. This is extremely important since different applications can need different type of information about the system operating conditions. Moreover, DSOs can also have the necessity to look at different parameters

and quantities of the grid in order to assess the grid performance or to evaluate the power quality conditions (possible presence of over- or under-voltages, or overloads of grid assets, etc.).

### 2.1.2 Data-driven state estimation approach

In alternative to classical WLS estimation approaches, data-driven approaches can also be conceived to perform the state estimation in distribution grids. To build data-driven monitoring models, the main requirement is to have reliable training data representing the behaviour of the grid depending on the current topology (which needs to be known) and the current scenario of power generation and consumption. The training data can be obtained from load flow data, either directly received from a DSO or generated and extracted from a power flow simulation tool. In the SOGNO project, Artificial Neural Networks (ANN) are exploited as a data-driven technique to perform the state estimation. To this end, an ANN is trained in such a way that it can map the system input (or measured grid variables) to the states (voltage magnitude and voltage angle have been chosen as representative state variables of the system in this context) of the distribution system. In fact, ANN consists of several layers, each containing a certain number of neurons. The ANN architecture used in the SOGNO monitoring system includes three layers: an input, a hidden and an output layer (see Figure 3).

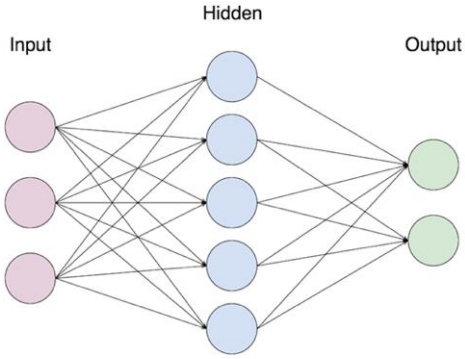


**Figure 3: Artificial neural network architecture**

The neurons in these layers are connected to each other through weights and biases that are synthesized by performing a training algorithm so that the ANN can learn to capture the non-linear correlations between input and output data sets. By providing training data (input and output data sets, which in the SE context correspond to starting measurements and grid state, respectively) the weights and biases are adjusted so that the distance between actual and predicted values would be below a specific threshold.

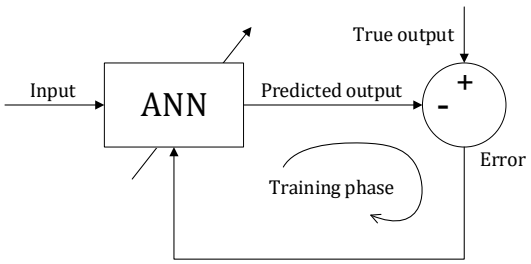


**Figure 4: Artificial neural network training process**

Compared to the WLS-based approach, the computational cost for performing state estimation in the data-driven monitoring approach is low as it does not involve matrix inversion operations. In runtime, upon receiving the measured values (input data), the ANN-based estimator very quickly calculates the grid states so that these can be immediately processed in other distribution automation functions. At the same, an extensive training of the grid model can also lead to very

good accuracy performance, which can be comparable to those of traditional algorithms based on WLS approaches.

## 2.2 Power control

The power control (PC) service aims to optimize the distribution grid power flows (at both MV and LV level) to prevent possible contingencies (e.g. violation of the voltage limits, overloading of grid components, etc.) and to foster a more efficient and reliable system operation. This is obtained through the smart control of the active and reactive power injected (or consumed) by converter-based components connected to the grid. While converters that are available today in the market do not always guarantee this feature, this requirement can be considered as realistic in future scenarios where the availability of communication capabilities will allow to enable the smart grid.

The PC service is based on the monitored grid state as provided by the synchronously running SE service. First, the state of the art power control is presented in subsection 2.2.1. It summarizes the grid code analysis of deliverable D2.2 and presents the essentials for the active control of Distributed Energy Resources (DERs) by means of coordinated schemes. Based on this, subsection 2.2.2 presents a coordinated control scheme that is based on a consensus approach. This exemplary algorithm is supposed to enhance the performance with respect to voltage profile and necessary active power curtailment. The output of the PC service is the pair of active and reactive power set points for each converter-based component in the grid. Subsection 2.2.2 presents the theory of the algorithm while section 3.2 provides the results achieved with this algorithm.

### 2.2.1 Grid codes and state of the art power control

Grid codes, standards and guidelines define the DER grid interconnection and operation including grid support. The previous deliverable D2.2 has outlined the variety of grid supporting functions from DER. A straightforward way that has proven to be effective is the Q(U) control. The reactive power infeed of the DER is controlled based on the measured terminal voltage and hence, directly affecting the voltage. For evaluating the voltage, one of the following methods shall be used:

- Positive sequence of the symmetrical components
- Average voltage of a three phase system
- Voltage of every phase to determine the reactive power for each phase independently

Figure 5 shows the droop curve that is prescribed by the German standard VDE AR-N 4105 [6] for the connection of generating units to the low and medium voltage grid. This standard is chosen as a reference as it imposes rather strict requirements for the connection and the operation of renewables in the distribution grid. It is configured for a maximum and minimum value according to cosφ = 0.95 for plants with a nominal apparent power up to 4.6 kVA and cosφ = 0.9 for plants with a higher nominal apparent power. The droop control of the DER operates with the set points determined by the curve in figure and the current voltage measured at the terminals of the DER connection, constrained by the operation limits of the DER.

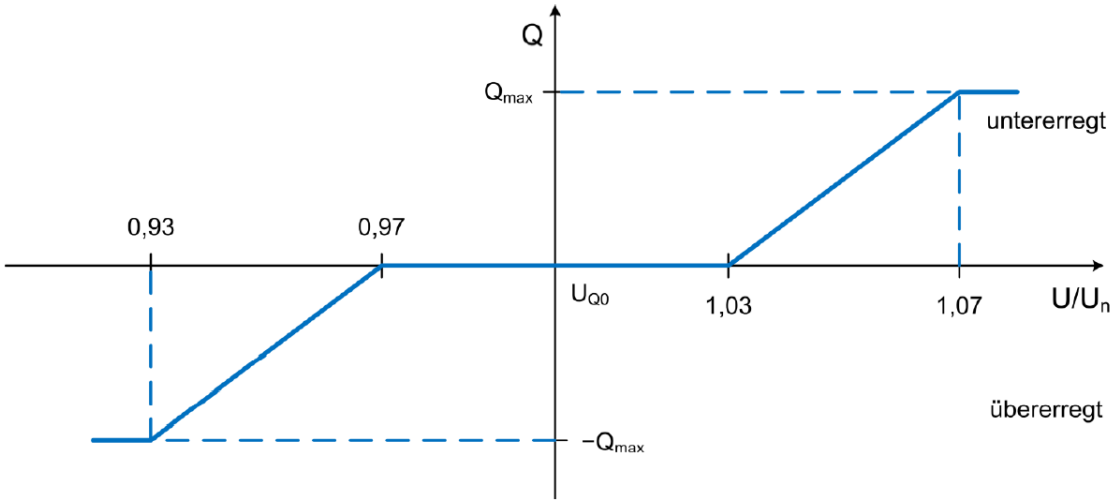


**Figure 5: Standard Q(U) droop curve according to VDE AR-N 4105**

Another option to restore the voltage is a P(U) control that limits the active power at over-voltage nodes in the grid. However, this control acts only to avoid the disconnection of the generating unit. Due to the high impact of the active power on the distribution grids this counteracts a rising voltage. The implementation depends solely on the manufacturer. The VDE standard does not enforce a P(U) control. Instead, it is only required that the individual plant is capable to reduce its active power output based on an external signal sent by the DSO. Based on a power curtailment signal, this reduction takes place in steps, i.e. each plant may be forced to reduce its active power injection from a value of 100% of the nominal active power to 60%, 30% or 0%. The reduction of the active power based on a remote signal will be referred to as active power curtailment in the following. The activation of active power curtailment by the DSO is not specified in detail since it is part of the grid security management. With respect to the validation in section 3.2 it is assumed that the DSO will activate the curtailment whenever the maximum permissible voltage threshold is exceeded.

Similarly to the active power curtailment by the DSO in critical situations, the possible usage of external input signals for the DER provides a new dimension for the power control. This enables an expansion of the aforementioned active power curtailment where it was only possible to force the PV plant into a limited selection of states. Instead of automatic controllers, or in addition to, external set points for active and reactive power may be directly imposed by the DSO overriding other set points (Figure 6). The increasing requirement in LV grid codes (and already prevailing MV grid codes) for DER to be able to use external control signals extends the possibility for more controllability and flexibility for the system operator. This potentially enables the DSO to react to commands from the Transmission System Operator (TSO), e.g. the request for active power limitation to avoid a congestion, or act based on the observed system state, e.g. to avoid an emergency situation.

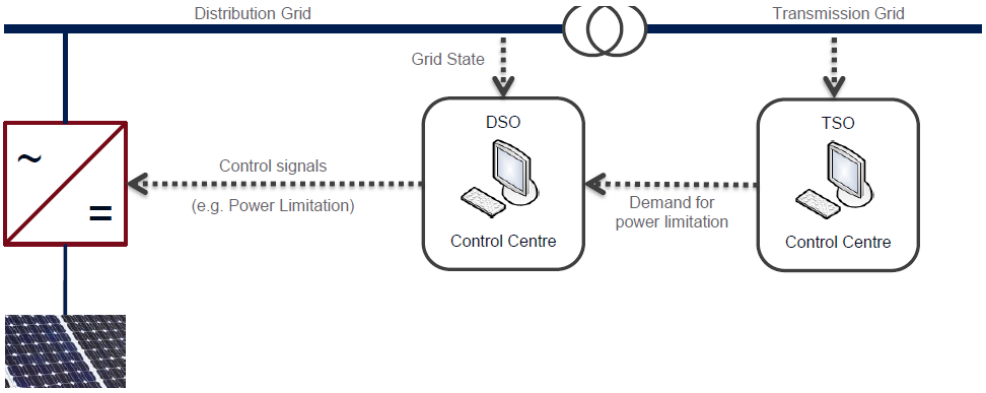


**Figure 6: External control of active/reactive power set points by system operator [7].**

However, the options are not limited to emergency scenarios. These control signals can also be utilized in normal operation. The DSO can use the external control signals to adjust the power flow in the distribution in its favor. The DSO may send active and reactive power set points to keep the voltage of a feeder within the limits during generation peaks. The full reactive power capacity could be utilized before any active power has to be curtailed. Or the losses in the grid may be minimized using a coordinated voltage control scheme for the grid. These kinds of approaches could allow minimizing the power curtailments for distributed generation based on renewable energy sources, thus fostering their operation in the distribution system.

The execution of such approaches requires additional computational power to run algorithms that can provide an optimized power flow for the grid or a system state within the operational limits. Moreover, the value of these algorithms increases with the reliability, flexibility and speed of the communication since the response time to any kind of event or desired action is lowered and the operational safety margin can be reduced. The SOGNO solution that is based on the ViSA together with a 5G communication to the controllable devices provides the computational power in the cloud and a flexible communication cost-efficiently, as it requires a minimal amount of hardware. This leads to the possibility to look into algorithms that can help to achieve a better management of DER and the distribution grid.

### 2.2.2 Distributed consensus-based power control

In a passive distribution grid, the voltage profiles tends to decrease along the feeder, whereas, the presence of distributed generators may cause an increase of the voltage values resulting in possible overvoltage events.

The effect of the injection of active and reactive power to the grid is described by the branch-flow model:

$$v_i = v_0 + \sum X_{ij}\left(s_j^g - s_j^c\right) \tag{6}$$

Where $s_j^g$ is the complex power $(p_j^g + jq_j^g)$ injected at node $j$, whereas $s_j^c$ the complex power absorbed at node $j$. $v_i$ and $v_0$ are the voltage at node $i$ and at the slack bus respectively. $X_{ij}$ is the mutual voltage-to-power-injection sensitivity factor [8] which defines the sensitivity of the voltage node to the variation of active and reactive power injections.

$$X_{ij} = r_{ij} + jx_{ij} \tag{7}$$

Where:

$$\begin{cases} r_{ij} = \frac{dv_i}{p_j^g} = -\frac{dv_i}{p_j^c} \\ x_{ij} = \frac{dv_i}{q_j^g} = -\frac{dv_i}{q_j^c} \end{cases}$$

The equation clarifies that a positive imbalance between generation and load causes an increase of the voltage on the subsequent nodes of the slack bus due to the export of energy. This variation of the voltage along the feeder can generate events where voltage exceeds the voltage limit imposed by the guideline for distributed energy resources.

As mentioned before, in order to comply with the limits, local voltage control is applied to the PV inverters consisting of injection/absorption of reactive power $Q_{PV}$ and limitation of active power injection $P_{PV}$. These strategies are based on incremental local feedback laws. With this approach, each PV independently acts on the grid without a coordination with the rest of the installed PVs.

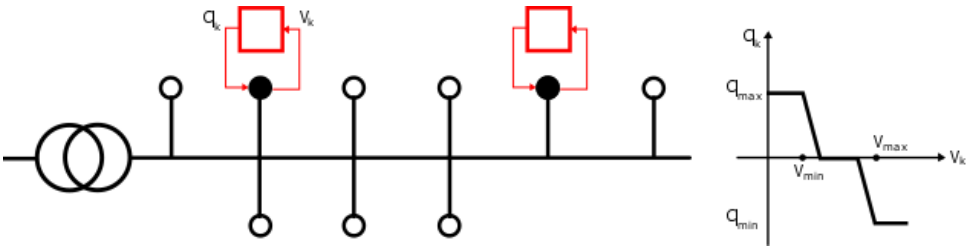


**Figure 7: Example of the typical reactive power control based on local feedback**

A different approach can be found in [9] [10] [11] [12] where PVs are used in a coordinated way to compensate for voltage violations. Among them, the approach defined in [11] [12] has been adopted as starting point for the design of the SOGNO power control service, because of its intrinsic feedback control behavior which guarantees robustness to model mismatch, rejection of disturbance, dynamic responsiveness, minimal computational effort. All these aspects, especially the minimal computation effort, are particularly interesting features for a real-time control application that needs to control multiple DERs.

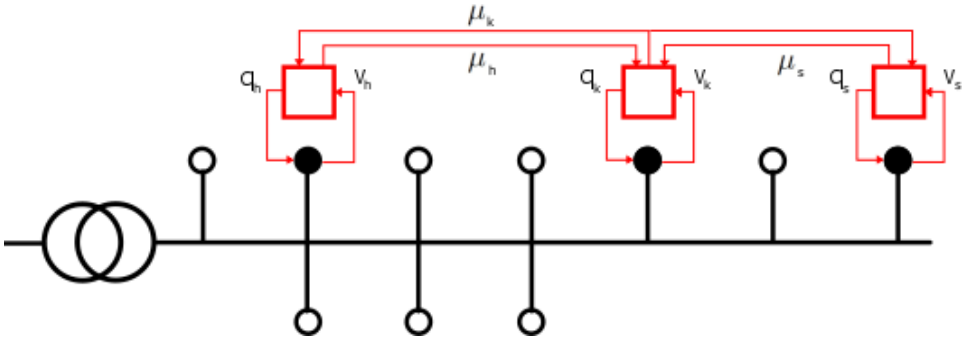


**Figure 8: Distributed reactive power control**

This approach can be implemented in a distributed way by making the distributed energy resources communicating among them or by solving element-wise the matrix by vector multiplication, so that each reactive power control output will depend only on the results of the calculation of only some elements of the vector. In this second case, even though the solution is not physically distributed, the sparsity of the matrix guarantees that the solution is distributed.

The definition of the control output is derived from the solution of the minimization of power losses on the grid, resulting in the minimization of the voltage deviation. This task is assigned to the PV, resulting in the following quadratic function and constraints:

$$\min_{q_{PV}} q_{PV}^T X^{IM} q_{PV} \tag{8}$$

$$subject\ to \quad \begin{matrix} v_{min} \leq v \leq v_{max} \\ q_{PV\,min} \leq q_{PV} \leq q_{PV\,max} \end{matrix}$$

The solution of the optimization problem follows the approach in [12] and it is based on the well-known dual decomposition method [13].

This optimization process starts with the definition of the Lagrangian function, which allows to reformulate the constrained minimization problem in terms of Lagrangian multipliers. Based on the definition in [12], the Lagrangian is expressed as follows:

$$L(q_{PV}, \lambda_{min}, \lambda_{max}, \mu_{min}, \mu_{max}) = q_{PV}^T X q_{PV} + \lambda_{min}(v_{min} - v) + \lambda_{max}(v - v_{max}) + \mu_{min}(q_{PV\,min} - q_{PV}) + \mu_{max}(q_{PV} - q_{PV\,max}) \quad (9)$$

where $\lambda_{min}, \lambda_{max}, \mu_{min}, \mu_{max}$ are the vectors of lagrangian multipliers associated to the voltage and power constraints

From the theory of dual decomposition, the problem in (3) can be reformulated as:

$$L \max_{\lambda,\mu} \left( \inf_{q_{PV}} \{L(q_{PV}, \lambda_{min}, \lambda_{max}, \mu_{min}, \mu_{max})\} \right) \quad (10)$$

The algorithm to solve 5 is based on the iterative execution of the following steps:

1) dual-ascent steps on the dual variables $\lambda_{min}, \lambda_{max}, \mu_{min}, \mu_{max}$
2) unconstrained minimization on the primal variable $q_{PV}$

The dual-ascent step is based on the theory described in [13], which applied to the problem (5), can be used to obtain the iterative algorithm for step 1):

$$\mu_{max,h}(k+1) = [\mu_{max,h}(k+1) + \gamma_Q(q_{PV,h} - q_{PV\,max})]_0^\infty \quad (11)$$

$$\mu_{min,h}(k+1) = [\mu_{min,h}(k+1) + \gamma_Q(q_{PV\,min} - q_{PV,h})]_0^\infty$$

$$\lambda_{max,h}(k+1) = [\lambda_{max,h}(k+1) + \alpha_Q(v_h - v_{max})]_0^\infty$$

$$\lambda_{min,h}(k+1) = [\lambda_{min,h}(k+1) + \alpha_Q(v_{min} - v_h)]_0^\infty$$

The calculation of step 2) follows the logic presented in [12], and aims at solving $\arg\min_{q_{PV}} L(q_{PV}, v)$, therefore from $\frac{\partial L}{\partial q_{PV}} = 0$, the updated reactive power injections of the PVs result in:

$$q_{PV}(k+1) = -\left(\lambda_{max,h}(k+1) - \lambda_{min,h}(k+1)\right) - G_Q\left(\mu_{max,h}(k+1) - \mu_{min,h}(k+1)\right) \quad (12)$$

where $G_Q$ is defined as $X^{-1}$.

The same approach can be applied to the active power control of the DGs, where the calculation of $G_P, \gamma_Q$ are based on $X^{RE}$.

## 2.3 Power Quality Evaluation

The annual cost of Power Quality disturbances on distribution grids in the EU has been estimated to be €150 Billion, of which €86.5 Billion (58%) is due to dynamic phenomena such as temporary dips and short interruptions [14]. These huge costs can be alleviated through continuous grid monitoring and grid awareness as provided by the mass-deployable low-cost APMUs and SOGNO Power Quality Evaluation (PQE) and other services.

A power quality (PQ) problem is defined as any problem that causes voltage, current, or frequency deviations in the supply and may result in failure or mal-operation of end-user equipment. There are four major factors that cause an increased need for DSOs to solve and prevent power quality problems in distribution networks [15]:

1. Increased use of power quality-sensitive equipment
2. Increased use of equipment that generates power quality problems
3. Increased inter-connectedness of power systems
4. Deregulation of the power industry

| Example waveshape or RMS variation | Causes | Sources | Effects | Examples of power conditioning solutions |
|---|---|---|---|---|
| | Impulsive transients (Transient disturbance) | - Lightning<br>- Electrostatic discharge<br>- Load switching<br>- Capacitor switching | - Destroys computer chips and TV regulators | - Surge arresters<br>- Filters<br>- Isolation transformers |
| 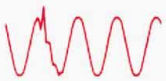 | Oscillatory transients (Transient disturbance) | - Line/cable switching<br>- Capacitor switching<br>- Load switching | - Destroys computer chips and TV regulators | - Surge arresters<br>- Filters<br>- Isolation transformers |
| | Sags/swells (RMS disturbance) | - Remote system faults | - Motors stalling and overheating<br>- Computer failures<br>- ASDs shutting down | - Ferroresonant transformers<br>- Energy storage technologies<br>- Uninterruptible power supply (UPS) |
| | Interruptions (RMS disturbance) | - System protection<br>- Breakers<br>- Fuses<br>- Maintenance | - Loss production<br>- Shutting down of equipment | - Energy storage technologies<br>- UPS<br>- Backup generators |
|  | Undervoltages/ overvoltages (steady-state variation) | - Motor starting<br>- Load variations<br>- Load dropping | - Shorten lives of motors and lightning filaments | - Voltage regulat<br>- Ferroresonant transformers |
| | Harmonic distortion (steady-state variation) | - Nonlinear loads<br>- System resonance | - Overheating transformers and motors<br>- Fuses blow<br>- Relays trip<br>- Meters misoperate | - Active or passiv filters<br>- Transformers with cancellati of zero sequenc components |
| 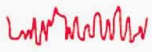 | Voltage flicker (steady-state variation) | - Intermittent loads<br>- Motor starting<br>- Arc furnaces | - Lights flicker<br>- Irritation | - Static VAR systems |

**Figure 9: Power Quality problems**

As discussed in SOGNO deliverable D2.2, the SOGNO PQE service provides continuous real-time situational grid awareness to the electricity grid operators about the quality of the power supply in their grid and, in case anomalies are detected, triggers suitable countermeasures to prevent asset stress or failures, and outages. The produced power quality information can be used as input for more complex management and SOGNO control functions by the DSOs to efficiently operate their grid. In this regard, control or optimization functionalities built based on the PQE service can lead to:

- reduced costs by reducing outages and their associated regulator fines;
- reduced asset failures due to low power quality;
- reduced time to identify outages related to poor power quality;
- improved service quality and efficiency of the power delivery.

The SOGNO PQE service is provided by the Advanced Power Measurement Unit (APMU) device that is being developed by MAC, as shown in the following:

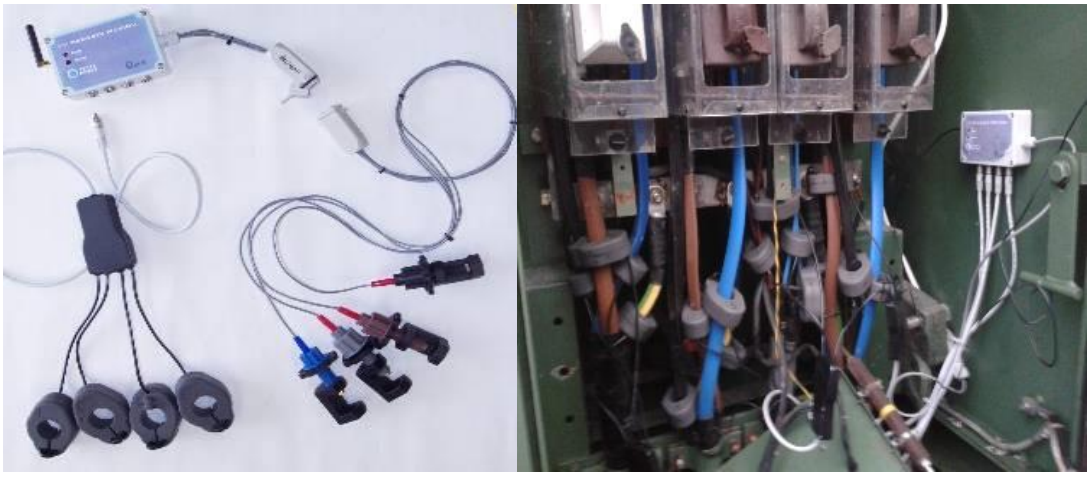

**Figure 10: APMU deployed on a 4-Feeder LV Network.**

On LV and MV lines, the APMU measures:

- Classical electrical quantities, including voltage, current, power and frequency.
- Advanced power quality parameters, including current flow direction, harmonics, reactive power, power factor, earth fault currents.
- Further advanced power quality parameters and smart event monitoring, such as unbalanced phases, voltage sags & dips. over-voltage, over-current, and overload detection, using algorithms that run in the APMU and are dynamically updated for local grid-edge intelligence.

The algorithms are updated as required depending on the operational/business monitoring objectives of the DSO for specific parts of their networks or issues that they are encountering. There could be straightforward changes to Over-Voltage/Current thresholds or as complex as defining new PQ indices or potential fault conditions to be monitored.

While current power quality monitoring units that compute PQ parameters already exist in the market, the innovative added value of the SOGNO solution is the implementation of new functionalities including: (a) providing grid-edge processing and dynamic DSO-defined algorithms, (b) using a low-cost device that enables mass deployed network monitoring to generate real-time data, even in very large distribution grids at MV, but particularly at LV, and (c) integration into the SOGNO ecosystem and all of its other services. The information directly provided by the APMU can be optionally complemented by the results of SE or by additional post-processing algorithms implemented in the SOGNO ViSA cloud platform for the computation of other power quality indicators.

The PQE outputs of the APMUs are communicated in real-time to the ViSA and, finally, transmitted to the grid operators to give them awareness on the current status of the power quality in the grid. The different power quality indicators can be constantly shown in the visualization tool of the DSO or could trigger specific alarms if the related values exceed specific thresholds. For instance the following figure shows some typical examples of SOGNO PQE service user interface parameters from MAC's cloud-based visualisation platform at http://gridwatch.cloudapp.net

- Currents of 3 phases & Neutral from one Feeder

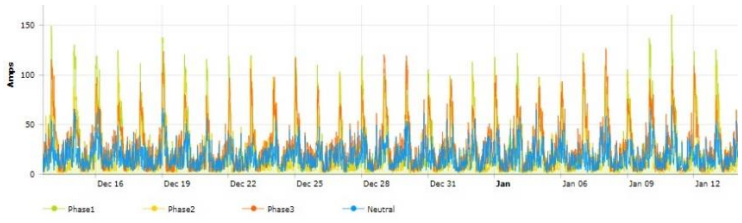

- Current detail showing Neutral current

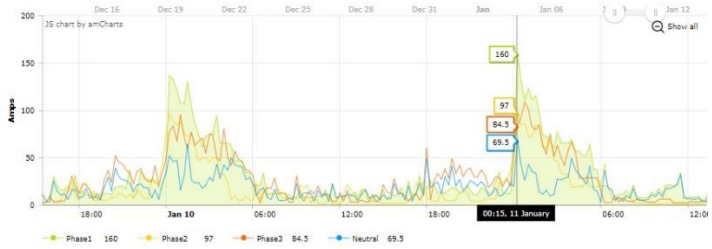


- Voltages of 3 phases from one Feeder

- Active Power for 3 phases from one Feeder

- Frequency for 3 phases from one Feeder

- Power Factor for 3 phases from one Feeder

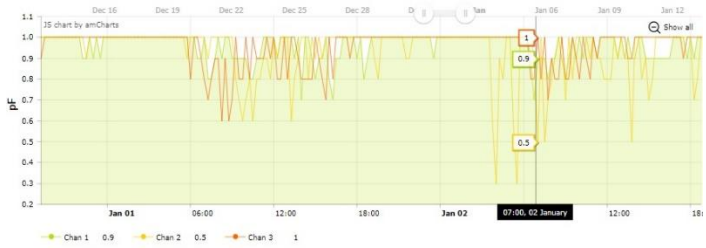


**Figure 11: PQE Service User Interface examples of monitored parameters.**

Being a monitoring service, the SOGNO PQE runs continuously with a reporting rate of the monitored parameters to the control centre, typically well below a minute.

The PQE service's APMU devices continuously monitor and provides standard power quality parameters, including (see Annex A3.1):

- Current (A) - Phase 1, Phase 2, Phase 3, Neutral Current, Flow Direction.
- Voltage (V) - Phase 1, Phase 2, Phase 3
- Power - Active Power (kW), Apparent Power (VA), Reactive Power (Var)
- Harmonic Distortion (current & voltage) THD & Individual harmonics

The SOGNO PQE Service can dynamically load algorithms over-the-air (OTA) as simple JSON scripts that run in the APMU devices for local grid-edge intelligence. An example JSON script is

shown in Annex A3.2. These algorithms can address the operational/business monitoring requirements of each DSO for specific parts of their networks or issues that they are encountering. So for instance in some substations, or parts of the grid, the operations staff may be concerned about, one or more of the following use cases:

- Imbalance across 3 phases (leading to stresses on some phases),
- Excessive earth fault currents leakage and possible safety issues,
- Too high reactive power or low power factor resulting in reduced delivery capacity,
- Potential harmonics due to certain loads.
- Etc.

The algorithms could be straightforward changes to Over-Voltage/Current thresholds (as in the A3.2 example) or as complex as defining new PQ parameters or potential fault conditions to be monitored, such as:

- Over-voltage, over-current, and overload detection
- Excessive earth fault currents
- LV outage detection
- Persistent unbalanced phases
- Voltage Sag and Flicker Detection

However, it is expected that future algorithms will be more complex by defining more sophisticated grid parameters or potential fault conditions to be monitored, exploiting the security and low-latency features of 5G to better meet the operational needs of DSOs. For instance, the following have already been suggested by DSOs and are looking promising:

- Using LV monitoring to determine MV voltages.
- Using LV monitoring to detect MV lines down or fuse blown.

The SOGNO PQE dynamically loaded algorithms will enable sophisticated distributed real-time intelligent monitoring and grid-awareness right to the grid edge, in low-cost mass-deployed APMU devices to provide the PQE service data to:

- DSOs' operational field staff who "need to know urgently" about events on the grid as they occur on their mobile devices to help them prevent asset stress or failures, and outages.
- The DSO's backend SOGNO services, and Distribution Management System, at all times.

Each APMU supports up to 4 feeders and is powered from one of the voltage lines being monitored. In the WP5 pilots, for LV networks MAC's Planar Magnetic Current Sensors and industry standard voltage G-Clamps are used, and for MV networks ALTEA's high voltage sensors are deployed. More details on the sensors and measurement units deployed in the SOGNO field trials are provided in Deliverable D5.1. Existing voltage sensors deployed by the DSO can also be facilitated if available.

### 2.3.1 Power Quality Standards and Indices

The SOGNO Advanced Power Quality Measurement Units (APMUs) provide the real-time measurements and awareness of Power Quality (PQ) for the SOGNO Power Quality Evaluation (PQE) service.

Power Quality refers to the condition of the electrical supply as presented at a customer load. This is the most important power distribution system feature after Security of Supply which ensures a continuous availability of power. Power Quality concerns any manifestation of voltage or current deviations that can result in the failure or mal-operation of customer equipment. Typically, the most pertinent parameters are associated with the voltage waveform. These include

(a) the magnitude and balance of the three-phase voltages,
(b) transient fluctuations and
(c) individual and total voltage harmonics and inter-harmonics.

Power Quality refers to a set of electrical boundaries defined by various documented rules designed to allow electrical equipment to function in its intended manner without significant loss

of performance or life expectancy, this includes the steady and stable supply of electricity delivered by the grid. In order to achieve this aim it is necessary to constantly and vigilantly monitor the power conditions within an electrical network.

With increased globalization of industry, including the free transport of electrical distribution and production equipment, it will be increasingly necessary for power quality to be consistently monitored and regulated. The EU Directive 89/336 for Electromagnetic Compatibility (in 1989) [16], aimed to ensure the reliability and power quality of distribution networks (and proper operation of equipment connected to them). This EMC Directive led to a 1989 definition of the physical characteristics of the LV and MV distribution systems by the organization UNIPEDE, and finally in 1994 the EN50160 standard on "Voltage characteristics of electricity supplied by public distribution systems". This standard was developed by a working group under CENELEC (European Committee for Electrotechnical Standardization) and was given the designation European Norm 50160, or EN50160 [17].

EN50160 defines, describes and specifies the main characteristics of the Voltage at a network user's supply terminals in public low voltage, medium and high voltage AC electricity networks under normal operating conditions. This standard describes the limits or values within which the voltage characteristics can be expected to remain at any supply terminal in public European electricity networks. EN50160 defines and in some cases provides measurement methods and compliance levels for 10 characteristics of the supply voltage:

- Power frequency
- Supply voltage variations
- Rapid voltage changes (and Flicker)
- Supply voltage dips
- Short interruptions
- Long interruptions
- Temporary over-voltages
- Supply voltage unbalance
- Harmonic voltage
- Mains signalling voltage

However, power quality is not just voltage quality, it also includes current quality. Based on the best practices of national regulators and DSOs, the International Standard IEC61000-4-30 [18] builds on EN50160 (and other standards) to help to provide a common framework for quality of supply regulation and globally acceptable limits [19].

The International Standard IEC61000-4-30, "Testing and measurement techniques – Power quality measurement methods" regulates the measurement methodologies and creates the ability to directly compare results from different analyzers [20]. The standard is periodically updated as the industry evolves and new measurement scenarios are discovered or required. Since its introduction in 2003, the standard has been updated several times and is currently on its 3rd Edition.

IEC61000-4-30 defines the measurement method, accuracy and time aggregation to verity power quality parameters in the following 3 performance classes to obtain repeatable and comparable results[1]:

- Class A – must comply to the highest performances and accuracy level to obtain repeatable and comparable results
- Class S – accuracy levels are less stringent. Class S Power quality analysers can be used for statistical surveys and contractual application where comparable measurements are not required. The SOGNO APMU adheres to this Class S.
- Class B (obsolete) – This class was introduced at the 1st and 2nd editions of the standard to avoid making may instrument obsolete. In this class the standard required

[1] Additionally, the IEC 62586-1 defines EMC, safety and environmental requirement for power quality analyzers in different installation conditions and the IEC 62586-2 defines the test and uncertainty requirement to comply with IEC 61000-4-30 class A.

that the measurement method and accuracy will be defined by the manufacturer in the instrument datasheet. In the 3rd addition, this performance class was removed.

Standards were created to provide an equal starting point to Power Quality Evaluation and to help show the same values. However, in many cases limiting the information to standards prevented the troubleshooting field engineer from monitoring the anomalies, not to mention identifying their source. The APMU provides continuous measurement of available information. There is no limit on the available data, since no thresholds or setups are used. In addition, it measures both in accordance to IEC61000-4-30 and cycle-by-cycle in order to guarantee a complete view of the electrical network. Furthermore, the evaluation according to the latest IEEE 519 is also achievable due to the continuous waveform recording. Using the APMU for Power Quality Evaluation ensures that anomalies are not only be monitored, but their causes can also be identified.

#### 2.3.1.1 Power Quality Evaluation KPIs

Following are the parameters defined in the IEC 61000-4-30 standard:

- Power frequency
- Magnitude of supply voltage
- Flicker (by reference to IEC 61000-4-15)
- Supply dips/swells
- Voltage Interruptions
- Voltage unbalance
- Voltage harmonics (by reference to IEC 61000-4-7)
- Voltage Inter-harmonics (by reference to IEC 61000-4-7)
- Mains signalling
- Under- and over-deviation

In the 3rd addition the following parameters were introduced:

- Rapid voltage changes
- Flicker class F1
- Magnitude of the current
- Current unbalance
- Current harmonics (by reference to IEC 61000-4-7)
- Current inter-harmonics (by reference to IEC 61000-4-7)

The APMU sensors constantly measure voltage and current on all phases at each monitored point (of up to 4 feeders) on the distribution network, and the AMPU provides the following indices from the IEC 61000-4-30 standard, as well as some additional Power Quality parameters that are most relevant for DSOs and the SOGNO PQE service (see Annex A3.1).

1. Power Frequency
2. Magnitude of supply Voltage (V) - Phase 1, Phase 2, Phase 3
3. Voltage Interruptions
4. Supply Voltage unbalance
5. Voltage harmonics - THD & Individual harmonics
6. Under- and over-deviation
7. Rapid voltage changes
8. Magnitude of the Current (A) - Phase 1, Phase 2, Phase 3, Neutral Current, Flow Direction.
9. Current unbalance
10. Current harmonics - THD & Individual harmonics
11. Power - Active Power (kW), Apparent Power (VA), Reactive Power (Var)
12. Power Factor

### 2.3.2 Power Quality Evaluation Added Value for DSOs

As discussed earlier, the most pertinent power quality parameters for DSOs, include

a. the magnitude and balance of the three-phase voltages,
b. transient fluctuations and
c. individual and total voltage harmonics and inter-harmonics.

While the effects of voltage and transient fluctuations are clear, the impact of harmonics, power factor and voltage regulation on the operation of distribution networks can be more subtle but no less important, so they are now discussed in more detail in the following subsections.

#### 2.3.2.1 Power Quality and Harmonics Issues

Harmonics can have adverse effects on the distribution network. If nonlinear loads produce unwanted harmonics, they can cause grid equipment failure as a result of insulation breakdown, arcing and overheating. As such, this aspect of power quality management is of high importance to both DSOs and users of electrical power networks.

Cable connections, particularly those underground, can introduce power-frequency resonance points to the local distribution system. Any unwanted harmonic currents injected at these resonance points will be amplified and result in severe distortion to the local system voltage. It is particularly important that all details of such cable connections, internal networks and plant, including any reactive power devices, be monitored to assess and identify an optimal solution for all neighbouring installations.

The SOGNO APMUs measure Total Harmonic Distortion (THD) of both Voltage (THDV) and Current (THDI) and individual harmonics, as shown in the following Power Quality Evaluation (PQE) screen-grabs from an APMU running in a substation near to a large photovoltaic (PV) source, and displaying up to the 7$^{th}$ harmonic:

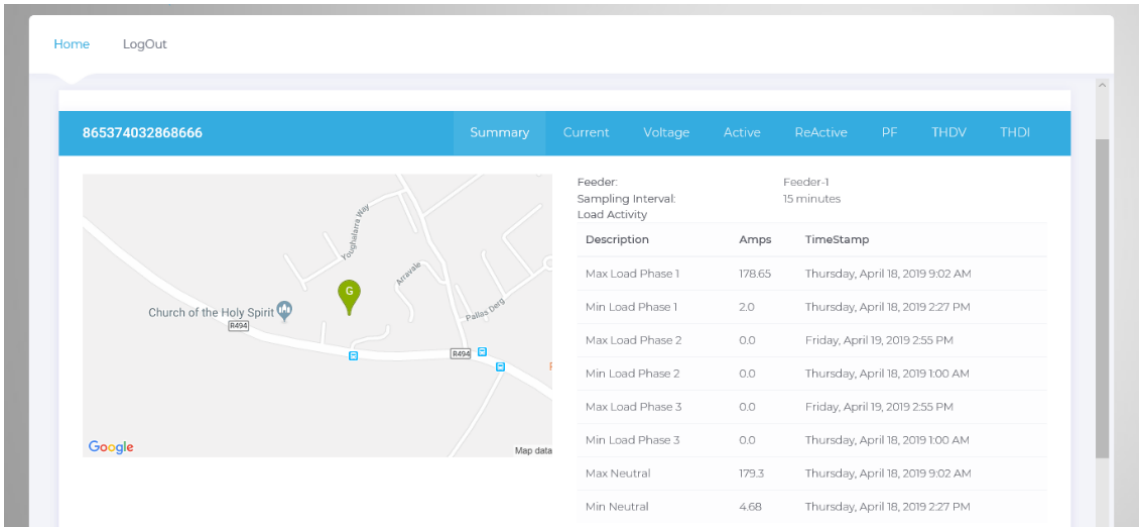


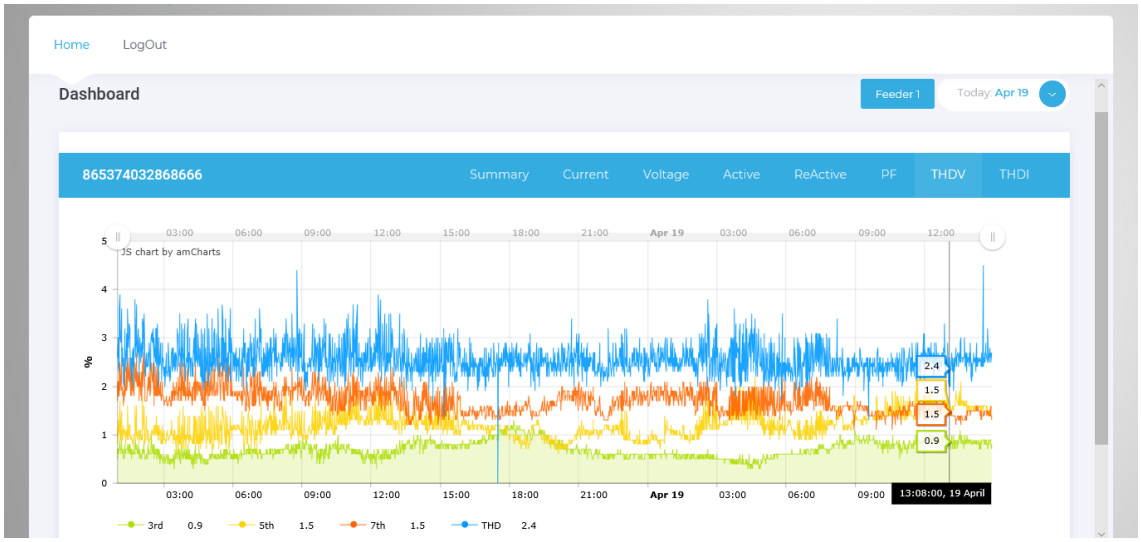

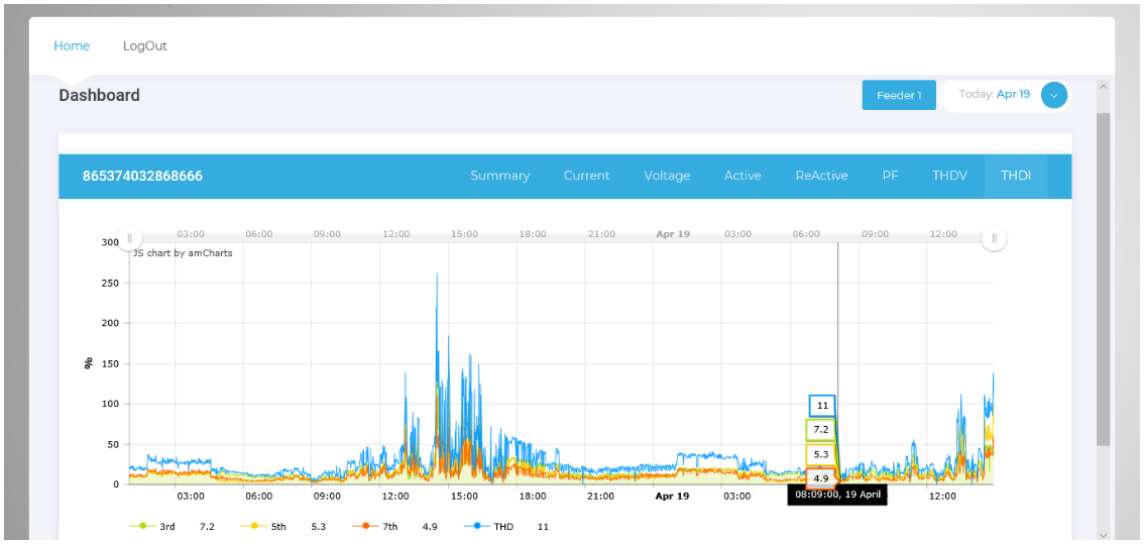


**Figure 12: PQE display of APMU real-time harmonic measurements**

Harmonics are not a new phenomenon and have been an issue on AC power systems since their invention. Harmonics can damage users' and system equipment. They may also interfere with telecommunication. Harmonics cause higher losses through increased currents in the power system. Power System Harmonics are an issue on every major power distribution system and DSOs utilize international standards for their management. The SOGNO PQE service and APMUs facilitate DSO's grid awareness through their measurement, modelling and mitigation strategies. In line with their Grid Code requirements (For instance, in Ireland these are described in [21] and [22]). DSOs need to continuously monitor and be aware of their distribution grids for the presence of power system harmonics.

#### *2.3.2.1.1 Impact of Harmonics in Distribution Grids and use of SOGNO APMUs*

Harmonics are any signal or wave that occurs at a frequency that is an integer multiple of the fundamental 50 Hz sinusoidal voltage waveform. The net effect of these harmonics is that they combine with the voltage (or current) waveform and are superimposed onto it, thereby inflicting a distortion. This means that the smooth sinusoidal aspect of the 50Hz voltage (or current) waveform may be destroyed. The Figure below portrays this additive effect for a single phase and its detrimental impact on the 50Hz voltage (or current) waveform.

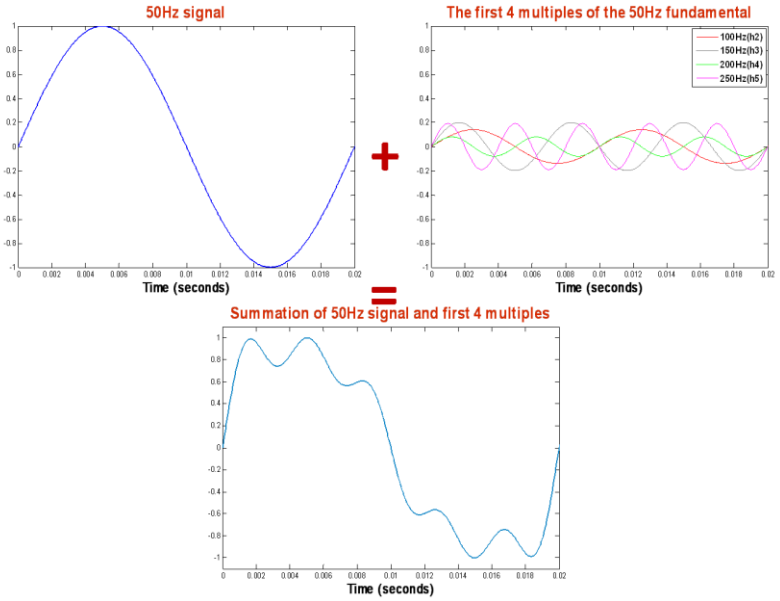


**Figure 13: First 4 voltage harmonics & resulting distortion.**

#### *2.3.2.1.2 Sources of Harmonics*

The principal cause of current harmonics on power distribution systems is non-linear customer loads. A linear load is one which, when applied with a steady-state, single-frequency sinusoidal voltage results in the flow of a purely sinusoidal current of equal frequency and proportional magnitude. Such devices include incandescent lightbulbs and ovens and, as such, historically represented most of the domestic electrical demand on the power system. The current drawn is not directly proportional to the magnitude and/or phase of the voltage for non-linear loads. Therefore, non-linear loads result in the flow of transient or steady-state currents with frequencies other than that of the supplied steady-state, single-frequency sinusoidal voltage. These harmonic currents will interact with the system impedance and cause a harmonic voltage distortion.

Many types of power system devices result in the flow of distorted currents. A few of these are listed as follows:

| **Power Electronics** | **ARC devices** | **Saturated ferromagnets** |
|---|---|---|
| Power converters | Fluorescent lighting | Transformers |
| Variable frequency drives | ARC furnaces | Motors |
| DC motor controllers | Welding machines | Generators |
| Static var Compensators | | |
| Power supplies, UPS and Battery Chargers | | |
| Inverters (as in the PC service described in section 2.2) | | |

**Table 1: Sources of Harmonic injections from customer installations**

Specifically, all power electronic devices, switch-mode power supplies common in household and industrial appliances, and variable frequency drives are non-linear as they utilize current in abrupt short pulses. Plant with ferromagnetic cores such as power transformers, motors and generators may also promote harmonic currents by drawing non-sinusoidal current if they enter their magnetic saturation regimes. Devices that utilize arcing such as furnaces, welders and fluorescent lighting are also known harmonic current sources.

#### *2.3.2.1.3 Harmonic problems an increasing concern in the management of Distribution Grids*

The increasing prevalence of power electronics on power distribution systems is directly contributing to the increased presence of harmonic currents and voltages. The power converters used in wind turbines are of concern, especially where they are in isolated regions of the electrical network. The presence of harmonic currents even within IEC61000 standard limits [23] may not be a problem, but if they are present and the local electrical network has a resonance around that harmonic frequency then a severe harmonic voltage may appear as well. This voltage distortion is experienced by all customers connected to the local electricity network and can have a detrimental impact on the performance and lifetime of connected devices.

Power converters, such as those found in Inverters (see PC service in section 2.2), battery chargers, Uninterrupted Power Supplies (UPS), electronic ballast lighting, and variable frequency drives are intrinsic components of many large-scale demand customers. These may influence harmonic voltages with respect to any harmonic currents produced at each frequency multiple. Although the harmonic injections of most consumer equipment is limited by the IEC61000 standard, some significant customer loads may be in close proximity to other customers or cables which can have undesirable interactions.

The influx of more cables onto the network can intensify the magnitude of the voltage waveform distortion by changing the network impedance. Therefore, cables may amplify any harmonic injections present. It is worth noting that the cables themselves do not introduce harmonics. Instead, they can serve to lower the frequency at which system resonance occurs due to the capacitance distributed along the cable length. Any harmonic current injections occurring at a resonant frequency can invoke a significant harmonic voltage which is undesirable. Cables are also subject to a phenomenon whereby the effective resistance of the conductor increases with frequency. This skin effect can limit the power transfer capability of the cable.

#### *2.3.2.1.4 Consequences of Harmonic distortion*

Harmonic related distortions can result in the failure or mal-operation of customer equipment and power system plant. The existence of harmonic currents imposes an ampacity limit on the magnitude of the customer load that can be served as they needlessly waste some of the current carrying capacity of the conductors. The additional harmonic currents also increase the total system current flowing. This has immediate consequences since higher losses are observed when power is converted to waste heat, due to the product of the conductor resistance and the current squared.

The presence of harmonic currents and voltages results in additional heating of power system plant. Generators, motors and transformers are susceptible to additional heating increased flux losses, which decreases the power capability and their lifetime. These magnetic eddy currents are proportional to frequency so higher harmonic orders imply higher currents flowing, thereby increasing the heating experienced by the plant and possibly shortening its lifespan. A number of harmonics can also place a rotational torque on motors which may require additional power to overcome. Some harmonic orders may also cause current to flow in the neutral wire which requires it to be oversized to avoid excessive heating. This wire provides a low impedance connection that carries current to ground for an item of plant to prevent the manifestation of spurious hazardous voltages.

Capacitors are often utilized on the power distribution system for reactive power support and power factor correction. However, as their reactance is inversely proportional to frequency, they provide a low-impedance path. Conversely, inductive reactance increases with frequency. There exists an impedance-frequency resonance point when the capacitive and inductive reactance is equal in a local network. Any small harmonic current injected at this parallel resonance point will result in large voltage harmonics and associated voltage distortion. The presence of harmonic currents or a potentially excessive voltage at a harmonic resonance point serves to dramatically shorten the life cycle of the capacitor bank.

Telecommunications interference is a much-maligned result of unbalanced audio-frequency harmonics present in the power system. These may couple with neighbouring metallic communication circuits and excite unacceptable noise levels due to the appearance of spurious AC currents and voltages in the telecommunications circuits. Exposure to harmonic distortions between 500Hz and 1200Hz ($10^{th}$ to $24^{th}$ harmonic) are particularly problematic since this is the bandwidth utilized by voice telephony. Fiber networks are impervious to this noise since optical signals do not interact with electrical channels.

Most modern electronic circuits employ a triggering system to convert the AC voltage waveform to a usable DC power source. These rectifier devices often rely on detecting the zero-crossing of the x-axis of the AC voltage to determine the frequency of the system power supply. This timing signal detection may function incorrectly and misfire if the voltage waveform has undergone harmonic distortion since multiple crossings may occur. The potentially high frequencies associated with the distortion pattern can cause end-use consumer equipment to fail.

The following Figure illustrates triggering as the sinusoidal voltage waveform crosses the x-axis, denoted by a red *. In the rightmost figure, the same waveform is subject to harmonic distortion. The zero-crossings are now shown by a green • but they do not necessarily coincide with the original 50Hz firing points and multiple points can occur in a short timeframe. For examples there are 4 such crossings in the 0.009 to 0.011 range, implying a frequency of 750Hz, but none overlap with the desired 50Hz crossing point at 0.01s

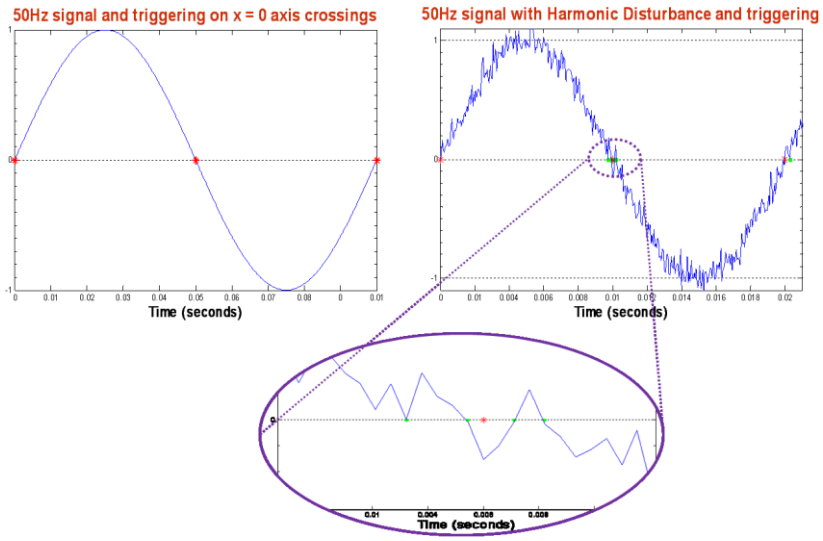


**Figure 14: Impact of harmonics on zero-crossing detection**

#### *2.3.2.1.5 Standards for Harmonics in Distribution Grids and using SOGNO PQE Service to enforce them*

The distortion limits due to harmonics are outlined in IEC/TR3 61000-3-6 [23]. These denote the total cumulative distortion permitted at the Point of Common Coupling for the combined contributions from all associated connections.

In Ireland, both the Grid Code (CC10.13) and Distribution Code (DCC9.5.1) [21] [22] place the onus of responsibility on the end user to ensure that their plant is compliant and does not result in the level of distortion or fluctuation of the supply voltage at their connection point to exceed that allocated to them. Lower voltage limits are specified in the Distribution Code (DCC6.8.3) to ensure compliance with the CENELEC Standard EN 50160 [24].

The SOGNO APMUs and PQE service can provide the DSO with a real-time itemised allocation of spectral emissions for any customer. These allocation details can be then compared to the maximum emissions permitted from a customer's site and must be less than those in the IEC/TR3 61000-3-6 planning standard [23] since (1) other customers at the same location will be allocated a portion of the tolerated range for injections on a fair and appropriate basis and (2) a safety margin is retained for operational prudence and / or future developments.

Normally it is the customer's responsibility to ensure that their facility is standards and Grid Code compliant, and the DSO assists with clarification of the harmonic voltage distortions permitted at their point of connection to the network. Any customer seeking to modify their reactive power characteristic, be it through requesting a cable connection or modifications to their turbine types, internal network, transformers, filters or reactive power support, communicate the updated parameters to the DSO early in the connection-to-the-grid process. This can minimize the customer's risk in the event of a harmonics issue being identified since any mitigation strategy may require a significant lead time to implement. This is beneficial to both parties since the DSO may enhance their model and identify proposed limits at a sufficiently early stage. If a harmonics issue is identified, the customer can be advised of such limits which may aid in their selection process for suitable turbine types and / or necessary filtering prior to any outlay of significant capital resources. In addition to harmonic emission limits, the DSO will also provide impedance loci for the power system at the customer's connection point. Each of these loci is a discrete polygonal envelope which represents a bound on the network impedance for one or more harmonic frequencies. Several impedance loci are typically provided spanning the full range harmonic orders. These loci are formed by plots of reactance (X) vs resistance (R) and reflect the influence of numerous different configurations of the distribution system at those frequencies, including significant outages with a view to accounting for many of the feasible operational regimes. A customer's proposed load may be prevented from connecting to the power system until such time that all appropriate harmonic limitation mechanisms are in place, and the DSO can confirm them using the SOGNO APMUs and PQE service.

The following figure illustrates planning of the Impedance loci for the first harmonic orders (A-G). Each of the scenarios denotes a network configuration that was considered in the analysis covering all aspects of normal system operation from the most onerous Summer Night Valley minimum load case to the Winter Peak maximum demand scenario. The envelope captures the effects of alternate line flows, loadings and dispatches in the interim. The margin accounts for the retained overhead up to the Planning limits in IEC/TR3 61000-3-6 for future development and distribution system safety. The Impedance loci for the harmonic order *E* may be beneficial to describe a spectral region of concern with a single bound in order to accurately specify a filter without it being centred at an inopportune frequency.

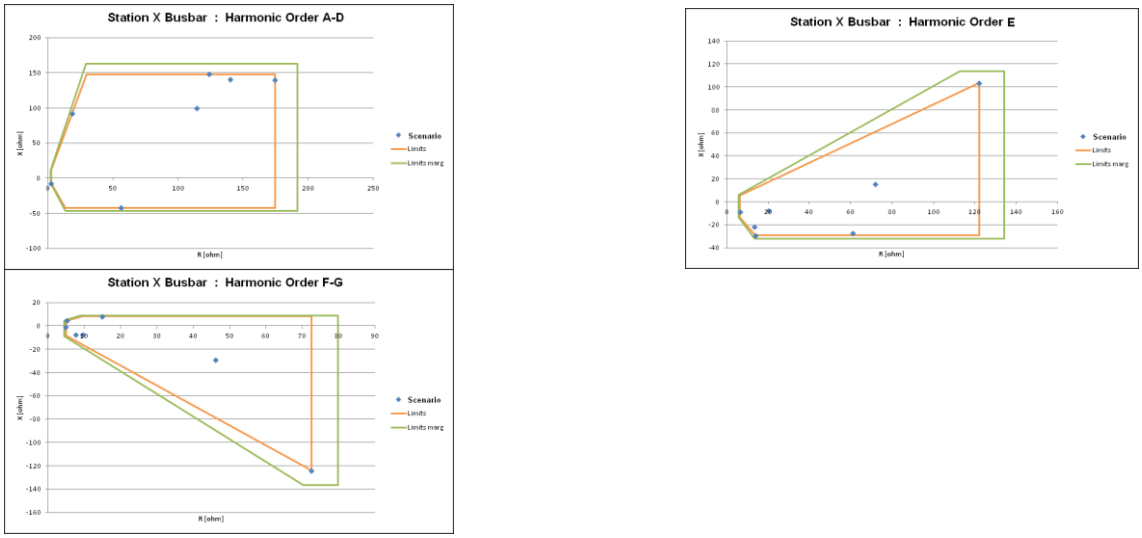


**Figure 15: Impedance loci for harmonic orders (A-G).**

Once the customer has received their allocated limits and impedance loci, they can select appropriate turbines and any required filters to comply with their allotment at each harmonic frequency to ensure that they do not interact detrimentally with neighbouring customers. The DSO can continuously monitor their adherence to their allocated impedance loci using the SOGNO APMUs and PQE service.

#### *2.3.2.1.6 Strategies to use PQE Service to Mitigate Harmonics Problems in Distribution Grids*

There are several strategies for DSOs to mitigate harmonic issues in their distribution grids. However, the selection of a solution from all the prescribed options is non-trivial. This is primarily due to interactions with neighbouring customers increasing the complexity of the analysis and uncertainty over the final connection method to be constructed. For example, if a customer opts to connect via high voltage underground cable, they may introduce an impedance-frequency resonance point in the local network, which will limit the harmonic current injections for all contributing plants. These interactions become increasingly complex as other nearby customers may also select cables as their preferred connection method. Ideally all details of customers' cable connections, internal networks and plant including reactive power devices, should be known to the DSO, but this is not always the case. However, the DSO can use the SOGNO APMUs and PQE service to continuously monitor their grid and help to assess and identify an optimal solution for each "problem" customer's region of influence.

There is no predetermined mitigation proposal or associated order of preference, as each option must be analysed in a case specific context to identify the most cost-effective and enduring solution. It is also important to note that any future connection method modification may require a revision of the solution to be applied. There is a possibility that no single viable approach may be identified, and a combination of the following mitigation strategies will be required (adapted from [25]). The responsibility for each option can reside with the relevant DSO or the customer or both (denoted in parentheses below), depending on the outcome of a cost-benefit analysis.

However, in all cases the DSO can use the SOGNO APMUs and PQE service to continuously monitor and assess if the mitigation strategy is working or needs to be enhanced.

| | |
|---|---|
| **Harmonic Injection limitation (Customer)** | This is the simplest mechanism for controlling the system harmonic distortion. If minimal harmonic currents are injected onto the distribution network, there will be a diminished magnitude for the associated harmonic voltage distortion arising from these currents interacting with the system harmonic impedance. These injection limits will be calculated by the DSO and communicated to the customer after the customer requests analysis to ensure compliance with the IEC-61000-3-6 standard and the Grid or Distribution Codes. This mitigation strategy compliments each of the alternate options as it does not interact with any plant thereby potentially further altering the system impedance. It is worth noting that selecting an alternate turbine type may facilitate compliance with the imposed harmonic limits without requiring any additional measures. |
| **System Reinforcement (DSO)** | This option involves increasing the strength of the power distribution system in the region where the customer(s) is located. Typically, this approach alters the system impedance observed at each harmonic order, effectively allowing any injections that manifest close to a parallel resonance point to be tuned up the frequency spectrum by means of an increased inductance. The reinforcements required to modify the system impedance can involve the commissioning of additional power transformers or construction of new overhead lines. The commissioning of this plant can involve significant lead-times and costs. Furthermore, it is important that the permanent connection methods associated with all influencing plants must be known in advance of selection of this strategy. This is to account for the change in system impedance with the addition of new or expanded customer internal electrical networks and devices or the construction of new power system infrastructure |
| **Isolation transformers (DSO / Customer)** | Some higher frequencies can be attenuated by certain transformer configurations. This is particularly true for triple n harmonics (those that are odd multiples of 3) since any associated zero sequence harmonic currents will flow to ground through the neutral of a wye-delta transformer providing the currents are balanced and in-phase. This solution is not applicable for all harmonic orders as the harmonic currents may not be in-phase with each other and will therefore pass through the transformer. The commissioning of a transformer for this solution may involve a long lead-time and/or incur significant expense depending on whether the transformer is located at a transmission system voltage level or as a step-up or generator transformer on the distribution system or internal customer network. |
| **Passive Filter (DSO / Customer)** | There are numerous configurations associated with this mitigation approach ranging from a simple inductive reactor to dampen the harmonics to complex multi-stage filters tuned to block multiple harmonic frequencies. The fundamental mechanisms of harmonic filtering devices require the inductive and capacitive components to resonate at select frequencies, thereby presenting a virtual short-circuit or low impedance path to ground for any injected harmonic currents at that or nearby harmonic orders. This implies that the harmonic voltage at the filter's resonant frequency will be negligible whilst still maintaining the desired system impedance, and hence voltage, at the fundamental 50Hz frequency. Harmonic filters may equally be utilised to counteract the resonances imposed by uncontrolled capacitances presented by local cables by selectively tuning the resonant points away from harmonic injections as required.<br>Filters may present a cost-effective solution in many cases depending on the number and spectral range of the harmonics to be eradicated, although, they can add an additional level of complexity to the operation of the system. Such filters are designed based upon a specific system impedance and if that impedance changes due to new power system infrastructure the filter may lose effectiveness and permit excessive harmonic emissions onto the power |

| | |
|---|---|
| | distribution grid. As impedance values vary by season due to changes to the generation portfolio dispatched and associated network configurations, passive filters may not be a future-proof solution unless strict design criteria are employed. |
| **Active Filter (DSO / Customer)** | This is a relatively recent development for controlling any harmonic distortion. Active filters are derived from passive versions and offer similar functionality except that they can account for variation of the distribution grid impedance over time. As the reactors and capacitance automatically retunes to attenuate select frequencies, the filter offers a stable solution for any harmonic problem. However, this may be an expensive approach since active filter technology is still very much in its infancy. Further considerations must be given to possible complex interactions between neighbouring active filters as any changes to the impedance initiated by one filter may automatically result in the retuning of another device in the locality, resulting in a circular effect. |
| **Overhead Line (DSO / Customer)** | Underground cables typically exhibit characteristics that result in resonance at low order ($5^{th}$ – $7^{th}$) harmonic injections. Overhead lines do not typically exhibit such resonances. Harmonic injection limits will still apply to applicants connecting via overhead lines to ensure minimal high frequency currents are present at higher order harmonics or if the background harmonic distortion is already significant at a node. |

#### 2.3.2.2 Power Factor and Voltage Regulation

Power factor correction and voltage regulation are closely related. In many cases, the desired voltage regulation is costly to obtain. Larger or paralleled conductors to reduce voltage drop under load are, in many cases, the proper solution (adapted from [26], [27], [28]).

However, power factor correction may also be justified for four reasons:

1. To improve voltage
2. To lower the cost of electric energy, when the electric utility rates vary with the power factor at the metering point
3. To reduce the energy losses in conductors
4. To utilize the full capacity of transformers, switches, overcurrent devices, buses, and conductors for active power only, thereby lowering the capital investment and annual costs

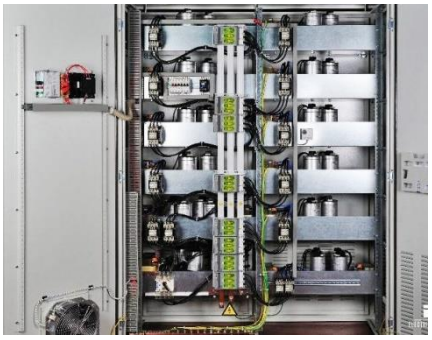

DSOs can use the SOGNO APMUs and PQE service to continuously monitor the power factor and voltage at key points in their distribution grid and assess if their power factor correction and voltage regulation strategies are working or need to be enhanced.

##### *2.3.2.2.1 Voltage Regulation*

The goal of good voltage regulation is to control the voltage of the system so that it will stay within a practical and safe range of voltage tolerances under all design loads. Voltage at any utilization equipment should be within the guaranteed operative range of the equipment.

The type and size of wires or cables, types of raceways, reactances of transformers and cables, selection of motor-starting means, circuit design, power factor correction, and the means and degree of loading all affect voltage regulation.

Voltage regulation in any circuit, expressed in percentage, is:

((No-load Voltage – Full-load Voltage) x 100 ) / (No-load Voltage)

When it is not economical to control voltage drop through conductor sizing, circuit design, or other means, voltage regulators may be needed. Several types of voltage regulators, either automatic or manual, are available for all types and sizes of loads from individual electronic devices to the equipment for an entire laboratory or department store.

Voltage regulators are frequently used by electric utility companies in their distribution system feeders and are seldom needed within commercial buildings, except for use with electronic equipment.

Normally, the power and light distribution system within large commercial buildings can be designed economically and adequately without the use of large voltage regulators.

#### *2.3.2.2.2 Power Factor Correction*

When the type of load to be installed in a commercial building will result in a poor power factor, then the DSO can do continuous evaluation using the SOGNO PQE service to determine if and when installing capacitors is justified, either to stay within the required power factor range in order to avoid penalty payments or to obtain a continued reduction in their electric bill.

As discussed in the last subsection, care should be taken when adding capacitors to ensure that no resonant conditions could exist with the fundamental or harmonic frequencies. This is particularly true if SCR drives are used.

When large machines (like blowers, or refrigeration or air compressors) are to be installed, the DSO can use their APMUs and PQE service to determine whether it would be economical to install a synchronous motor and utilize it for power factor correction. The cost of the synchronous motor with its controller can be compared with the cost of a squirrel-cage motor with its simpler controls plus separate static capacitors.

The SOGNO PQE service can also help with better utilization of electrical machines and reduction of losses:

(a) Generators and transformers are sized according to the apparent power S. At the same active power P, the smaller the reactive power Q to be delivered, the smaller the apparent power. Thus, by improving the power factor of the installation, these machines can be sized for a lower apparent power, but still deliver the same active power.
(b) The power losses of an electric conductor depend on the resistance of the conductor itself and on the square of the current flowing through it. Since, with the same value of transmitted active power, the higher the cosφ, the lower the current, it follows that when the power factor rises, the losses in the conductor on the supply side of the point where the power factor correction has been carried out will decrease.

### 2.3.2.3 Reactive Power and Compensation Solutions

The total power, the so-called apparent power, of a distribution network is composed of active and reactive power as in the following figure:

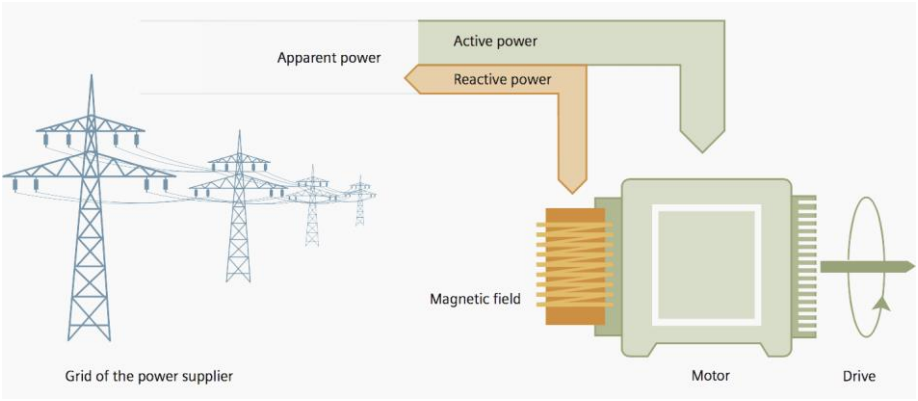


**Figure 16: Composition of the total power of a transmission grid**

While the power consumers connected into the distribution network transform the active power into active energy, the reactive energy pertaining to the reactive power is not consumed. The reactive power at the consumer side is merely used for building up a magnetic field, for example, for operating electric motors, pumps, or transformers (adapted from [29] [30] [31] ).

Reactive power is generated when power is drawn from the supply network and then fed back into the network with a time delay. This way it oscillates between consumer and generator. This constitutes an additional load on the network and requires greater dimensioning in order to take up the oscillating reactive power in addition to the active power made available. As a consequence, for DSOs, less active power can be transported. However, they can use the SOGNO APMUs and PQE service to continuously monitor reactive power and implement compensation strategies at key points in their grid to optimize their active power distribution.

The Reactive Power Compensation strategies can include the use of capacitors for single, group, and central configurations, as follows:

#### 2.3.2.3.1.1 Single compensation

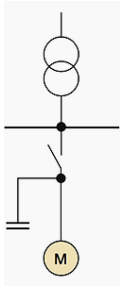


In single compensation, the capacitors are directly connected to the terminals of the individual power consumers and switched on together with them via a common switching device. Here, the capacitor power must be precisely adjusted to the respective consumers. Single compensation is frequently used for induction motors.

Single compensation is economically favorable for:

- Large individual power consumers
- Constant power demand
- Long ON times

However, as load is taken off the feeder lines to the power consumers, a continuous adjustment of the capacitor power to its reactive power demand is not possible.

#### 2.3.2.3.1.2 Group compensation

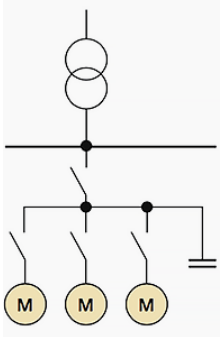


With group compensation, each compensation device is assigned to a consumer group. Such a consumer group may consist of motors or discharge lamps, for example, which are connected into supply together through a contactor or switch.

Group compensation has the same advantages and disadvantages as single compensation.

#### 2.3.2.3.1.3 Central compensation

Reactive power control units are used for central compensation, which are directly assigned to a switchgear unit, distribution board, or sub-distribution board and centrally installed there. Control units contain switchable capacitor branch circuits and a controller which acquires the reactive power present at the feed-in location. If it deviates from the set-point, the controller switches the capacitors on or off step by step via contactors.

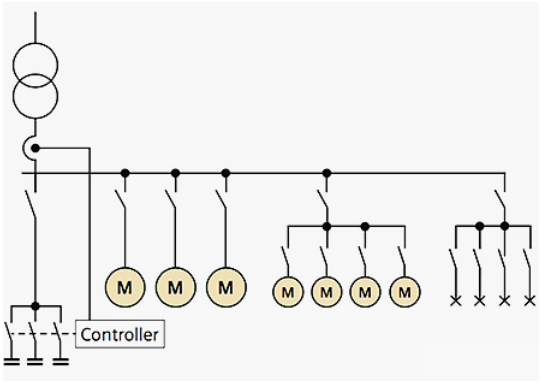


The capacitor power is chosen in such a way that the entire installation reaches the desired cos φ, and can be continuously monitored by the SOGNO APMUs and PQE service.

Central compensation is recommended in case of:

- Many small power consumers connected into supply
- Different power demands and varying ON times of the power consumers

# 3. Validation and KPI of system awareness services

The validation of the state estimation and the power control service will be based on simulations. The validation of the power quality service was done in laboratories as the service itself requires real data to test the service. Hence, the service validation is not directly connected to trial sites of WP5. However, the analysis of the field trial results in WP5 should further validate these results. Each validation cycle aims to yield KPI of the respective services in order to evaluate the performance. This way it is ensured that the individual services work properly.

## 3.1 State estimation

The validation of the state estimation service is carried based on the scheme in Figure 17. It takes into account both SE algorithms described in section 2.1 and deliverable D2.2.

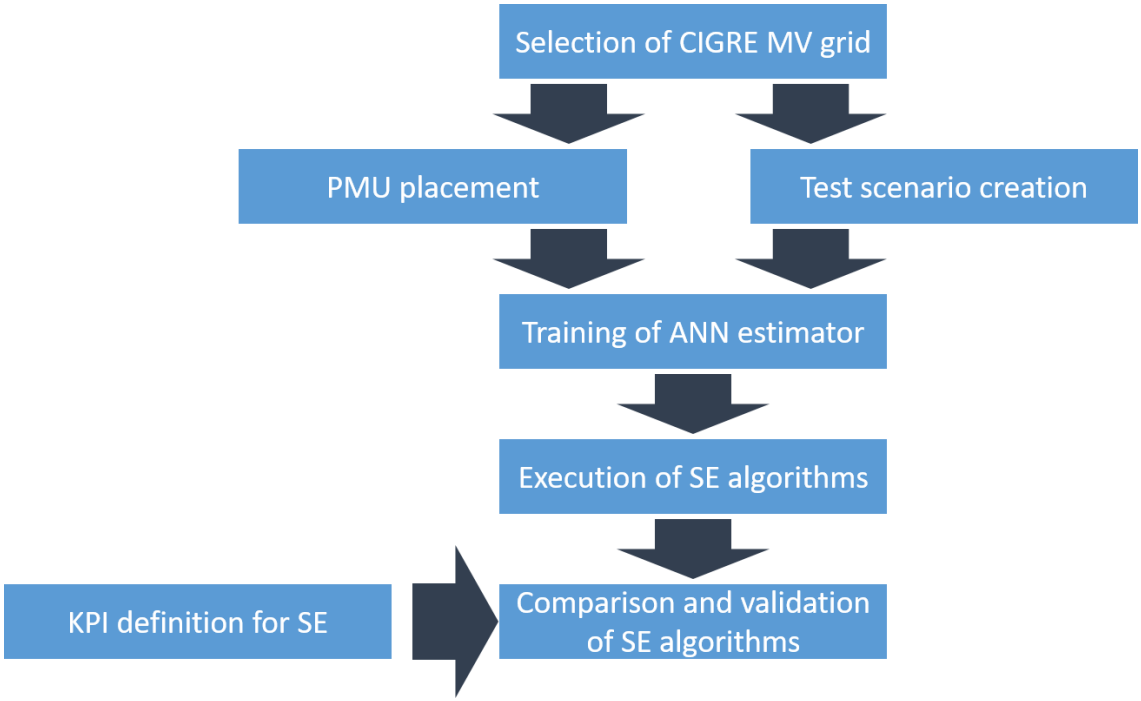


**Figure 17: State estimation validation process.**

### 3.1.1 Test grid and PMU placement

The test grid is the European MV standard network provided by the Conseil International des Grands Réseaux Électriques (CIGRE) [32]. It is chosen as it describes a widely accepted standard grid with the essential characteristics of current distribution grids in Europe. The grid is divided in three areas. Only one area of the grid, presented in Figure 18 is exploited for evaluation of state estimation performance. The topology, line parameters and power injection are presented, respectively, in Annex A2 (Table A-6,

Table A-7 and

Table A-8). The network is three phase. Considering that the line parameters and the power injections are balanced, the results are presented only for voltages estimated at phase A, considering that the same result is valid for phases B and C. The lines are built with the same type of cable, which has resistance per kilometer equal to $0.6033\ \frac{\Omega}{km}$, reactance per kilometer

equal to $1.01\ \frac{\Omega}{km}$ and susceptance per kilometer equal to $47.493 \cdot 10^{-6}\ \frac{S}{km}$. The conductance is approximated as null. Thus,

Table A-7 contains only the length of the cables for each line. The Artificial Neural Network (ANN) estimator utilizes the aforementioned data in Common Information Model (CIM) format.

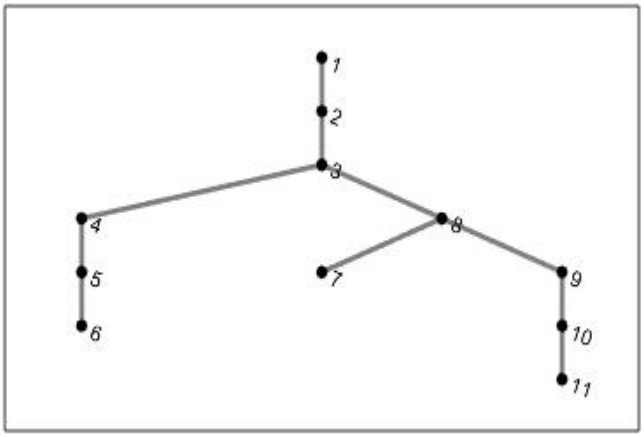


**Figure 18: Topology of portion of CIGRE Network exploited for evaluation of state estimation performance**

It is considered that measurements of voltage magnitude are provided at nodes 1, 7, 8, 10 and 11. Current magnitude measurements are provided at branches 1, 7, 9 and 10. These measurements are assumed to have a maximum error equal to 0.5%. The error is assumed to have Gaussian distribution with null average value, and standard deviation equal to one third of the maximum error.

### 3.1.2 Training phase of ANN estimator

The ANN estimator is trained by generating a large number of power flow scenarios. 2250 scenarios are generated by means of GridLabD software[2]. In each scenario, apparent power injections are extracted considering a Gaussian probability distribution with average value equal to the reference apparent power, presented in

Table A-8, and relative standard deviation equal to $\frac{100\%.}{3}$. The power factor is fixed and equal to the nominal power factor. In this way, 99.7 % of the extracted active and reactive power injections are included between 0% and 200% of the nominal active and reactive powers. The other cases are discarded.

The measurement values, corresponding to voltage magnitudes and nodes 1, 7, 8, 10 and 11 and current magnitudes at branches 1, 7, 9 and 10, are extracted for each scenario and corrupted with an error with null average value and a relative standard deviation equal to $\frac{0.5\%.}{3}$. The corrupted measurement value constitute the training set of the ANN estimator. The reference values are the voltage phasors at each node, in each of the 2250 power flow scenarios.

[2]Available online at: https://www.gridlabd.org/

### 3.1.3 Testing phase of ANN estimator

Once the state estimator has been trained, it can be exploited for testing purposes. With GridLabD software, 750 scenarios are generated. The power injection and the random errors are extracted with the same methodology presented in the training phase. The true value of voltage phasors are stored for derivation of mean, standard deviation and Root Means Square (RMS) of state estimation error. Such metrics are calculated to evaluate the performance of the state estimator.

### 3.1.4 WLS estimator as reference case

The classical state estimator, applied in power system, is based on the Weighted Least Square (WLS) approach [1]. Such estimator is exploited as reference for evaluation of the performance of the ANN estimator. Considering that power injection and power flow measurements are normally exploited, it is necessary to implement the non-linear version of the WLS [1]. However, given that the non-linearity are limited by the proximity of the voltage magnitude to the nominal voltage, as well as the proximity of voltage phase angle to 0 crad, it is possible to exploit the formulas for propagation of uncertainty to know the expected uncertainty. The reliability of such approach has been demonstrated in literature [33].

For the purpose of comparison, the WLS estimator exploits the same set of measurements provided by the ANN estimator. Therefore, voltage magnitudes measurements are considered at nodes 1, 7, 8, 10 and 11 and current magnitudes measurements are considered at branches 1, 7, 9 and 10. Measurement errors are expected to have null average value and a relative standard deviation equal to $\frac{0.5\%.}{3}$.

Furthermore, to have a proper comparison with the ANN estimator, the information provided in the training phase of the ANN estimator, in terms of expected range of variability of power injection and voltage at the slack bus is to be provided to the WLS estimator. With regards to power injection, in order to replicate the same knowledge of the ANN estimator, pseudo measurements [34], with relative maximum error equal to 100% and Gaussian distribution, are considered. With regards to voltage at the slack bus, a measurement value with expected average value and standard deviation similar to the one observed in the training phase is included as additional measurements.

### 3.1.5 Results of ANN estimator

The ANN estimator provides estimation of the values that are not directly measured. Therefore it provides the voltage magnitude of nodes 2, 3, 4, 5, 6 and 9. Voltage phase angle is not directly measured, so it is provided for all the nodes of the grid. For the sake of simplicity, the results of voltage phase angle error are presented only for nodes 2, 3, 4, 5, 6 and 9. In Figure 19: Histogram of error of voltage estimation at node 2. (a) histogram of voltage magnitude error. (b) histogram of voltage phase angle error

and Figure 20 the probability distributions of voltage phasors estimation at node 2 and 3 are presented. It can be observed that the probability distributions of the errors are not exactly Gaussian. Nevertheless, they are statistically quantified by means of standard deviation and average values in Table 2.

It is possible to observe that voltage magnitude relative standard deviation is in the range of 0.1 %, while voltage phase angle standard deviation is in the range of 1.5 crad. A certain amount of average error is also present. It is in the order of 0.03% for voltage magnitude and 0.25 crad for the voltage phase angle. Considering that both errors of voltage magnitude and phase angle have

a bias and a random components, the Root Means Square Error (RMSE) is used as metric to aggregate them, in Table 3.

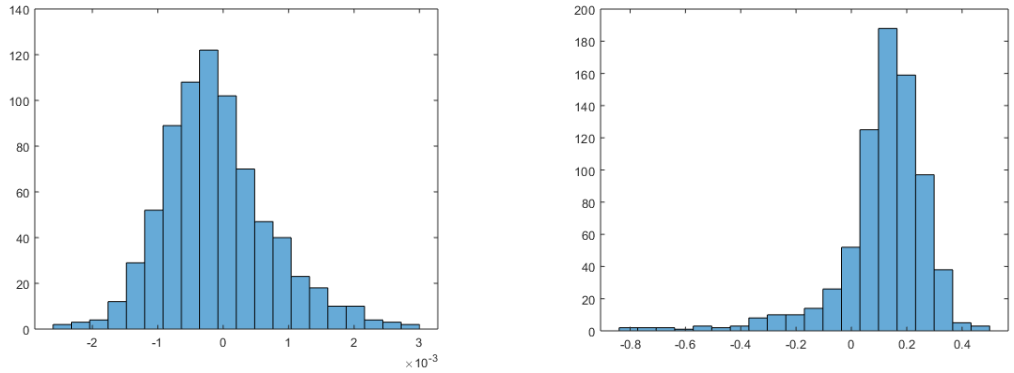


(a) (b)

**Figure 19: Histogram of error of voltage estimation at node 2. (a) histogram of voltage magnitude error. (b) histogram of voltage phase angle error**

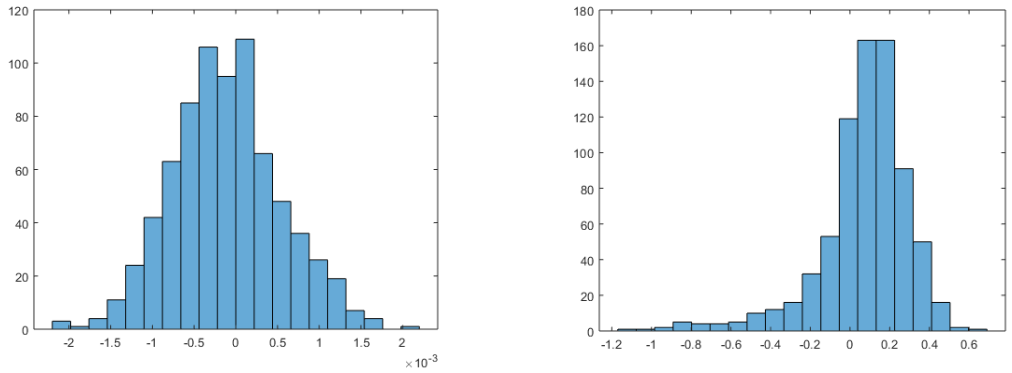


(a) (b)

**Figure 20: Histogram of error of voltage estimation at node 3. (a) histogram of voltage magnitude error. (b) histogram of voltage phase angle error**

**Table 2: Standard deviation and mean value of estimation error of ANN estimator**

| **Node** | **2** | **3** | **4** | **5** | **6** | **9** |
|---|---|---|---|---|---|---|
| Relative standard deviation of error of voltage magnitude [%] | 0,083 | 0,067 | 0,07 | 0,067 | 0,052 | 0,104 |
| Standard deviation of error of voltage phase angle [crad] | 16,481 | 23,154 | 23,172 | 19,823 | 23,892 | 22,73 |
| Relative mean error of voltage magnitude [%] | -0,01 | -0,011 | 0,075 | -0,001 | 0,255 | 0,203 |
| Relative mean error of voltage phase angle [crad] | 11,479 | 7,025 | 6,842 | 6,367 | 15,483 | 7,943 |

**Table 3: RMSE of ANN estimator**

| Node | 2 | 3 | 4 | 5 | 6 | 9 |
|---|---|---|---|---|---|---|
| Relative RMSE of voltage magnitude [%] | 0,084 | 0,068 | 0,102 | 0,067 | 0,260 | 0,228 |
| RMSE of voltage phase angle [crad] | 20,076 | 24,182 | 24,146 | 20,808 | 28,457 | 24,063 |

### 3.1.6 Results of WLS estimator

In this section the performance of the reference WLS estimator is evaluated. WLS estimators in presence of input Gaussian distributed measurement error provide a Gaussian distributed state estimation error [WLS]. Similarly, if the input measurement error has null average, also the state estimation error has null average [WLS]. Consequently, it is sufficient to use the standard deviation to represent the statistical distribution of the WLS state estimation error, in Table 4. By comparing Table 4 with Table 3, valid for the ANN case, we can observe that the voltage magnitude state estimation error is in the same range. The WLS provides slightly better voltage magnitude accuracies in all nodes. Considering that no information on phase angle were provided, both ANN and WLS present large phase angle uncertainties. The WLS provides slightly better results in all nodes.

**Table 4: Standard deviation of estimation error of WLS estimator**

| Node | 2 | 3 | 4 | 5 | 6 | 9 |
|---|---|---|---|---|---|---|
| Relative standard deviation of error of voltage magnitude [%] | 0.076 | 0.078 | 0.079 | 0.079 | 0.081 | 0.080 |
| Standard deviation of error of voltage phase angle [crad] | 8.759 | 8.800 | 8.803 | 8.805 | 8.808 | 8.808 |

## 3.2 Power Control

The power control service is to be validated for a scenario tailored to the future orientation of the service. The newly developed coordinated reactive power control is to be compared against the state of the art reactive power droop curve (see section 2.2 for details). This leads to a schematic validation process of the power control service as shown in Figure 21.

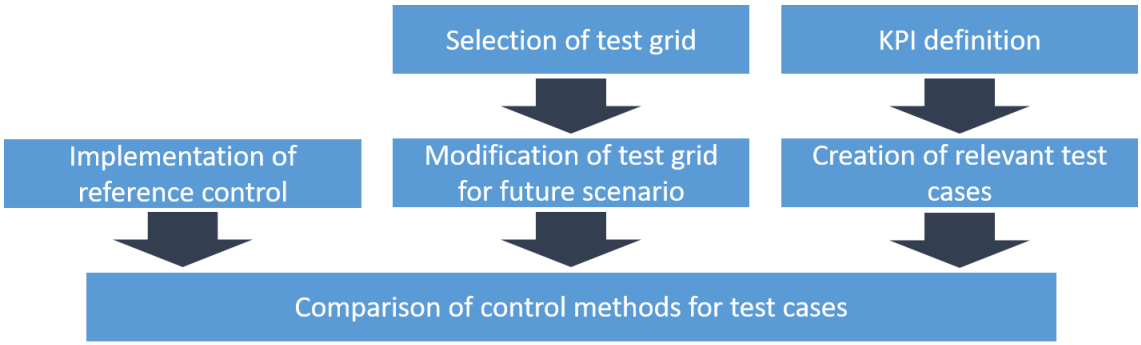


**Figure 21: Power control validation process**

At first a suitable test grid is picked and then slightly modified to encompass a high share of renewables in order to represent a meaningful scenario. In parallel the reference reactive power control is implemented. An active power curtailment is added that complies with the German standard [6] and can be used to complement each reactive power control method. Based on the identification and definition of suitable key performance indicators, the relevant test cases are created. The execution of all them serves for the comparison of the methods and hence, enables the evaluation.

### 3.2.1 Selection and modification of test grid

Figure 22 shows the selected grid that is a slightly modified grid of the Bornholm grid in [35]. It is a small radial grid representing a residential area in Bornholm that can be used to study the impact of an increasing share of renewables on LV grids. It contains 22 LV buses with a total of 52 residential customers.

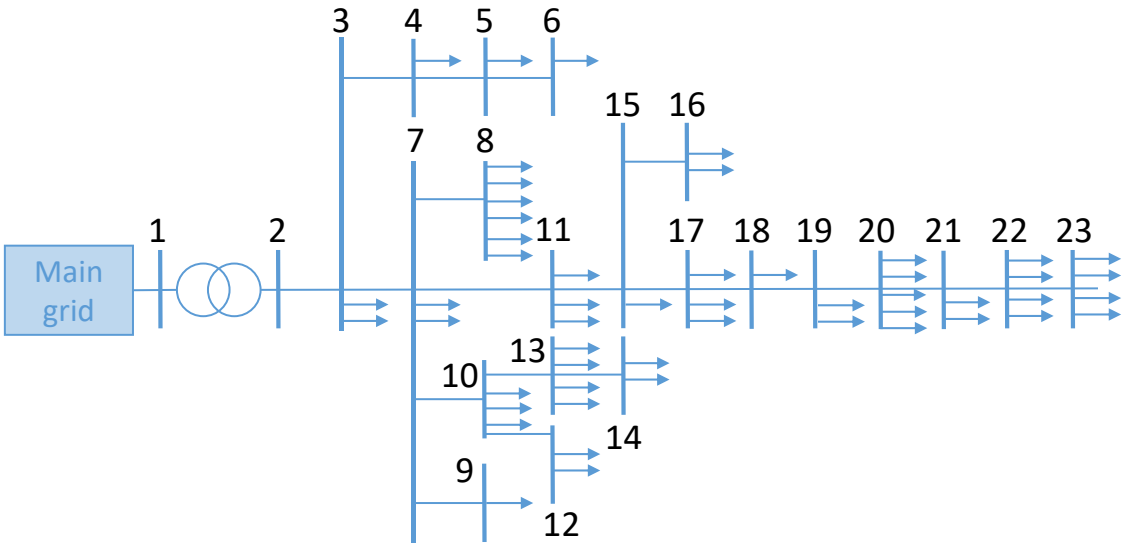


**Figure 22: Bornholm LV test grid**

All of the customers in the grid are residential households. Therefore, each load is modelled with a nominal value of 4 kW that is equal to the typical value for residential households. Each customer receives an individual daily load profile. Since the loads at each bus are assumed to be directly connected to this bus, the loads at each bus are lumped together in all following analysis.

We define the PV penetration as the total installed PV capacity divided by the maximum aggregated load. According to [35] we use a PV plant with a fixed size of 5.2 kWp as the reference PV plant size in the Bornholm grid. According to section 2.2 the cosφ is 0.95 for a symmetrical connection of such a PV plant. The daily generation profile is calculated with a previously developed PV profile generator [36]. In order to represent a future scenario for this service, it is assumed that every household installs one standard PV plant which results in a PV penetration of 130%. Higher and lower penetration rates can be achieved by the connection and disconnection of these standard PV plants. In general, the critical hours in an LV grid with a high share of renewables occur in summer during the day as the highest irradiation leads to the maximum active power infeed by PV. Thus, the simulations are carried for a random day.

### 3.2.2 Implementation of reference control

The reactive power control is based on the reactive droop curve in VDE AR-N-4105 [6] in Figure 5. The terminal voltage input to the control may fluctuate fast due to changes in the loads. To

avoid the consequence of oscillatory control behavior, the input voltage is filtered with an added moving average filter of 10 min to handle fast fluctuations of the voltage. The filtered voltage is processed according to the droop curve. The maximum available reactive power is set to 1.71 kVar in order to reach the cosφ of 0.95 at nominal power.

$$Q_{max/min} = \pm \tan \varphi \times P_{nom} \quad (13)$$

The resulting reactive power set point is assumed to be applied instantaneously by the converter of the PV plant.

As explained in section 2.2 the DSO has the possibility to remotely activate power curtailment of the PV plants within the grid when the grid stability is endangered. This case is considered whenever a nominal voltage of 1.05 pu is exceeded. In this case the active power set points of the PV plant are lowered from 100% nominal power to 60% and respectively 30% and 0% if it is necessary in order to reduce the voltage level to less than 1.05 pu. As the change between these discrete steps may result in oscillatory behavior, the same moving average of 10 min is applied. A change in the active power set point of the PV plant is assumed to have immediate effect.

### 3.2.3 KPI definition and creation of test cases

One of the major issues that is caused by a high penetration of renewables in the distribution grid is the violation of the voltage limits along the feeder. The adjustment of reactive power infeed may be used to compensate a voltage rise caused by renewables. Thus, one performance indicator is the voltage profile at the individual nodes when the respective control scheme is activated. Other simpler metrics like the percentage of customers seeing a non-compliant voltage or the accumulated time of can be derived based on the voltage profiles.

Whenever the reactive power control does not succeed to keep the voltage within the limits, active power curtailment is the last measure to enforce the limits. During the critical time steps that require the curtailment of active power available energy is inevitably lost. So another key performance indicator of the control scheme is the resulting curtailed energy which is a major economic concern. Some national regulations prescribe that curtailed energy of renewables must still be monetarized and hence, causes higher electricity prices.

In order to explore these indicators for the classic droop based reactive power control and the coordinated reactive power control, several cases are considered for the test scenario:

- Case 1: Reference case with local reactive power droop curves and no active power curtailment
- Case 2: Local reactive power droop curves and step-wise uniform active power curtailment
- Case 3: Local reactive power droop curves and step-wise individual active power curtailment
- Case 4: Coordinated reactive power control without active power curtailment
- Case 5: Coordinated reactive power control and step-wise individual active power curtailment

Case 1 depicts the reference case with the local reactive power droop curves. It does not consider active power curtailment so the resulting voltage profile shows the direct impact of the reactive power control. Case 2 and 3 consider the local control with active power curtailment. In case 2 the DSO does only have the information that somewhere in the grid occurs an overvoltage and consequently, he uses active power curtailment as a measure. Typically active power curtailment will be forced upon all PV plants in a region uniformly, i.e. if any voltage violation is known then all PV plants will curtail active power. However, when the DSO is assumed to have detailed information about the voltages in the grid, an individual active power curtailment is possible at buses with overvoltages is possible. Only the PV plants at buses with voltage violations retrieve the curtailment signal. This is treated in case 3.

Case 4 and 5 contain the coordinated reactive power control with or without active power curtailment. A uniform active power curtailment is not considered because a coordinated control

requires the individual terminal voltages anyway. Thus, the availability of a coordinated control implies the availability of active power curtailment for individual PV plants. A potential case 6 with coordinated active and reactive power control is not considered because current regulations for small renewable installations do not enforce the possibility to freely adjust the active power infeed. This case would be of vital interest if battery storages are assumed to be in place.

### 3.2.4 Test case results

**Case 1:** Reference case with local reactive power droop curves and no active power curtailment

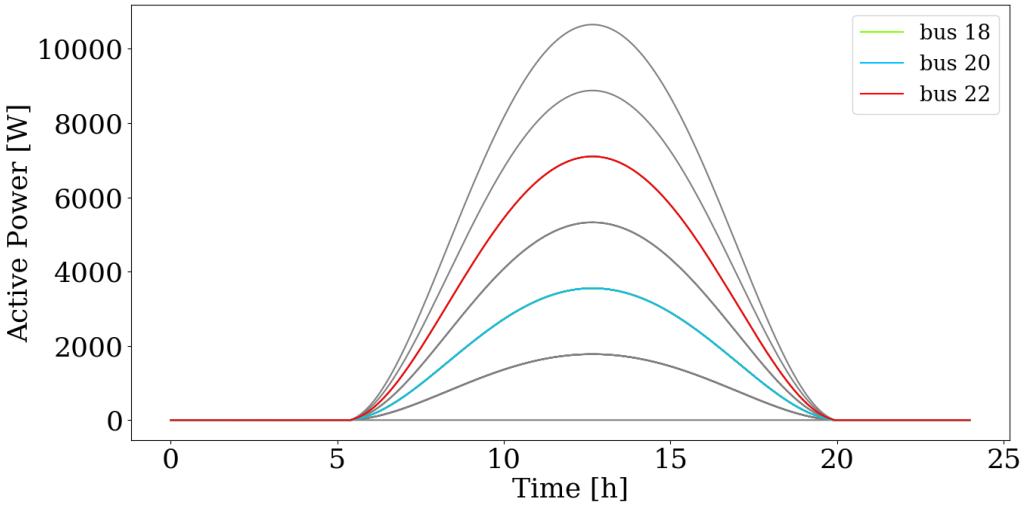


**Figure 23: Injected active power without active power curtailment**

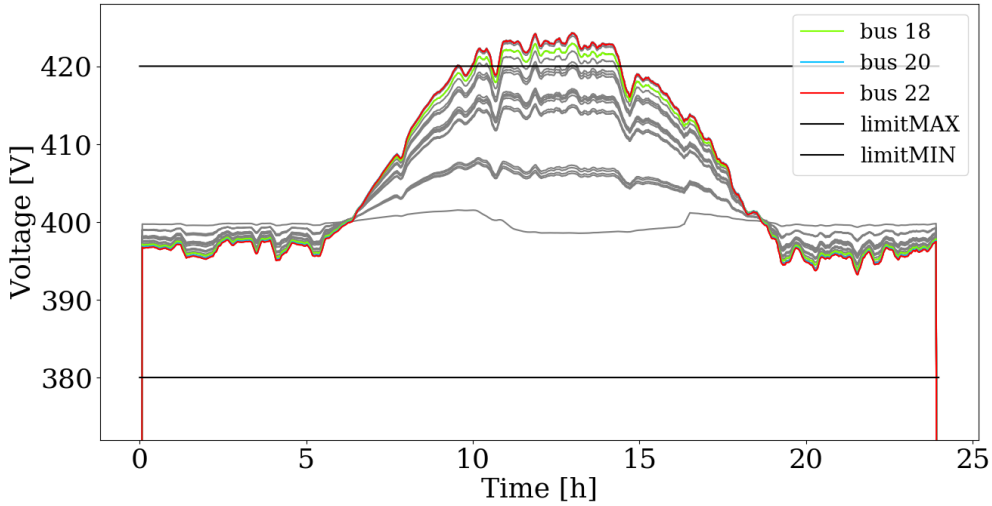


**Figure 24: Voltage magnitudes for droop curve control without active power curtailment**

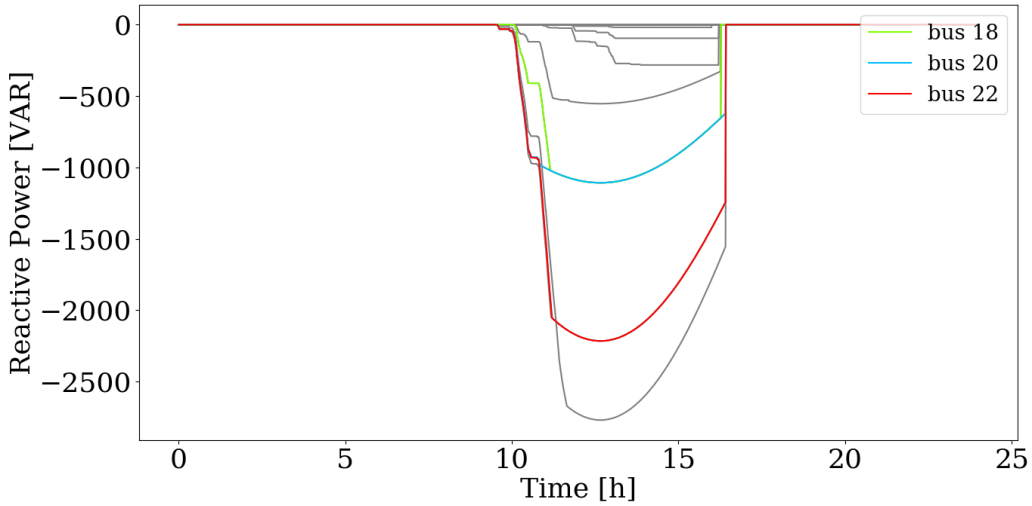


**Figure 25: Injected reactive power for droop curve control without active power curtailment**

The injected active power equals the available power of the PV plants because no active power curtailment is applied. Thus, the injected active power follows the ideal curve of the solar irradiation of a summer day. The only difference is the scaling because all PV plants at each bus are aggregated in analogy to the loads.

The voltage raises due to the high active power infeed and reaches the threshold of 1.05 pu at several buses at the end of the feeder during noon time. The PV plants at the buses with a voltage above the deadband value of 1.03 pu absorb reactive power in order to mitigate the voltage rise. However, this is not enough to compensate voltage rise at 3 buses that remain outside the voltage limit.

**Case 2:** Local reactive power droop curves and step-wise uniform active power curtailment

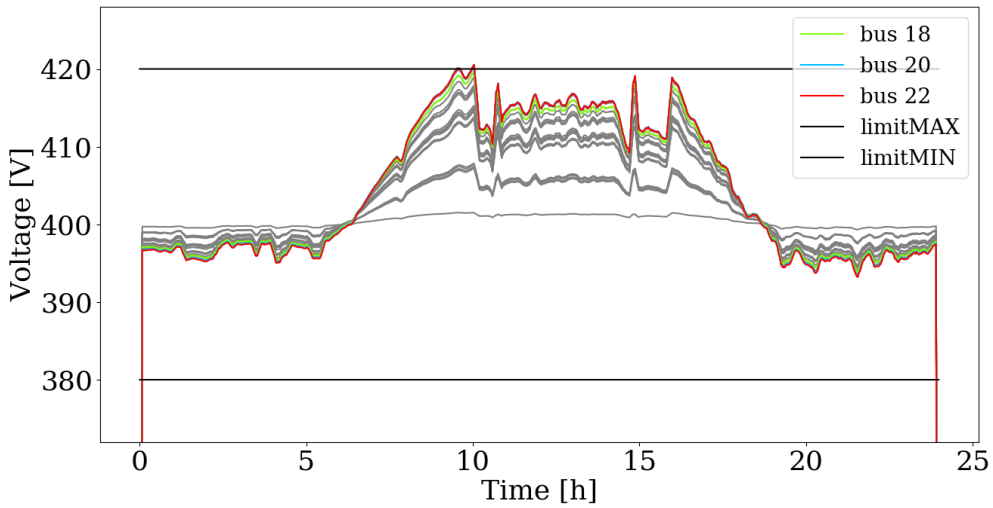


**Figure 26: Voltage magnitudes for droop curve control with step-wise uniform active power curtailment**

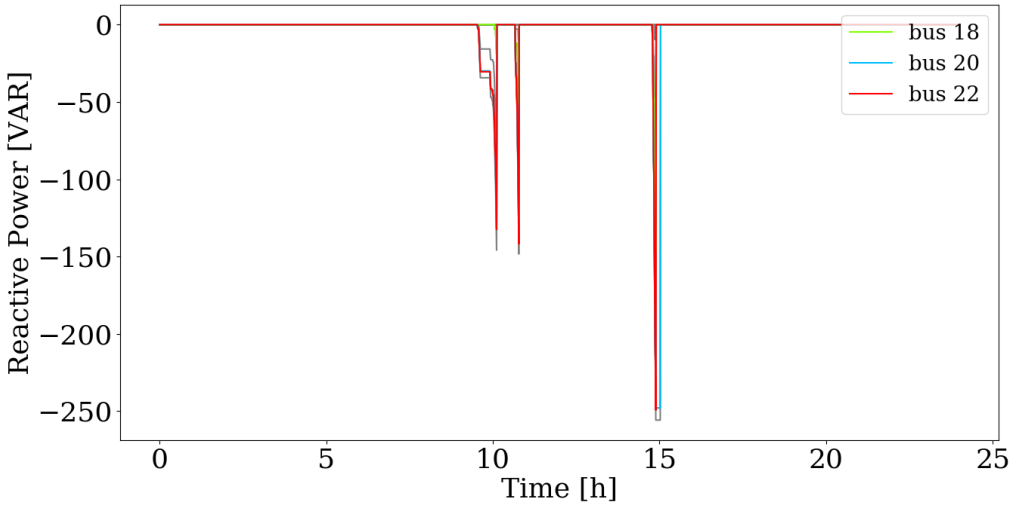


**Figure 27: Injected reactive power for droop curve control with step-wise uniform active power curtailment**

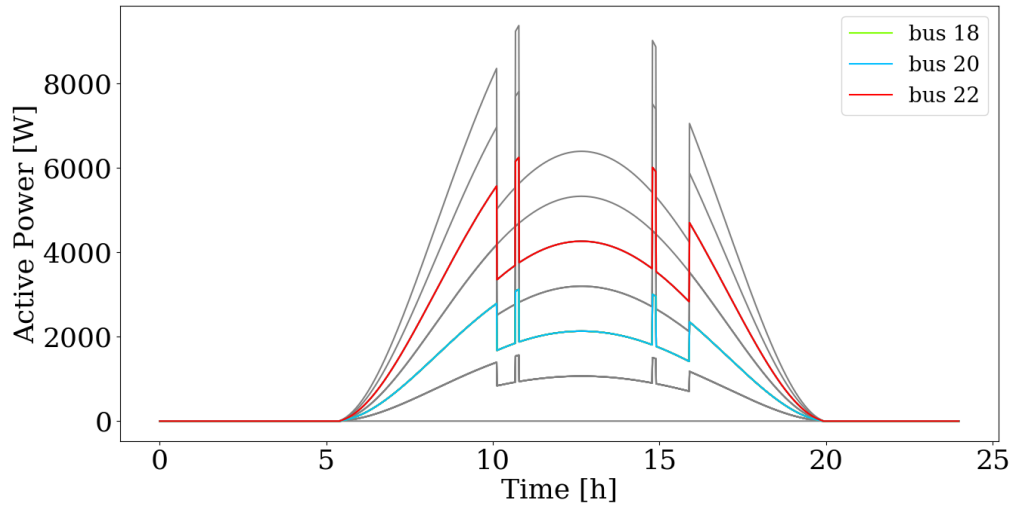


**Figure 28: Injected active power for droop curve control with step-wise uniform active power curtailment**

The implementation of the active power curtailment results in a significant improvement of the voltage profile. Whenever a single bus with installed PV leaves the voltage limit, active power curtailment is imposed on all nodes. This resembles the situation that the DSO knows only that an overvoltage occurs in the grid but not where. Due to the massive curtailment that is imposed in the grid, a complementary reactive power compensation is almost not required anymore as the voltage drop due to curtailment in the whole grid is very high.

**Case 3:** Local reactive power droop curves and step-wise individual active power curtailment

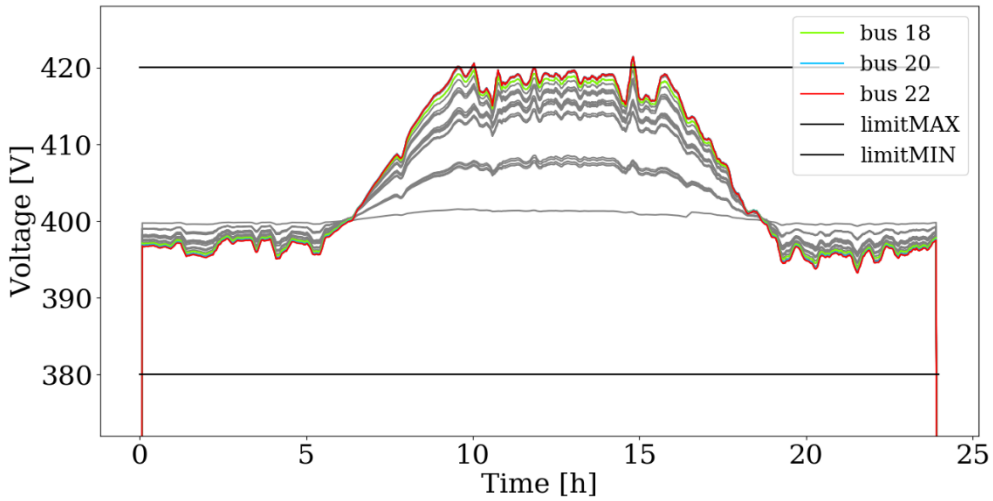


**Figure 29: Voltage magnitudes for droop curve control with step-wise individualized active power curtailment**

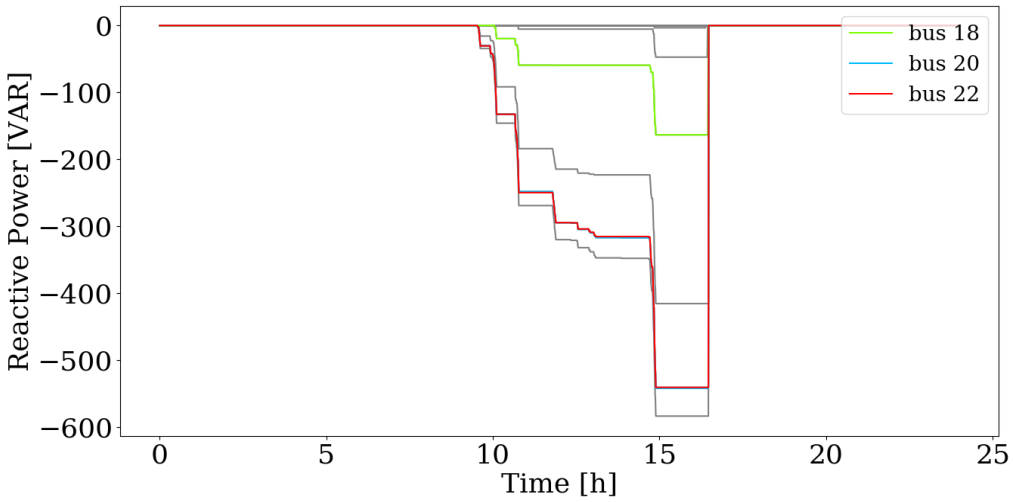


**Figure 30: Injected reactive power for droop curve control with step-wise individualized active power curtailment**

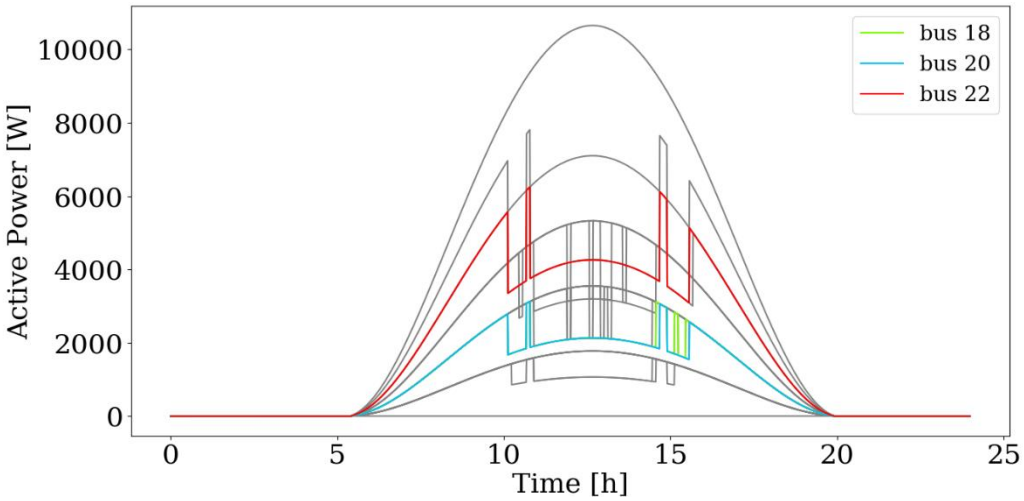


**Figure 31: Injected active power for droop curve control with step-wise individualized active power curtailment**

The results with the individual active power curtailment show the same improvement at the critical time steps as in case 2. At the same time the PV plants close to the feeder are curtailed less often because the threshold for the active power curtailment is activated less often. The reactive power compensation is decreased in comparison to case 1 because of the significant curtailment of 40% active power when the curtailment is activated.

**Case 4:** Coordinated reactive power control without active power curtailment

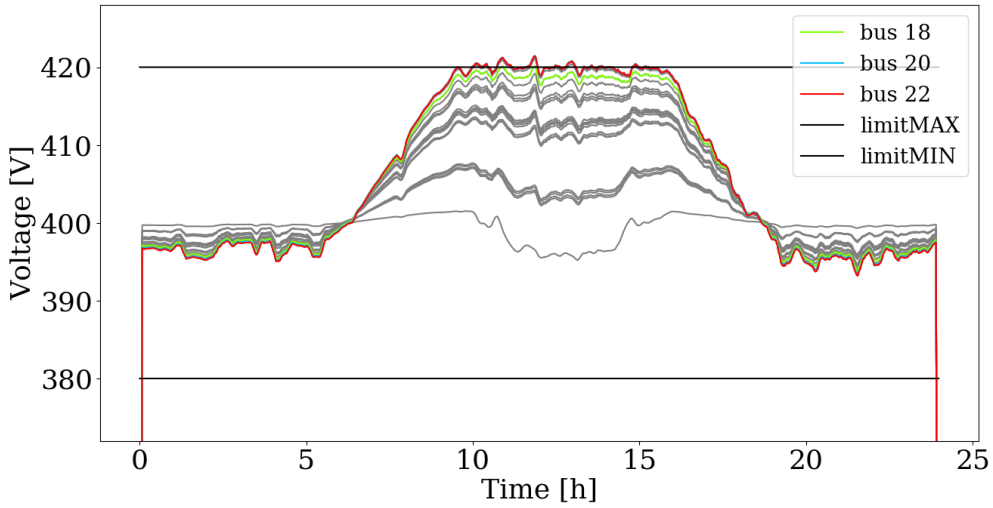


**Figure 32: Voltage magnitudes for coordinated reactive power control without active power curtailment**

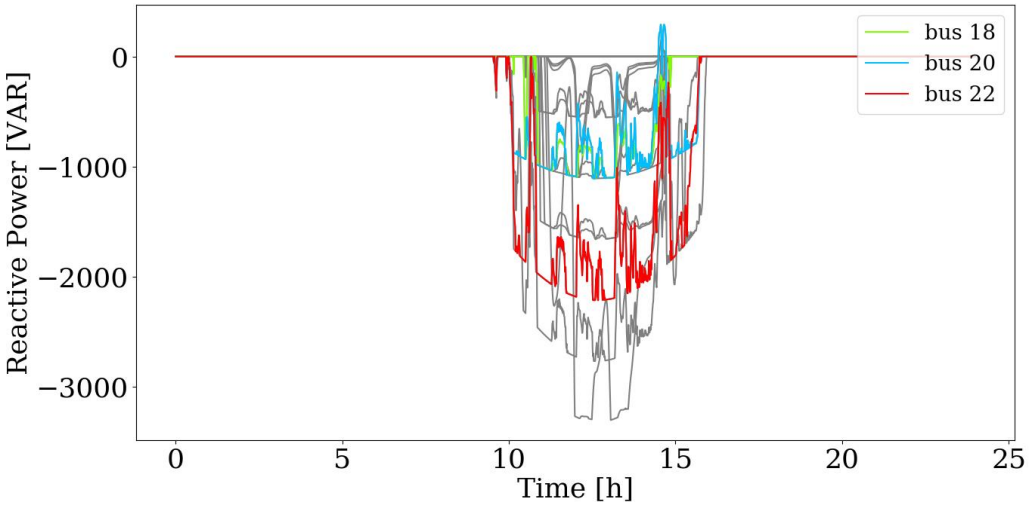


**Figure 33: Injected reactive power for coordinated reactive power control without active power curtailment**

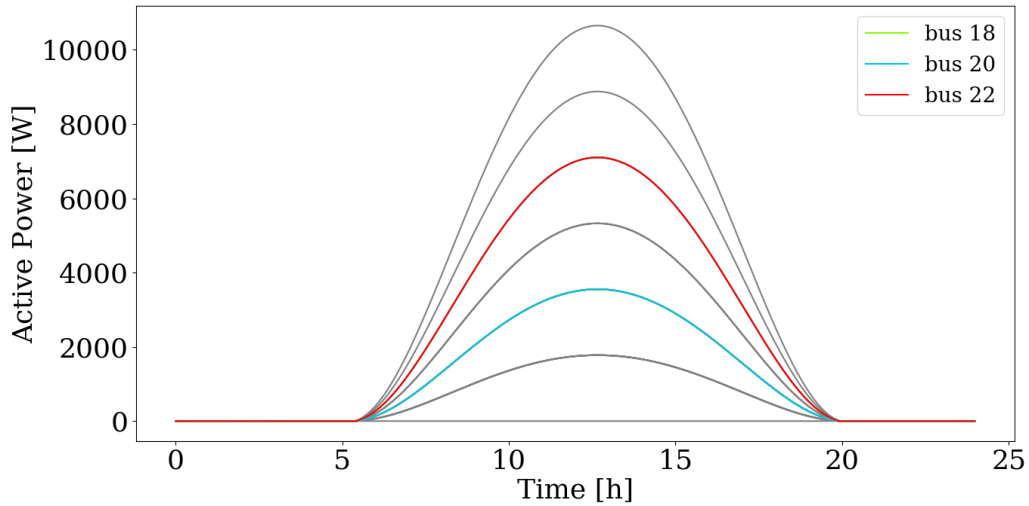


**Figure 34: Injected active power for coordinated reactive power control without active power curtailment**

The coordinated reactive power control shows a significant improvement in comparison to the local control in case 1. The voltage stays close to the permissible limit and violates the limit only for short durations. The reason can be seen in the reactive power infeed that is used for more PV plants than in case 1. The coordinated control approach does not contain a dead band for the reactive power control of an individual PV plant so PV plants close to the feeder contribute reactive power if the voltage at the end of the feeder raises significantly. Hence, the sharing of the reactive power contributions works as intended for the coordinated control.

**Case 5:** Coordinated reactive power control and step-wise individual active power curtailment

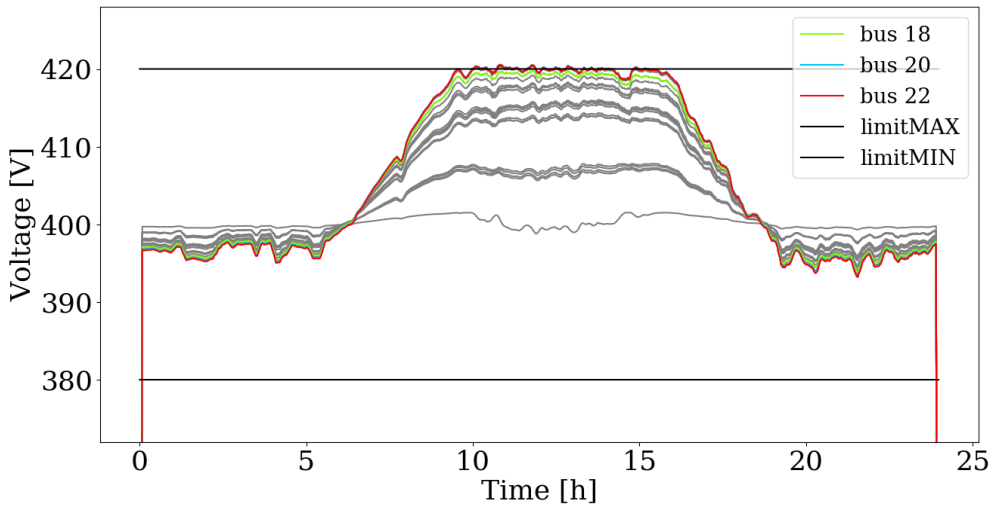


**Figure 35: Voltage magnitudes for coordinated reactive power control with step-wise individualized active power curtailment**

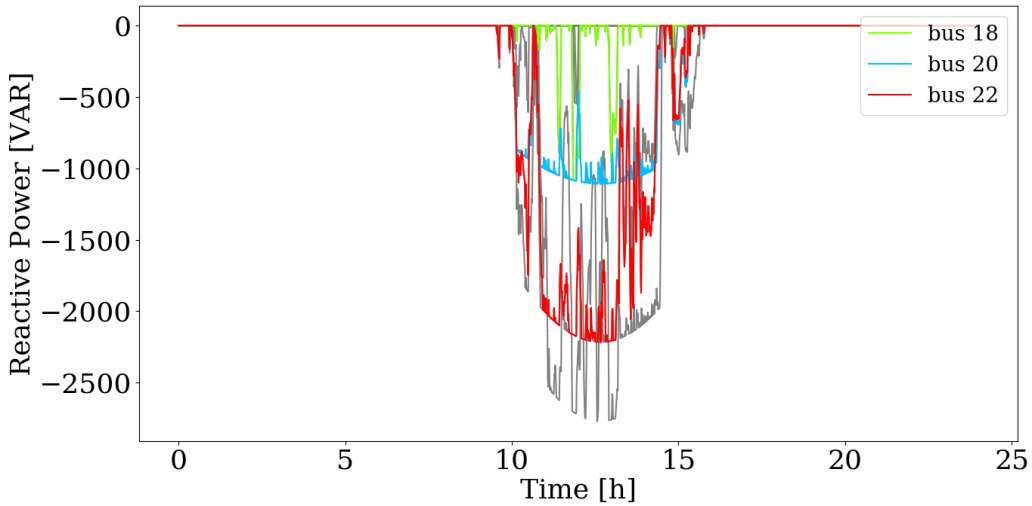


**Figure 36: Injected reactive power for coordinated reactive power control with step-wise individualized active power curtailment**

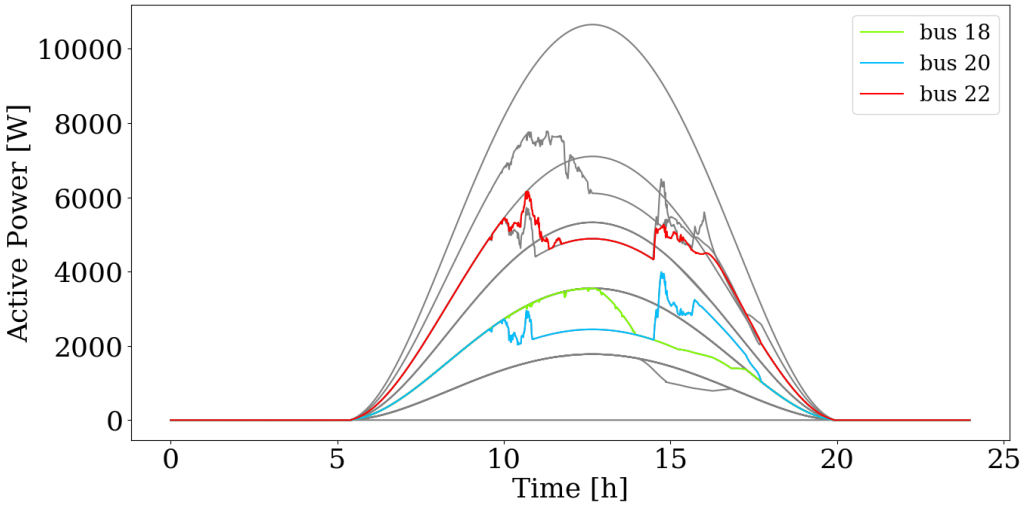


**Figure 37: Injected active power for coordinated reactive power control with step-wise individualized active power curtailment**

The integration of the option to curtail active power into the coordinated control improves the voltage profile compared to case 4. However, there occur some voltage limit violations as the moving average filter causes a delay in the reaction of the control to overvoltages. If the voltage limit send to the control is set to be a little bit lower, this can be compensated and it is expected to reduce or eliminate overvoltages. The active and reactive power injections are fluctuating more in comparison to the local control cases. At the same time the curtailed active power remains below the ones in case 2 and case 3 for most time steps.

### 3.2.5 Summary of results

The previous results indicate that the coordinated control methods improve the active power injection of the renewables at peak times and lead to a lower curtailed energy across the simulated summer day. In order to explicitly look at these quantities, Figure 38 shows the active power injection at all buses during the peak time while Figure 39 depicts the curtailed energy on the simulated day.

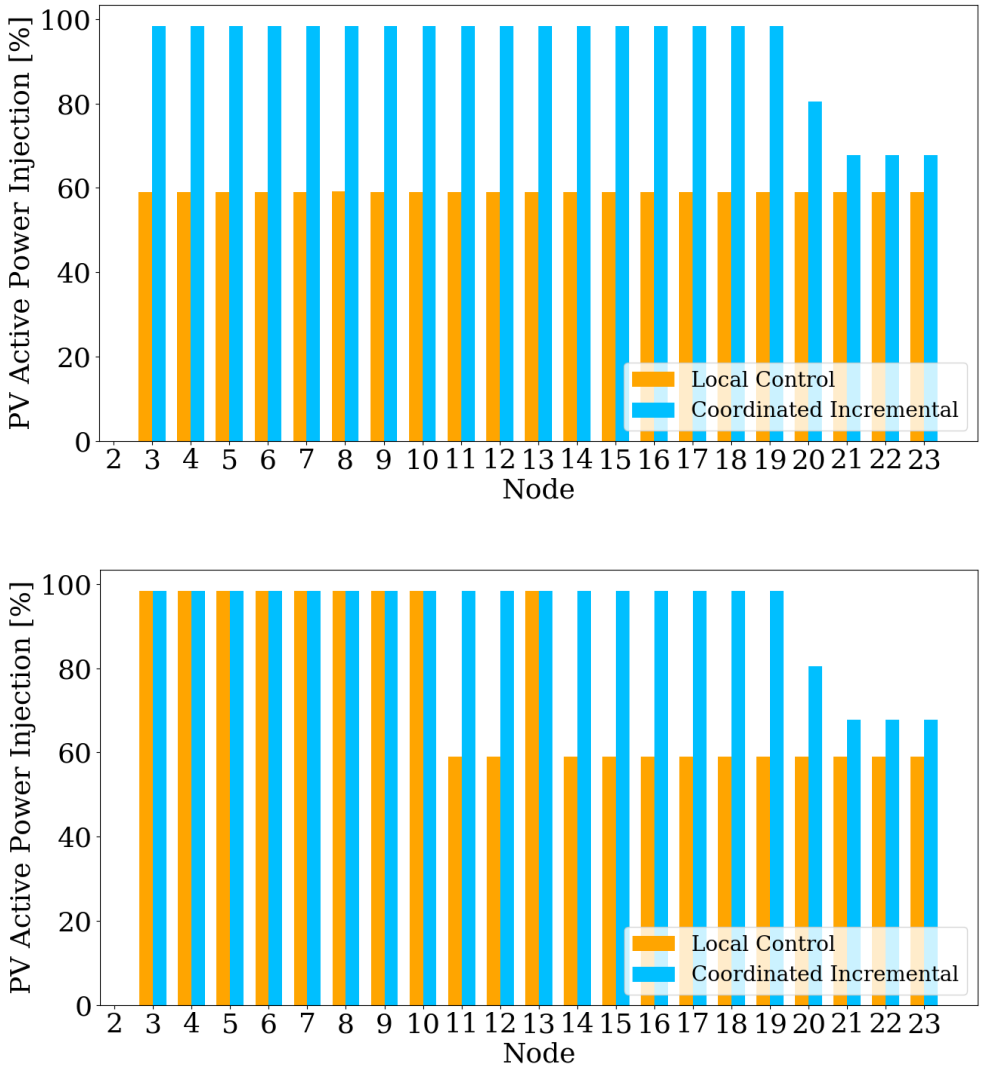


**Figure 38: Active power injection for each bus at noon time for coordinated control (case 5) compared to local control with uniform active power curtailment (case 2 in top figure) and individual active power curtailment (case 3 in bottom figure)**

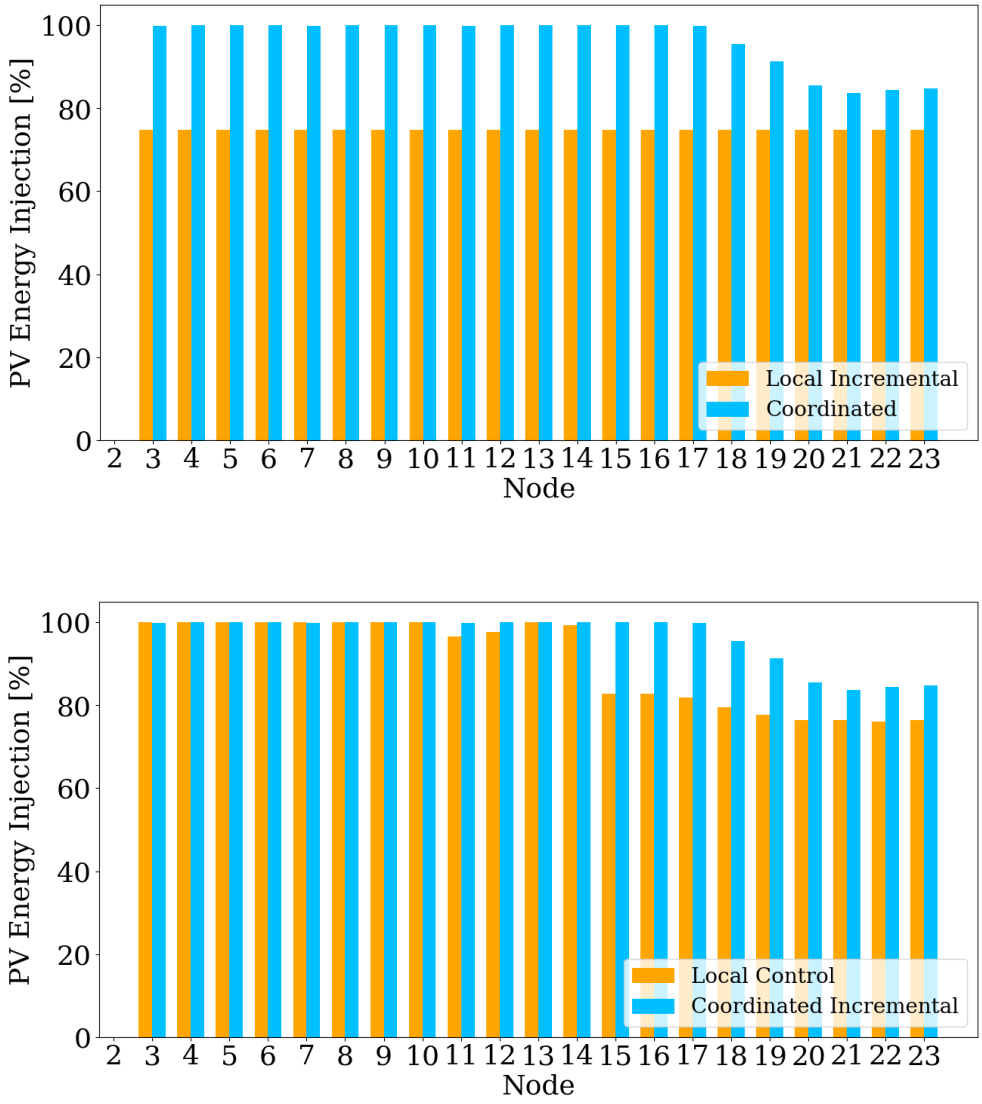


**Figure 39: Injected energy for each bus at noon time for coordinated control (case 5) compared to local control with uniform active power curtailment (case 2 in top figure) and individual active power curtailment (case 3 in bottom figure)**

The previous observations are very clear in these comparisons. During the peak time, the coordinated control curtails only the active power at the nodes at the end of the feeder to the minimum degree necessary. The individual active power curtailment that requires additional monitoring in the grid splits the grid into sections that receive the active power curtailment signal or not. The curtailed energy shows the impact over the time. While the coordinated control results only in lost energy at the last six buses, both active power curtailments for the local control show significantly more lost energy. Once again, the uniform active power curtailment proves to be unfavourably as it results in a loss of 25% energy at all PV plants. Due to the selective behaviour of the individual curtailment method, only 10% of the energy are lost. The cumulative lost energy with the coordinated approach is 4% with respect to the available energy.

Apart from the lost energy, the actual power quality delivered to the customers is of mayor relevance. Figure 37 shows the maximum voltage violation that the customer sees at each node. The buses close to the feeder do not show any voltage violation. Without any active power curtailment, the coordinated reactive power control reduces the occurring violations of the voltage threshold in comparison to the local control. Less buses are affected by voltage quality issues and others are affected by smaller overvoltages.

Lastly, Figure 41 shows the accumulated customer minutes with voltage violations for all buses that experience overvoltages during the simulation. The simple trade-off between voltage quality and preserved energy can easily be observed for the local control without curtailment, uniform and individual curtailment. The more active power is curtailed, the less the accumulated time of voltage quality problems at the customer side. Due to the fact that the coordinated control is operated very close to the threshold, small violations occur more often in comparison to the curtailment methods with the local control. A fine tuning of the parameters of the coordinated control together with an adjustment of the moving average filter is likely to reduce the voltage violations below the reference cases 2 and 3.

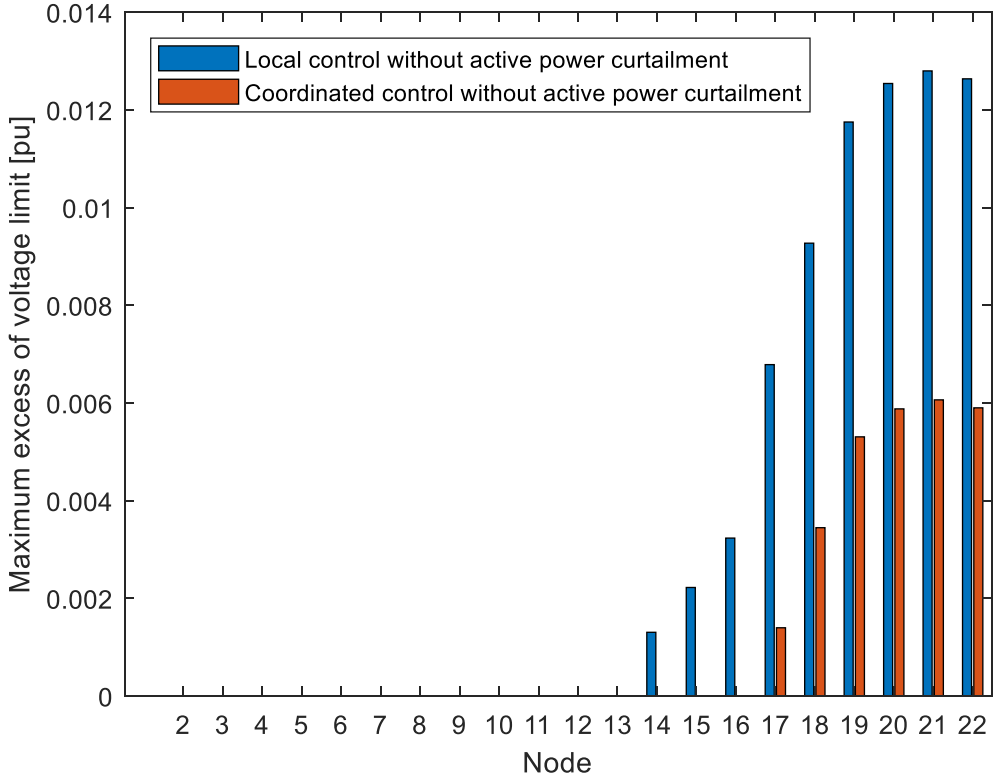

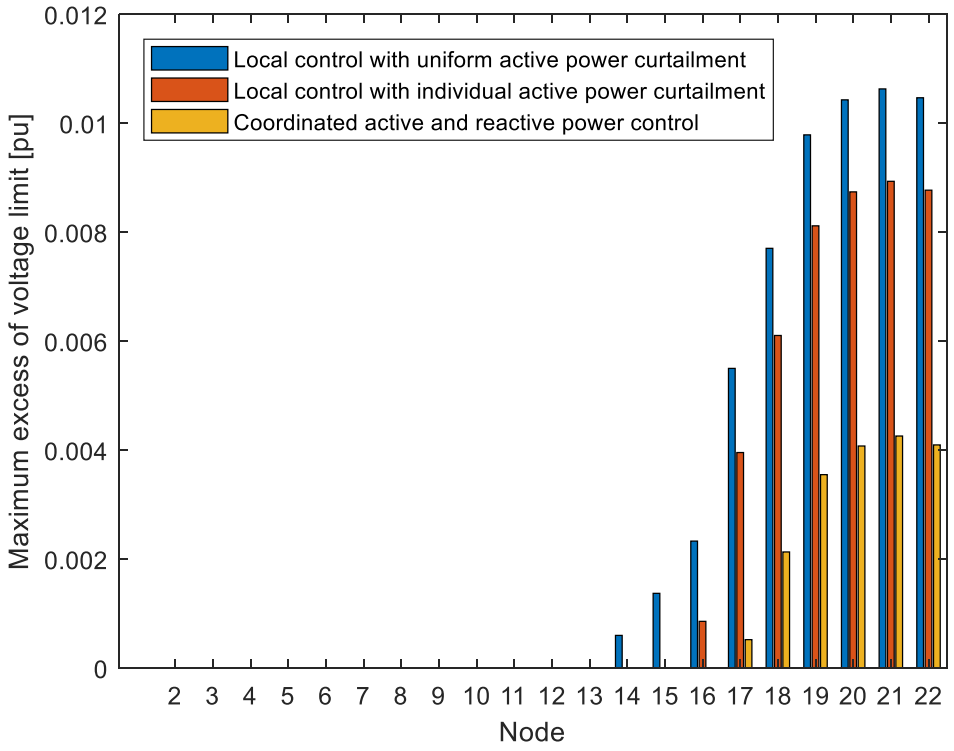


**Figure 40: Maximum voltage violation per node for cases without curtailment (top) and with curtailment (bottom)**

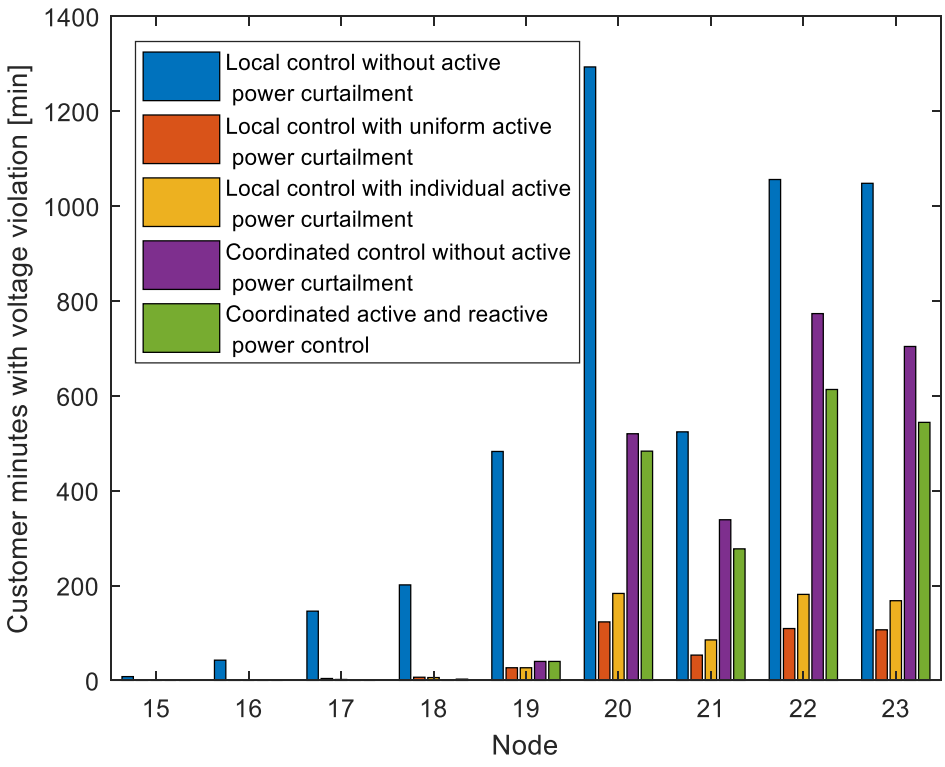


**Figure 41: Aggregated time of voltage violations for each relevant node**

## 3.3 Power Quality Evaluation

Validation of the PQE service and APMU devices focused on the fundamental classical parameters from IEC 61000-4-30, and power parameters as requested by the DSOs and required for other SOGNO services such as the Load Forecasting (as discussed in section 2.3.1). So the PQE and APMUs service KPIs to be verified are:

1. Power Frequency
2. Magnitude of supply Voltage (V) - Phase 1, Phase 2, Phase 3
3. Voltage harmonics - THD and Individual harmonics
4. Magnitude of the Current (A) - Phase 1, Phase 2, Phase 3.
5. Current harmonics - THD and Individual harmonics
6. Power - Active Power (Kw), Apparent Power (VA), Reactive Power (Var)

### 3.3.1 APMU Characterisation Tests

The APMU characterization Tests were designed and implemented by Altea and UniBo at the UniBo test facility during June-July 2019.

The tests aimed to compare the measurements of Power Quality parameters performed by the APMU device to the reference values of an instrument owned by the University of Bologna.

To verify the measurement results of the APMU it was necessary to compare them with a reference instrument. The proper reference for this test was the Fluke Calibrator 6105a[3] together with its Transconductance 52120a[4], capable of injecting up to 120 A and of applying up to 1000 V, while fixing for both all desired power quality parameters (e.g. harmonics, inter-harmonics, etc.).

The tests described in the following were defined by starting from the international standards: the IEC 61000-4-30 and the EN 50160. Briefly, the former lists and defines the parameters covering Power Quality, and it provides details on how devices must implement the relevant measurements; the latter specifies limits for voltage and frequency in the distribution network, so it was used to define the test protocol.

**Test description:**

According to the IEC standard on Power Quality the following parameters were selected to be measured:

1. Power frequency
2. Magnitude of voltage and current
3. Voltage and current THD
4. Individual harmonics of the voltage and the current (up to 50th is ok, but even standards stops at the 25th)
5. Apparent, active and reactive power

To ensure the reliability of the device measurements, THD and harmonics were measured in every test, even if not strictly related to the quantity under test. Therefore, an example of data collecting table could be:

| Test # | F [Hz] | \|V\| [V] | \|C\| [A] | THD [%] | S [VA] | P [W] | Q [Var] | 1st h [%] | 2nd h [%] | 3rd h [%] | Nth h [%] |
|---|---|---|---|---|---|---|---|---|---|---|---|
| 1 | | | | | | | | | | | |

The test conditions are reported in the following:

- Rated conditions: 230 V, 50 A, pure sinusoidal, no harmonics.
- Frequency: 49, 49.5, 50.5, 51 Hz.
    - Measured every 10 s, the accuracy should be ±0.01 Hz.
- Voltage magnitude: 207, 218.5, 241.5, 253 V.

[3] https://eu.flukecal.com/products/electrical-calibration/electrical-calibrators/6105a-6100b-electrical-power-quality-calibrat?quicktabs_product_details=4
[4] https://eu.flukecal.com/products/electrical-calibration/electrical-calibrators/52120a-transconductance-amplifier?quicktabs_product_details=4

- Measured 10 cycles, the accuracy should be ±0.1 Un.
- Current magnitude: 5%, 20%, 80%, 100%, 120% of 50 A.
  - Measured 10 cycles, the accuracy should be ±0.1 Un.
- Harmonics: according to the table (% with respect to the fundamental signal), each single harmonic is superimposed to the rated signal
  - Measured for 10 s, pure comparison

| 3 | 5 | 7 | 9 | 11 | 13 | 15 | 17 | 19 | 21 | 23 | 25 |
|---|---|---|---|---|---|---|---|---|---|---|---|
| 5% | 6% | 5% | 1.5% | 3.5% | 3% | 0.5% | 2% | 1.5% | 0.5% | 1.5% | 1.5% |

- Multiple harmonics: the THD limit is 8 %, hence a combination of harmonics is defined and superimposed to the fundamental signal.
  - Measured for 10 s, pure comparison

### 3.3.2 LV APMU Results

The LV APMU Device under Calibration (DUC) was an electronic device designed to measure voltage and current in a Low Voltage (LV) energy distribution network. It calculated, also, some power quality parameters. The test session was run on July 9th – 10th 2019 at the laboratory of Electric and Electronic Measurements of the University of Bologna, Electrical and Information Engineering Dept.

The test setup is shown in the following schematic and pictures:

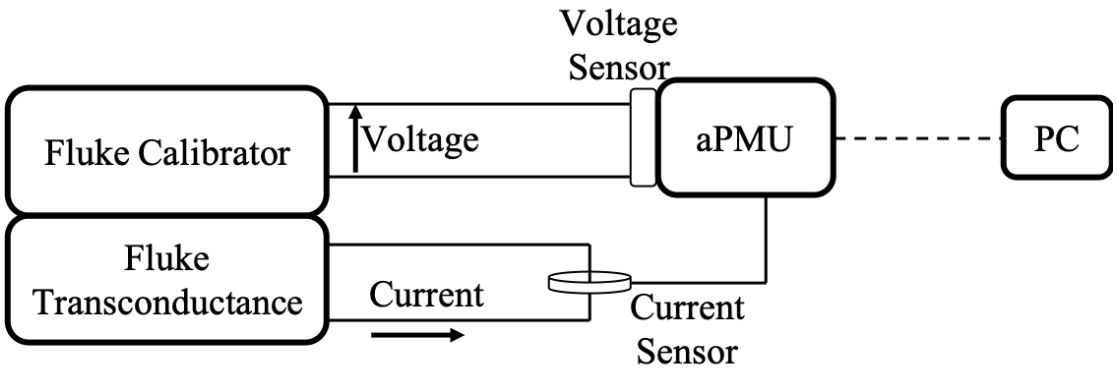


**Figure 42: Schematic of the LV APMU test setup**

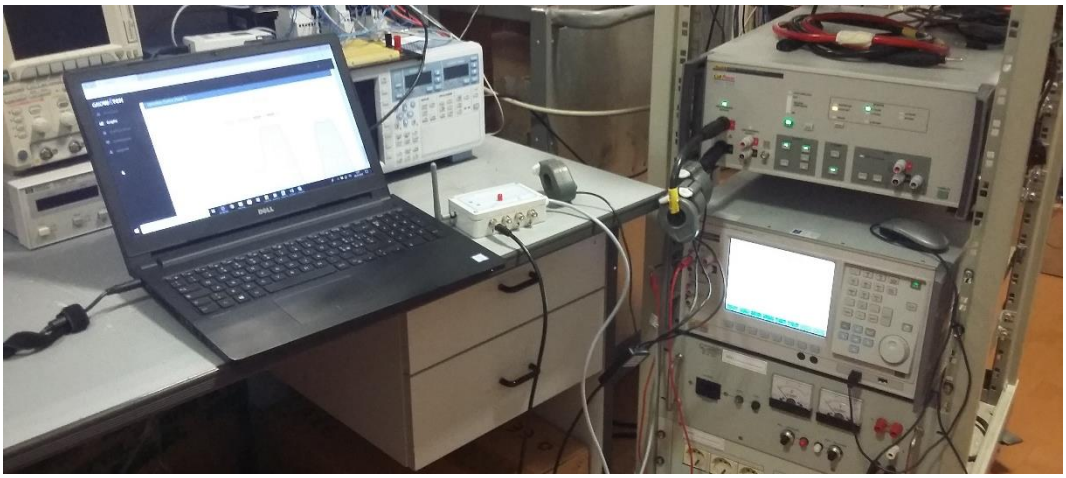

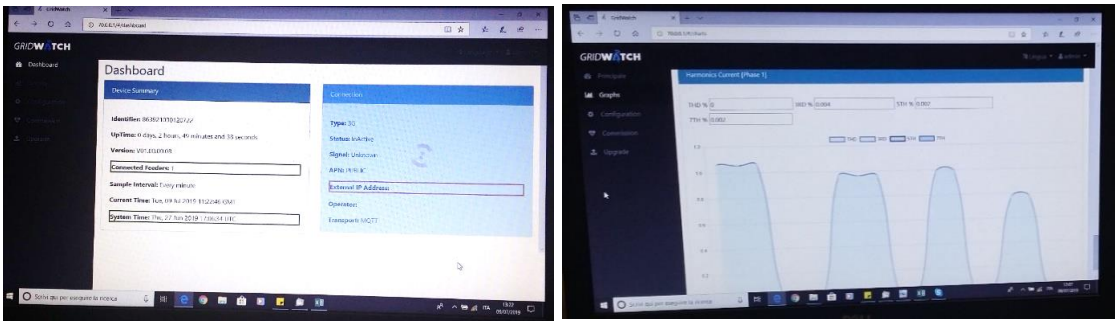


**Figure 43: LV APMU test setup**

1. The calibrator voltage output was connected in parallel to the 3 Phase inputs of "feeder 1", to run simultaneous measurements. The calibrator output was isolated from ground, fitting the operating conditions of the APMU. Voltage on Phase 3 supplied the auxiliary power to the APMU for the entire duration of the test session. The calibrator voltage output was never disabled, in order to avoid the APMU turning off.
2. The calibrator was connected to the ancillary transconductance to cover the range of rated primary current of the APMU. All 3 sensors dedicated to phase currents were mounted on the high-current coil of the transconductance, to run simultaneous measurements. The current sensor provided for the neutral conductor was not used. The primary current was flowing in the coil without interruptions during the test session.
3. A laptop was connected to the APMU Wi-Fi access point and logged into the APMU Gridwatch web interface; the parameters reported on the "Graphs" page were monitored to check fluctuations and recorded during each test:
    a. 3 RMS phase voltages,
    b. 3 RMS phase currents,
    c. 3 phase Active powers,
    d. 3 phase Apparent powers,
    e. THD of voltage and of current on phase 1,
    f. 3$^{rd}$ 5$^{th}$ and 7$^{th}$ harmonics of voltage and of current on phase 1.

#### 3.3.2.1 Observations on test conditions of the test protocol

The fundamental frequency is not an output of the APMU, so it could not be tested. Nevertheless, it was varied from 49 to 51 Hz as per the test protocol, to see if other parameters were affected.

Currently, the APMU provides a one point reading of Harmonics, RMS of voltage and current to give better visibility on the dynamic performance of the networks and their behavior (peaks etc.). However, it is planned shortly to implement an averaging embedded algorithm on a 10 s window in the AMPUs to comply with IEC 61000-4-30. So averaging is likely to improve system accuracy further. Harmonics and THD of Voltage and Current were displayed only for Phase 1, not for Phase 2 and 3.

For both Voltage and Current, only odd harmonics up to 7$^{th}$ order were available, so it was not possible to determine if the DUC complies with IEC 61000-4-30 for further harmonics.

#### 3.3.2.2 LV APMU test results and conclusions

The recorded test results are shown in A3.3. For voltage measurements, the accuracy was 0.5%, in line with Class S of IEC 61000-4-30 requirements. For current measurements, the accuracy was 1%, in line with Class S of IEC 61000-4-30 requirements. For Power measurements, the accuracy is 1%, in line with Class I of IEC 61000-4-7. The accuracy on the Harmonics measurements (Voltage or Current) was 0.5%, much better than requirements reported for Class I of IEC 61000-4-7 (5%).

The accuracy on THD (Voltage or Current) cannot be declared due to the measurements (THD up to 1%) occurring when the actual THD of injected signals was null. Since the THD threshold

value is 8%, 1% error is too high. Anyway, regarding this parameter there is not an explicit uncertainty class in the reference standards.

### 3.3.3 MV APMU Results

The DUC was an electronic device designed to measure voltage and current in a Medium Voltage (MV) energy distribution network, the model type was MV APMU. It calculated, also, some power quality parameters. The DUC was connected to an Altea CVS-P-24-O combined voltage and current sensor for MV distribution networks and stores their calibration coefficients. The DUC specifications were the following:

| **Voltage channel** | |
|---|---|
| Accuracy Class: | 0.5 % |
| Rated voltage input signal: | 1 V |
| Rated Frequency | 50 Hz |
| **Current channel** | |
| Accuracy Class: | 0.5 % |
| Rated current input signal: | 60 mV |
| Rated Frequency | 50 Hz |
| **Others** | |
| Power Input | 230 Vac / 50 Hz |
| Visualization | Web page on WiFi network |
| **Sensors** | |
| Type | CVS-P-24-O |
| CH1 S/N | 18054005 |
| CH2 S/N | 18054002 |
| CH3 S/N | 18054003 |
| Rated Voltage | 20/√3 kVrms |
| Rated Current | 100 Arms |
| Rated accuracy | 0.5 % |

The validation procedure consisted in the determination of the measurement error of the DUC. The following measurements were performed-:

- **PRIMARY VOLTAGE:** By applying to the inputs of the MV sensors connected to the DUC a reference voltage and by recording the corresponding indicators given by the DUC;
  - Accuracy Vs Test Voltage, test frequency: 50 Hz
- **PRIMARY CURRENT:** By applying to the inputs of the MV sensors connected to the DUC a reference current and by recording the corresponding indicators given by the DUC;
  - Accuracy Vs Test Current, test frequency: 50 Hz.

Some tests could not be performed imposing the primary voltage/current for safety or for limitations in the test setups, in these cases input signals were applied directly to the DUC:

- **LPIT SIMULATION:** By applying to the inputs of the DUC signals that are equivalent to a Low Power Instrument Transformer (LPIT), and by recording the corresponding indicators given by the DUC.
  - To evaluate the DUC dynamic range:
    - Overcurrent response;
    - Overvoltage response.
  - To analyze power measurements:
    - Apparent and active power.
  - The measurements are also repeated at various ambient temperatures:
    - Accuracy Vs Temperature.

The measurements were performed under the following conditions:

- With the DUC in thermal equilibrium at the temperature of 23 ± 2 °C for the last 4 h (excluding the Accuracy Vs Temperature measurement);
- With the antenna SMA connector shield of the DUC connected to earth;

- Powering the DUC with a sinusoidal voltage $U_A$ = 230 VRMS, frequency 50 Hz and distortion factor less than 1 %;
- With Firefox 66.0 web browser for data collection.
- Measurements Standards:

| DESCRIPTION | MANUFACTURER | MODEL | CERTIFICATE OF CALIBRATION |
|---|---|---|---|
| Comparator Unit | Altea | ACU-01 | UNIBO-3-3/2019 |

#### 3.3.3.1 Tests of primary voltage measurements with step-up transformer

Measurements were performed with the following setup: a high voltage sinusoidal signal generated by a Power Source (Chroma Power 61604) connected to a step-up transformer 100/√3 V: 36/√3 kV. The amplitude and frequency of the signal were controlled by the Power Source.

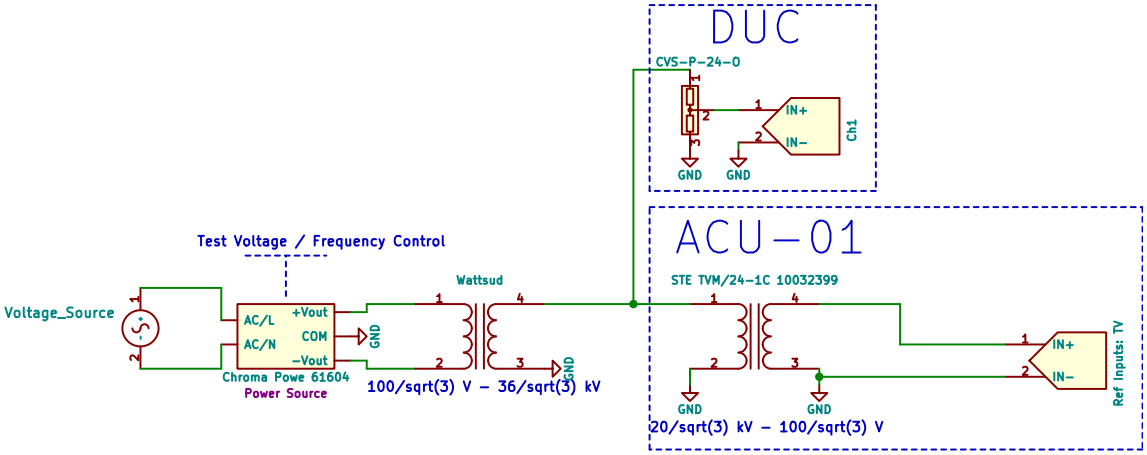


**Figure 44: Voltage test setup schematic**

This signal was injected into the DUC inputs through the CVS-P-24-O voltage sensors, and into the ACU-01 comparator unit.

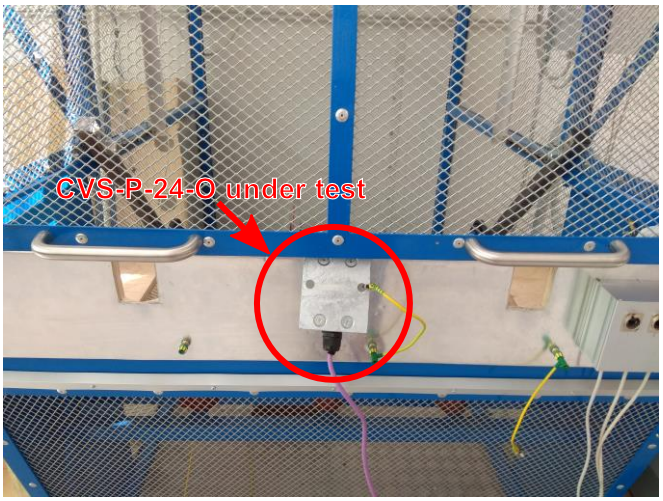


**Figure 45: CVS-P-24-O under test inside HV test cage**

**Test Result:** The error is below the 0.3 % from 30% to 120% of the nominal voltage.

#### 3.3.3.2 Tests of current measurement accuracy with step-down transformer

Measurements were performed with the following setup: a high current sinusoidal signal is produced by a step-down transformer (Carbognin) driven by the mains power voltage.

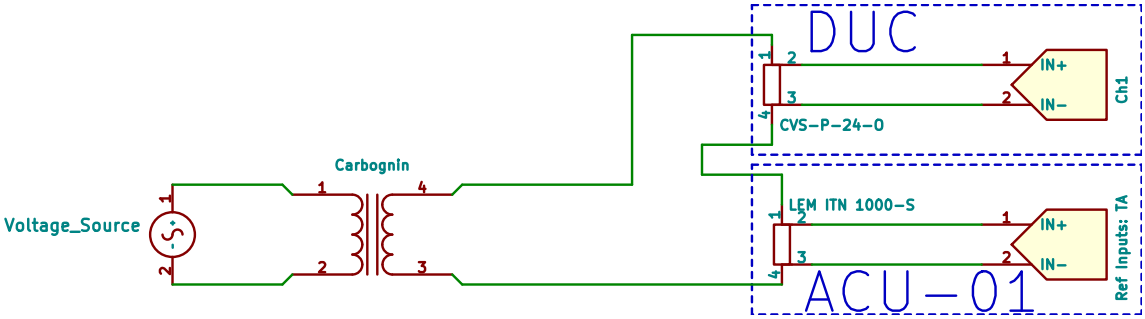


**Figure 46: Current test setup schematic**

This signal was fed to the DUC inputs through the CVS-P-24-O and to the ACU-01.

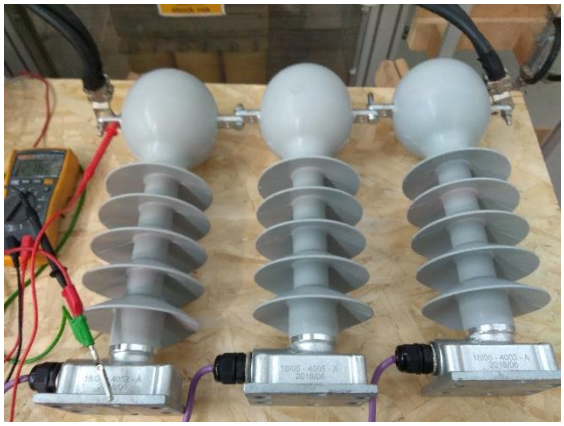

**Figure 47: CVS-P-24-O under test**

**Test Results:** The error is below 0.4 % from 14 A to 300 A.

#### 3.3.3.3 Tests of measurement accuracies with LPIT simulator

Measurements were performed with the following setup: a set of sinusoidal signals is generated by a low voltage arbitrary function generator (NI 9263) controlled by a software that simulates a sensor behavior. These signals were fed to the DUC and to an acquisition system (NI9239) that verified the generator output and calculated various power parameters (Real and Imaginary power, cos(ϕ), THD…).

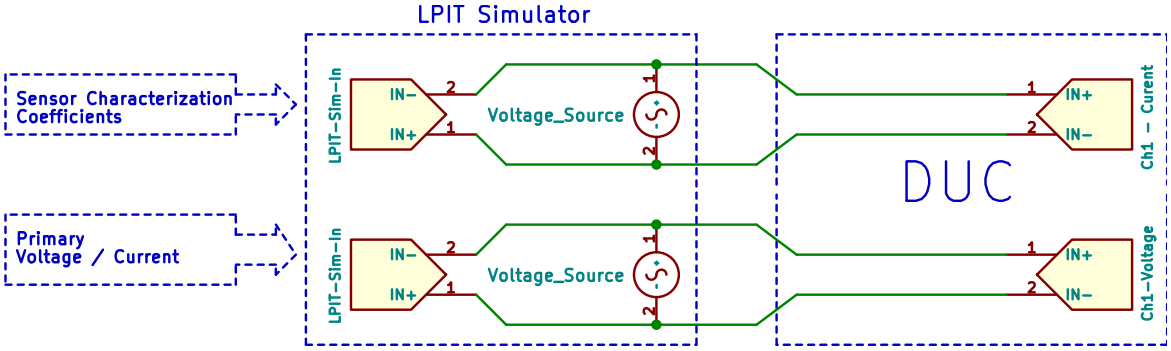


**Figure 48: LPIT simulator test setup schematic**

**Overcurrent response:** the error is below 0.5 % up to 400 A.

**Overvoltage response:** the error is below 0.5 % up to 45 kV.

**Apparent and Active Power measurement:** the error is below 0.5 % with resistive loads.

In the Accuracy Vs Temperature measurement, the DUC was put into a climatic chamber (Perani TC 250/70) that varied the ambient temperature from -5 °C 50 °C, 1 °C/minute of temperature variation, at least 1 hour in a stable temperature before taking the measurement. Figure 49 shows the DUC in the climate chamber

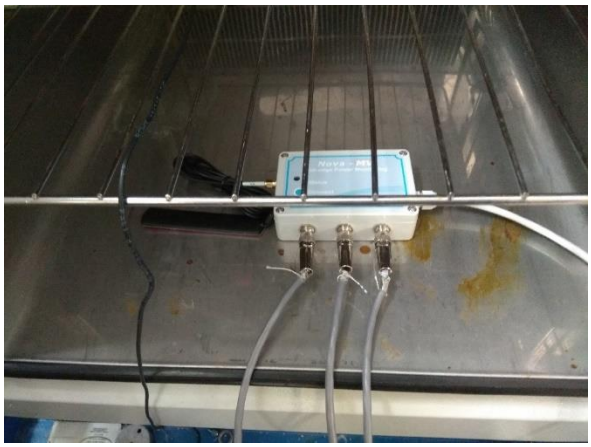

**Figure 49: DUC inside the climatic chamber for Accuracy Vs Temperature test**

Figure 50 displays the current ratio error against the temperature while Figure 51 shows the voltage ratio error against the temperature. It is evident that the error stays below 0.5 % for the tested temperature window in both cases.

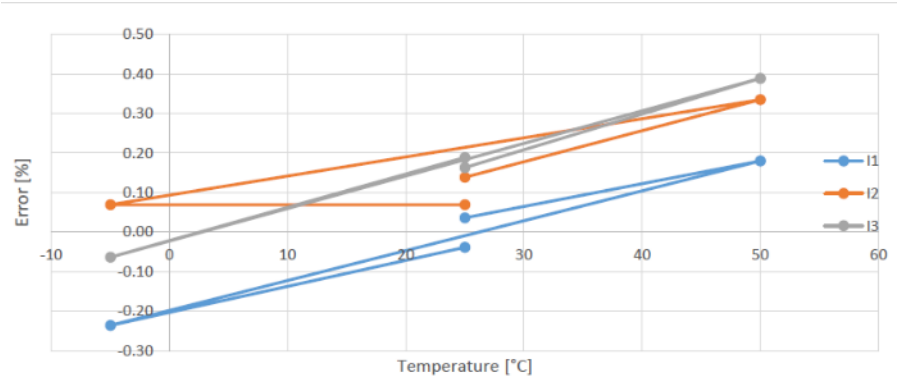


**Figure 50: Current Error vs Temperature**

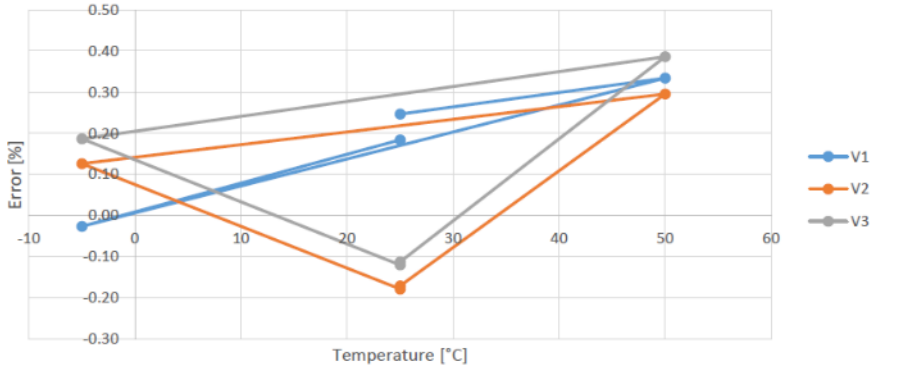


**Figure 51: Voltage Error vs Temperature**

#### 3.3.3.4 MV APMU Conclusions

For voltage measurements, the accuracy results are 0.5%, in line with Class S of IEC 61000-4-30 requirements. For current measurements, the accuracy results are 1%, in line with Class S of IEC 61000-4-30 requirements. For Power measurements, the accuracy is 1%, in line with Class I of IEC 61000-4-7. Thus, the MV APMU setup is in accordance to Class S which implies reliable power quality indices.

# 4. Documentation of the Application Programming Interface

These interfaces describe the interaction of the various services implemented within the scope of the EU project SOGNO. The fundamental architecture pattern is a combination of micro-services interacting via an MQTT broker. This pattern is used in information technology as it enables complex software instances to communicate with each other via defined endpoints independently of their implementation.

The services are mostly decoupled from each other and process a clearly defined task. This pattern enables a modular structure of the entire system, so that a failure of one or more services does not necessarily mean a failure of the entire system. In addition, new or existing services can be directly injected, deleted or updated without any significant impact on the rest of the system.

Figure 52 describes how the publish/subscribe mechanism between the services should be understood. As an example, let us assume that Service B is dependent on the input from Service A. Service A will publish its results on a specific predefined topic. The broker will forward the results from Service A to Service B, because Service B has subscribed to the topic before. The direction of the red components should be read as follows: Service A offers an interface that publishes its results in JSON format on Topic X. This JSON message is subscribed to by the B service. Once Service B has received these results, it can proceed with the data as its implementation requires.

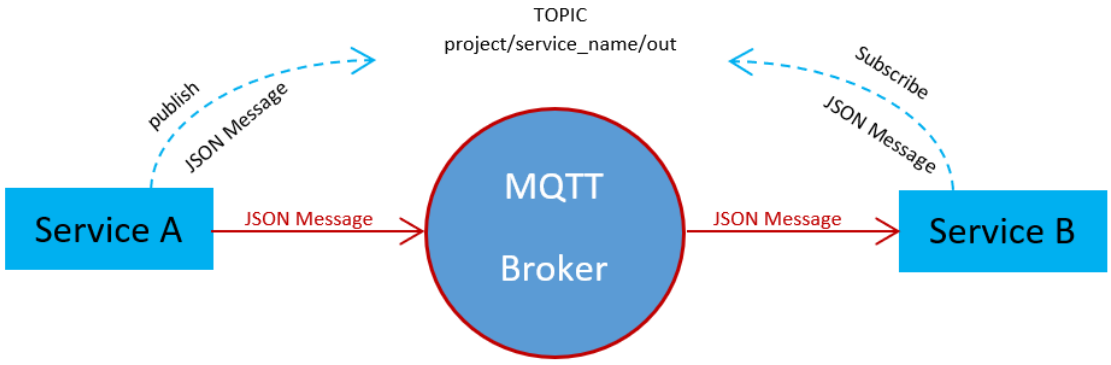


**Figure 52: Publish/Subscribe Mechanism**

There are services that publish different results on different topics. The topic naming follows a certain logic. This consists of the project name followed by the service name and then the direction separated by a slash, which separates the topic levels. If necessary, the results types will be appended to the end of the name as shown in the Table 5.

**Table 5: Logic of topic naming**

| LOGIC | EXAMPLE |
|---|---|
| PROJECT_NAME / SERVICE / DIRECTION [/ RESULT_TYP] | sogno / se / out<br>sogno / gui / out / flisr<br>sogno / gui / out / topology |

The usage of topic level separators allows to work with placeholders. While the character “+” stands for any content of a single layer, the character “#” can be used to select any content in layers afterwards. These are provided by the MQTT specification. For example, a service can be notified to all outgoing messages from any service with this simple topic name:

sogno / + / out / #

Figure 53 shows an overall view of the interaction of the services developed in this project from a logical point of view and illustrates the dependencies between the different services.

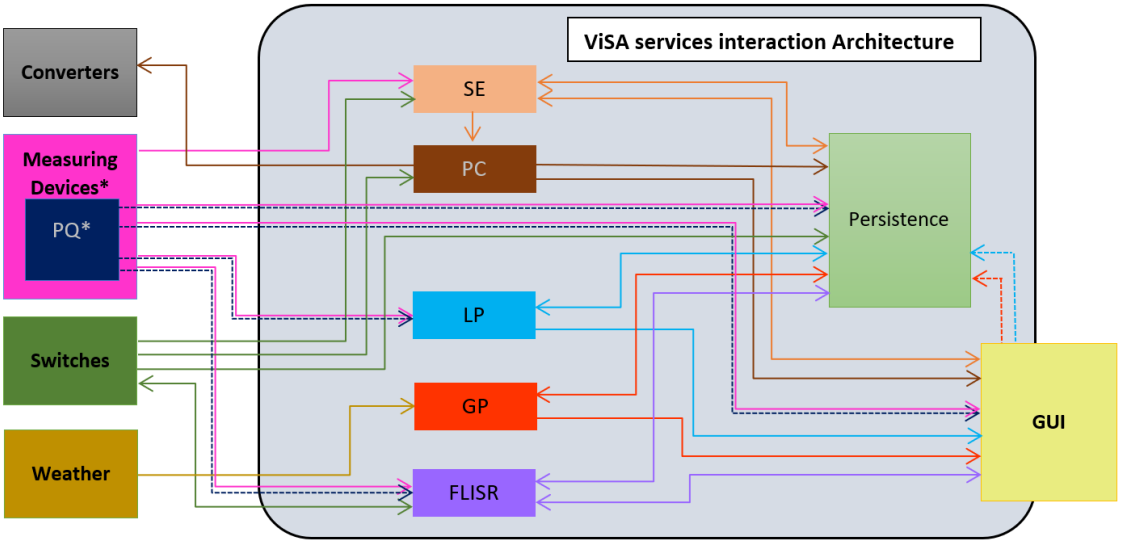


**Figure 53: ViSA Service Interaction Architecture**

* The output of the power quality evaluation is included in the message of the measuring devices.

## 4.1 The Interfaces

This section describes the endpoints for the corresponding services in this deliverable, namely SE, PQE and PC. The remaining services are part of other working packages and will be presented in the deliverables D3.3 and D4.3.

Basically, each service in this project will have two interfaces that will register a certain number of topics for publishing or subscribing. A complete list of the interfaces contained in the corresponding components were part of deliverable D2.2 and are described there individually.

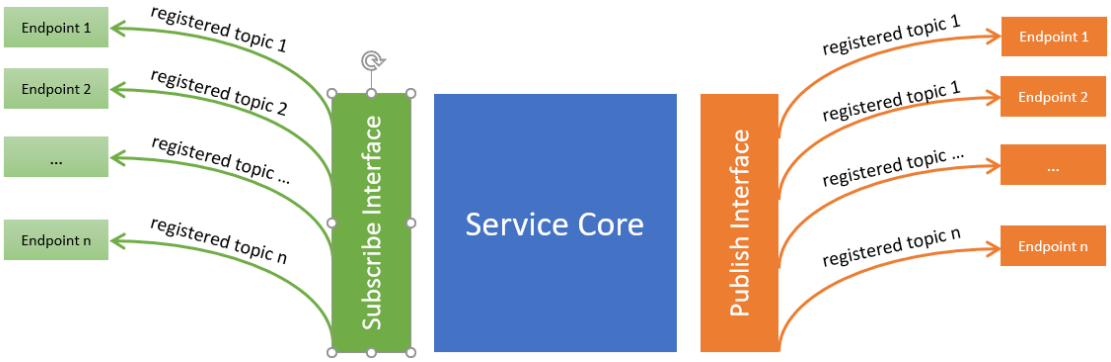


**Figure 54: A service with its publish and subscribe endpoints**

### 4.1.1 Measuring Devices and Power Quality Service

| Topic | Mechanism | Description | Payload |
|---|---|---|---|
| **sogno/md/out*** | publish | The endpoint on which the APMUs and the PQ service publish their measurements | In the annex |

** The measuring device message contains the results of the power quality service.*

### 4.1.2 Converters

| Topic | Mechanism | Description | Payload |
|---|---|---|---|
| **sogno/pc/out** | subscribe | The endpoint subscribed by the converters to receive the results of the power control service | See annex A1.4 |

### 4.1.3 Switches

| Topic | Mechanism | Description | Payload |
|---|---|---|---|
| **sogno/switch/out** | publish | The endpoint on which the switches publish their operational states. | See annex A1.3 |
| ***sogno/flisr/out**** | *subscribe* | *The endpoint subscribed by the switches to receive the commands from the FLISR service* | See the annex in D3.3 |

** For the sake of completeness, we have added this topic, although it is part of D3.3*

### 4.1.4 State Estimation

| Topic | Mechanism | Description | Payload |
|---|---|---|---|
| **sogno/se/out** | publish | The endpoint on which the state estimator publishes its results | See annex A1.2 |
| **sogno/md/out** | subscribe | The endpoint subscribed by the state estimation service to receive the measurement data | See annex A1.1 |
| **sogno/switch/out** | subscribe | The endpoint subscribed to by the state estimator to receive the operational states of the switches | See annex A1.3 |
| **sogno/db/out/topology** | subscribe | The endpoint subscribed by the state estimator to get the topology as CIM file from the persistence service when the system is restarted | See annex A1.5 |
| **sogno/gui/out/topology** | subscribe | The endpoint subscribed to by the state estimator to get the topology as CIM file from the GUI. This topology is sent as a CIM file | See annex A1.5 |

Since the CIM files can be very large, they will be sent compressed by the publisher using the python “zlib” library. The subscriber will decompress the message and then process it further. A small piece of python code for reading and compressing the CIM file could look like this:

```
import zlib

compressed_cim_file = None

with open('path/to/cim/cim.xml', 'rb') as cim_file:
    cim_file = cim_file.read()
    compressed_cim_file = zlib.compress(cim_file, zlib.Z_BEST_COMPRESSION)
```

The subscriber receives the compressed message as the payload of a message. It is assumed that the payload was stored in a variable called `compressed_cim_file`. The following code can be used to decompress the CIM file.

```
import zlib

decompressed_cim_file = zlib.decompress(compressed_cim_file)
```

### 4.1.5 Power Control

| Topic | Mechanism | Description | Payload |
|---|---|---|---|
| **sogno/pc/out** | publish | The endpoint on which the power control publishes its results | See annex A1.4 |
| **sogno/se/out** | subscribe | The endpoint subscribed by the power control to receive the state estimation results | See annex A1.2 |
| **sogno/switch/out** | subscribe | The endpoint subscribed by power control to receive the operational states of the switches | See annex A1.3 |

# 5. Conclusions

This deliverable provides an extension of the previous deliverable D2.2 with respect to main concepts for the system awareness services developed in the SOGNO project to support DSOs in managing distribution grids. Three services are developed in SOGNO to this purpose: state estimation, power control, and power quality evaluation. Additionally, all three services have been validated in simulations or laboratory tests.

The voltage and current measurements of the advanced power measurement unit (APMU) together with LV and MV transducers were tested in a full-sized laboratory setup. They provide an accuracy level within the class S of the relevant IEC standard. Thus, they are sufficient for the desired monitoring purposes. The newly developed coordinate control are compared to the state of the art solution according to current standards. For a possible future scenario with a grid including 100% renewables, the necessity of active power curtailment can be significantly reduced with the new control. Additionally, the voltage quality is improved with respect to maximum voltage violations that occur during critical time steps in the simulation. Both developed state estimation approaches show satisfactory accuracy level in the simulations of a test grid. The advantage of the monitoring results is evident since they can contribute to an improvement of existing control operations and upcoming coordinated control approaches.

Thus, the services developed in SOGNO allow a significant step forward for electricity grid operators to understand the behavior of their network, to identify possible issues or critical aspects, to evaluate the need of specific countermeasures for improving efficiency or operational performance, and to have more reliable decision-making process. SOGNO system awareness services are obtained through the use of low cost measurement devices, but still paying due attention to the accuracies in the measurement chain, thus making the up-front investment for DSOs more affordable while guaranteeing minimum accuracy performance for the monitoring tools. Additionally, newly developed control approaches enable a higher utilization of existing renewables and foster a higher penetration rate within distribution grids.

SOGNO proposes the concept of ViSA, namely a virtualized substation environment for the deployment of all the substation intelligence. The development of a modular structure enables simple interfaces for the services and hence, ensures interoperability with different services. At the same time, the virtualization allows minimization of hardware in the field and a distribution of computation and communication resources. This leads to the possibility to obtain scalability, as well as opening the possibility to provide the entire monitoring platform as a turnkey service for DSOs.

# 6. List of Tables

Table 1: Sources of Harmonic injections from customer installations ..... 26
Table 2: Standard deviation and mean value of estimation error of ANN estimator ..... 38
Table 3: RMSE of ANN estimator ..... 39
Table 4: Standard deviation of estimation error of WLS estimator ..... 39
Table 5: Logic of topic naming ..... 62
Table A-6 Topology of the test network ..... 81
Table A-7 Line parameters of the test network ..... 81
Table A-8 Power injection of the test network ..... 81
Table A-4: PQE output fields of each APMU ..... 81

# 7. List of Figures

Figure 1: Overview of SOGNO activities. ..... 7
Figure 2: Overview of input measurements to the WLS estimator ..... 10
Figure 3: Artificial neural network architecture ..... 12
Figure 4: Artificial neural network training process ..... 12
Figure 5: Standard Q(U) droop curve according to VDE AR-N 4105 ..... 14
Figure 6: External control of active/reactive power set points by system operator [7]. ..... 15
Figure 7: Example of the typical reactive power control based on local feedback ..... 16
Figure 8: Distributed reactive power control ..... 16
Figure 9: Power Quality problems ..... 18
Figure 10: APMU deployed on a 4-Feeder LV Network. ..... 19
Figure 11: PQE Service User Interface examples of monitored parameters. ..... 20
Figure 12: PQE display of APMU real-time harmonic measurements ..... 25
Figure 13: First 4 voltage harmonics & resulting distortion. ..... 25
Figure 14: Impact of harmonics on zero-crossing detection ..... 28
Figure 15: Impedance loci for harmonic orders (A-G). ..... 29
Figure 16: Composition of the total power of a transmission grid ..... 33
Figure 17: State estimation validation process. ..... 35
Figure 18: Topology of portion of CIGRE Network exploited for evaluation of state estimation performance ..... 36
Figure 19: Histogram of error of voltage estimation at node 2. (a) histogram of voltage magnitude error. (b) histogram of voltage phase angle error ..... 38
Figure 20: Histogram of error of voltage estimation at node 3. (a) histogram of voltage magnitude error. (b) histogram of voltage phase angle error ..... 38
Figure 21: Power control validation process ..... 39
Figure 22: Bornholm LV test grid ..... 40
Figure 23: Injected active power without active power curtailment ..... 42
Figure 24: Voltage magnitudes for droop curve control without active power curtailment ..... 42
Figure 25: Injected reactive power for droop curve control without active power curtailment ..... 43
Figure 26: Voltage magnitudes for droop curve control with step-wise uniform active power curtailment ..... 43
Figure 27: Injected reactive power for droop curve control with step-wise uniform active power curtailment ..... 44
Figure 28: Injected active power for droop curve control with step-wise uniform active power curtailment ..... 44
Figure 29: Voltage magnitudes for droop curve control with step-wise individualized active power curtailment ..... 45
Figure 30: Injected reactive power for droop curve control with step-wise individualized active power curtailment ..... 45
Figure 31: Injected active power for droop curve control with step-wise individualized active power curtailment ..... 46

Figure 32: Voltage magnitudes for coordinated reactive power control without active power curtailment ..... 46

Figure 33: Injected reactive power for coordinated reactive power control without active power curtailment ..... 47

Figure 34: Injected active power for coordinated reactive power control without active power curtailment ..... 47

Figure 35: Voltage magnitudes for coordinated reactive power control with step-wise individualized active power curtailment ..... 48

Figure 36: Injected reactive power for coordinated reactive power control with step-wise individualized active power curtailment ..... 48

Figure 37: Injected active power for coordinated reactive power control with step-wise individualized active power curtailment ..... 49

Figure 38: Active power injection for each bus at noon time for coordinated control (case 5) compared to local control with uniform active power curtailment (case 2 in top figure) and individual active power curtailment (case 3 in bottom figure) ..... 50

Figure 39: Injected energy for each bus at noon time for coordinated control (case 5) compared to local control with uniform active power curtailment (case 2 in top figure) and individual active power curtailment (case 3 in bottom figure) ..... 51

Figure 40: Maximum voltage violation per node for cases without curtailment (top) and with curtailment (bottom) ..... 53

Figure 41: Aggregated time of voltage violations for each relevant node ..... 53

Figure 42: Schematic of the LV APMU test setup ..... 55

Figure 43: LV APMU test setup ..... 56

Figure 44: Voltage test setup schematic ..... 58

Figure 45: CVS-P-24-O under test inside HV test cage ..... 58

Figure 46: Current test setup schematic ..... 59

Figure 47: CVS-P-24-O under test ..... 59

Figure 48: LPIT simulator test setup schematic ..... 59

Figure 49: DUC inside the climatic chamber for Accuracy Vs Temperature test ..... 60

Figure 50: Current Error vs Temperature ..... 60

Figure 51: Voltage Error vs Temperature ..... 60

Figure 52: Publish/Subscribe Mechanism ..... 62

Figure 53: ViSA Service Interaction Architecture ..... 63

Figure 54: A service with its publish and subscribe endpoints ..... 63

# 8. Bibliography


[1] A. Abur and A. Gomez-Exposito, Power System State Estimation: Theory and Implementation, New York, NY, USA: Marcel Dekker, 2004.

[2] W. M. Lin and J. H. Teng, "Distribution fast decoupled state estimation by measurement pairing," *Proc. IEEE, Generation Transmission and Distribution,* pp. 43-48, 1996.

[3] H. Wang and N. Schulz, "A revised branch current-based distribution system state estimation algorithm and meter placement impact," *IEEE Transactions on Power Systems,* pp. 207-213, 2004.

[4] M. Baran and A. Kelley, "A branch-current-based state estimation method for distribution systems," *IEEE Transactions on Power Systems,* pp. 483-495, 1995.

[5] M. Pau, P. A. Pegoraro and S. Sulis, "Efficient branch-current-based distribution system state estimation including synchronized measurements," *IEEE Transactions on Instrumentation and Measurement,* pp. 2419-2429, 2013.

[6] VDE, *VDE-AR-N-4105: Generators connected to the low-voltage distribution network - Technical requirements for the connection to and parallel operation with low-voltage distribution networks,* 2018.

[7] R. Bründlinger, "Review and Assessment of Latest Grid Code Developments in Europe and Selected International Markets with Respect to High Penetration PV," in *6th Inernational Workshop on Solar Integration*, Vienna, 2016.

[8] X. Z. a. L. C. M. Farivar, "Local voltage control in distribution systems: An incremental control algorithm," 2015 IEEE International Conference on Smart Grid Communications (SmartGridComm), Miami, FL, 2015, pp. 732-737..

[9] M. Brenna et al., "Automatic Distributed Voltage Control Algorithm in Smart Grids Applications," in IEEE Transactions on Smart Grid, vol. 4, no. 2, pp. 877-885, June 2013..

[10] D. K. M. e. al., "A Survey of Distributed Optimization and Control Algorithms for Electric Power Systems," in IEEE Transactions on Smart Grid, vol. 8, no. 6, pp. 2941-2962, Nov. 2017.

[11] R. C. G. C. a. S. Z. S. Bolognani, "Distributed Reactive Power Feedback Control for Voltage Regulation and Loss Minimization," *IEEE Transactions on Automatic Control,* pp. 966-981, April 2015.

[12] R. C. G. C. a. S. Z. S. Bolognani, "On the Need for Communication for Voltage Regulation of Power Distribution Grids," in IEEE Transactions on Control of Network Systems, vol. 6, no. 3, pp. 1111-1123, Sept. 2019.

[13] D. P. Bertsekas, "Nonlinear programming," Journal of the Operational Research Society 48.3 (1997): 334-334.

[14] R. Targosz, ""End use perceptions of Power Quality – A European Perspective"," EPRI PQA, 2007. [Online]. Available: http://www.academia.edu/8520180.

[15] Electrical Engineering Portal (EEP), ""Power Quality in industrial and commercial systems"," 2019. [Online]. Available: https://electrical-engineering-portal.com/download-center/ books-and-guides/electrical-engineering/power-quality.

[16] EEC, "Council Directive 89/336/EEC of 3 May 1989 on the approximation of the laws of the Member States relating to electromagnetic compatibility," 1989. [Online]. Available: https://eur-lex.europa.eu/legal-content/EN/ALL/?uri=CELEX%3A31989L0336.

[17] CENELEC TC8X, "European standard EN 50160 Voltage characteristics of electricity supplied by public distribution systems," 2006.

[18] IEC, "IEC 61000-4-30 - ELECTROMAGNETIC COMPATIBILITY (EMC) - PART 4-30: TESTING AND MEASUREMENT TECHNIQUES - POWER QUALITY MEASUREMENT METHODS," 2016.

[19] B. Kingham, ""Quality of Supply Standards: Is EN 50160 the answer?", Schneider Power Quality White Paper," [Online]. Available: https://www.oasis-open.org/committees/download.php/37248.

[20] ELSPEC, "Knowing IEC 61000-4-30 Class A," [Online]. Available: https://www.elspec-ltd.com/knowing-iec-61000-4-30-class-a/.

[21] ESB Networks, [Online]. Available: http://www.esbnetworks.ie/docs/default-source/ publications/distribution-code-v5-0.pdf?sfvrsn=6.

[22] EirGrid, "EirGrid Grid Code," [Online]. Available: http://www.eirgridgroup.com/site-files/library/EirGrid/GridCodeVersion6.pdf.

[23] IEC, "IEC/TR 61000-3-6 (ed2.0) Standard on Electromagnetic compatibility (EMC) Assessment of emission limits for the connection of distorting installations to MV, HV and EHV power systems," [Online]. Available: http://webstore.iec.ch/webstore/webstore.nsf/Artnum_PK/39088 .

[24] CENELEC, "EN 50160, Voltage characteristics of electricity supplied by public electricity networks," [Online]. Available: https://standards.globalspec.com/std/9943573/EN%2050160.

[25] EirGrid, ""An Information Note on Harmonic Issues and their impact on Customer connections", Eirgrid, Note 1,," 2013. [Online]. Available: http://www.eirgridgroup.com/site-files/library/EirGrid/ AnInformationNoteOnHarmonicIssuesv1.0.pdf.

[26] EEP - Electrical Engineering Portal, ""Good voltage regulation and justified power factor correction"," [Online]. Available: https://electrical-engineering-portal.com/ good-voltage-regulation-and-justified-power-factor-correction.

[27] IEEE, "IEEE Recommended Practice for Electric Power Systems in Commercial Buildings".

[28] ABB, ""Power factor correction and harmonic filtering in electrical plants"".

[29] EEP - Electrical Engineering Portal, ""Reactive Power and Compensation Solution Basics For Students"," [Online]. Available: https://electrical-engineering-portal.com/ reactive-power-and-compensation-calculation-basics.

[30] SIEMENS , ""Planning of Electric Power Distribution"".

[31] Federal Energy Regulatory Commission, ""Principles for Efficient and Reliable Reactive Power Supply and Consumption"".

[32] K. Strunz, E. Abbasi, C. Abbey, C. Andrieu, F. Gao, T. Gaunt, A. Gole, N. Hatziargyriou and R. Iravani, "Benchmark Systems for Network Integration of Renewable and Distributed Energy Resources," CIGRE, 2014.

[33] M. Pau., S. Sulis and P. A. Pegoraro, "WLS distribution system state estimator based on voltages or branch-currents: Accuracy and performance comparison," in *Instrumentation and Measurement Technology Conference (I2MTC)*, 2013.

[34] A. Angioni, T. Schlösser, F. Ponci and A. Monti, "Impact of Pseudo-Measurements From New Power Profiles on State Estimation in Low-Voltage Grids," *IEEE Transactions on Instrumentation and Measurement,* vol. 65, no. 1, pp. 70-77, 2016.

[35] J. Ø. a. G. Y. S. Hashemi, "A Scenario-Based Approach for Energy Storage Capacity Determination in LV Grids With High PV Penetration," *IEEE Transactions on Smart Grid,* pp. 1514-1522, May 2014.

[36] A. A. F. P. A. M. M.Pau, "A Tool for the Generation of Realistic PV Profiles for Distribution Grid Simulations," in *International Conference on Clean Electrical Power*, Otranto, Puglia, 2019.

# 9. List of Abbreviations

| | |
|---|---|
| ANN | Artificial Neural Network |
| API | Application Programming Interface |
| APMU | Advanced Power Measurement Unit |
| CIGRE | Conseil International des Grands Réseaux Électriques |
| CIM | Common Information Model |
| DER | Distributed Energy Resources |
| DSO | Distribution System Operator |
| DUC | Device Under Calibration |
| GUI | Graphical User Interface |
| JSON | JavaScript Object Notation |
| LPIT | Low Power Instrument Transformer |
| LV | Low Voltage |
| MQTT | Message Queuing Telemetry Transport |
| MV | Medium Voltage |
| PC | Power Control |
| PQE | Power Quality Evaluation |
| SE | State Estimation |
| SOGNO | Service Oriented Grid for the Network of the Future |
| ViSA | Virtualized Substation Automation |
| WLS | Weighted Least Squares |
| WP | Work Package |
| FLISR | Fault Location, Isolation, and Service Restoration |

# ANNEX

## A1 – Exemplary files for the JSON Message sent by the services and the CIM files used

### A1.1 - Example for the JSON Message from the measuring devices with power quality service results


```
{
  "identifier": "863921030120813-1",
  "readings": [
    {
      "timestamp": "2019-04-08T08:44:01",
      "source": "chan_1",
      "measurand": "activepower",
      "data": "-0.010"
    },
    {
      "timestamp": "2019-04-08T08:44:01",
      "source": "chan_2",
      "measurand": "activepower",
      "data": "0.001"
    },
    {
      "timestamp": "2019-04-08T08:44:01",
      "source": "chan_3",
      "measurand": "activepower",
      "data": "-0.001"
    },
    {
      "timestamp": "2019-04-08T08:44:01",
      "source": "chan_1",
      "measurand": "apparentpower",
      "data": "-0.010"
    },
    {
      "timestamp": "2019-04-08T08:44:01",
      "source": "chan_2",
      "measurand": "apparentpower",
      "data": "0.000"
    },
    {
      "timestamp": "2019-04-08T08:44:01",
      "source": "chan_3",
      "measurand": "apparentpower",
      "data": "0.037"
    },
    {
      "timestamp": "2019-04-08T08:44:01",
      "source": "chan_1",
      "measurand": "current",
      "data": "0.000"
    },
    {
      "timestamp": "2019-04-08T08:44:01",
      "source": "chan_2",
      "measurand": "current",
      "data": "0.000"
    },
    {
      "timestamp": "2019-04-08T08:44:01",
      "source": "chan_3",
      "measurand": "current",
      "data": "0.095"
    },
    {
      "timestamp": "2019-04-08T08:44:01",
      "source": "chan_N",
      "measurand": "current",
      "data": "0.308"
```

```
    },
    {
      "timestamp": "2019-04-08T08:44:01",
      "source": "chan_1",
      "measurand": "frequency",
      "data": "50.010"
    },
    {
      "timestamp": "2019-04-08T08:44:01",
      "source": "chan_2",
      "measurand": "frequency",
      "data": "50.000"
    },
    {
      "timestamp": "2019-04-08T08:44:01",
      "source": "chan_3",
      "measurand": "frequency",
      "data": "50.010"
    },
    {
      "timestamp": "2019-04-08T08:44:01",
      "source": "chan_1",
      "measurand": "powerfactor",
      "data": "-1.000"
    },
    {
      "timestamp": "2019-04-08T08:44:01",
      "source": "chan_2",
      "measurand": "powerfactor",
      "data": "-1.000"
    },
    {
      "timestamp": "2019-04-08T08:44:01",
      "source": "chan_3",
      "measurand": "powerfactor",
      "data": "0.053"
    },
    {
      "timestamp": "2019-04-08T08:44:01",
      "source": "chan_1",
      "measurand": "reactivepower",
      "data": "0.000"
    },
    {
      "timestamp": "2019-04-08T08:44:01",
      "source": "chan_2",
      "measurand": "reactivepower",
      "data": "0.00"
    },
    {
      "timestamp": "2019-04-08T08:44:01",
      "source": "chan_3",
      "measurand": "reactivepower",
      "data": "0.037"
    },
    {
      "timestamp": "2019-04-08T08:44:01",
      "source": "chan_1",
      "measurand": "volt",
      "data": "228.720"
    },
    {
      "timestamp": "2019-04-08T08:44:01",
      "source": "chan_2",
      "measurand": "volt",
      "data": "229.719"
    },
    {
      "timestamp": "2019-04-08T08:44:01",
      "source": "chan_3",
      "measurand": "volt",
      "data": "229.300"
    }
  ]
```

```
}
```

### A1.2 - Example for the JSON message from the switches

```
{
    "version": "1.0",
    "identifier": "756294756273",
    "type": "switch_input",
    "timestamp": "2019-04-08T08:44:01",
    "phase": "a",
    "action": "closed",
    "location": [
        {
            "node1": "863921030120813-1",
            "node2": "863921030120746-1"
        }
    ]
}
```

### A1.3 - Example for the JSON Message from the state estimator

```
{
    "version": "1.0",
    "type": "se_result",
    "nodes": [
        {
            "node_id": "863921030120813-1",
            "values": [
                {
                    "timestamp": "2019-04-08T08:44:01",
                    "phase": "a",
                    "measurand": "voltage_magnitude",
                    "data": 123
                },
                {
                    "timestamp": "2019-04-08T08:44:01",
                    "phase": "b",
                    "measurand": "voltage_magnitude",
                    "data": 123
                },
                {
                    "timestamp": "2019-04-08T08:44:01",
                    "phase": "c",
                    "measurand": "voltage_magnitude",
                    "data": 123
                },
                {
                    "timestamp": "2019-04-08T08:44:01",
                    "phase": "a",
                    "measurand": "voltage_angle",
                    "data": 123
                },
                {
                    "timestamp": "2019-04-08T08:44:01",
                    "phase": "b",
                    "measurand": "voltage_angle",
                    "data": 123
                },
                {
                    "timestamp": "2019-04-08T08:44:01",
                    "phase": "c",
                    "measurand": "voltage_angle",
                    "data": 123
                },
                {
                    "timestamp": "2019-04-08T08:44:01",
                    "phase": "a",
                    "measurand": "current_magnitude",
                    "data": 123
                },
                {
                    "timestamp": "2019-04-08T08:44:01",
                    "phase": "b",
```

```
        "measurand": "current_magnitude",
        "data": 123
    },
    {
        "timestamp": "2019-04-08T08:44:01",
        "phase": "c",
        "measurand": "current_magnitude",
        "data": 123
    },
    {
        "timestamp": "2019-04-08T08:44:01",
        "phase": "n",
        "measurand": "current_magnitude",
        "data": 123
    },
    {
        "timestamp": "2019-04-08T08:44:01",
        "phase": "a",
        "measurand": "current_angle",
        "data": 123
    },
    {
        "timestamp": "2019-04-08T08:44:01",
        "phase": "b",
        "measurand": "current_angle",
        "data": 123
    },
    {
        "timestamp": "2019-04-08T08:44:01",
        "phase": "c",
        "measurand": "current_angle",
        "data": 123
    },
    {
        "timestamp": "2019-04-08T08:44:01",
        "phase": "n",
        "measurand": "current_angle",
        "data": 123
    },
    {
        "timestamp": "2019-04-08T08:44:01",
        "phase": "a",
        "measurand": "active_power",
        "data": 123
    },
    {
        "timestamp": "2019-04-08T08:44:01",
        "phase": "b",
        "measurand": "active_power",
        "data": 123
    },
    {
        "timestamp": "2019-04-08T08:44:01",
        "phase": "c",
        "measurand": "active_power",
        "data": 123
    },
    {
        "timestamp": "2019-04-08T08:44:01",
        "phase": "a",
        "measurand": "reactive_power",
        "data": 123
    },
    {
        "timestamp": "2019-04-08T08:44:01",
        "phase": "b",
        "measurand": "reactive_power",
        "data": 123
    },
    {
        "timestamp": "2019-04-08T08:44:01",
        "phase": "c",
        "measurand": "reactive_power",
        "data": 123
```

```
                }
            ]
        }
    ],
    "lines": [
        {
            "line_id": "863921030173956-1",
            "values": [
                {
                    "timestamp": "2019-04-08T08:44:01",
                    "phase": "a",
                    "measurand": "active_power",
                    "position": "start_node **OR** end_node",
                    "data": 123
                },
                {
                    "timestamp": "2019-04-08T08:44:01",
                    "phase": "a",
                    "measurand": "active_power",
                    "position": "end_node",
                    "data": 123
                },
                {
                    "timestamp": "2019-04-08T08:44:01",
                    "phase": "a",
                    "measurand": "reactive_power",
                    "position": "start_node",
                    "data": 123
                },
                {
                    "timestamp": "2019-04-08T08:44:01",
                    "phase": "a",
                    "measurand": "reactive_power",
                    "position": "end_node",
                    "data": 123
                },
                {
                    "timestamp": "2019-04-08T08:44:01",
                    "phase": "a",
                    "measurand": "branch_current_magnitude",
                    "data": 123
                },
                {
                    "timestamp": "2019-04-08T08:44:01",
                    "phase": "a",
                    "measurand": "branch_current_angle",
                    "data": 123
                }
            ]
        }
    ]
}
```


### A1.4 - Example for the JSON Message from the power control service


```
{
    "version": "1.0",
    "type": "pwr_ctrl_result",
    "nodes": [
        {
            "node_id": "123456",
            "values": [
                {
                    "timestamp": "2019-04-08T08:44:01",
                    "phase": "a",
                    "measurand": "active_power_set_point",
                    "data": 123
                },
                {
                    "timestamp": "2019-04-08T08:44:01",
                    "phase": "b",
                    "measurand": "active_power_set_point",
                    "data": 123
                },
                {
```

```
                    "timestamp": "2019-04-08T08:44:01",
                    "phase": "c",
                    "measurand": "active_power_set_point",
                    "data": 123
                },
                {
                    "timestamp": "2019-04-08T08:44:01",
                    "phase": "a",
                    "measurand": "reactive_power_set_point",
                    "data": 123
                }
                {
                    "timestamp": "2019-04-08T08:44:01",
                    "phase": "b",
                    "measurand": "reactive_power_set_point",
                    "data": 123
                }
                {
                    "timestamp": "2019-04-08T08:44:01",
                    "phase": "c",
                    "measurand": "reactive_power_set_point",
                    "data": 123
                }
            ]
        }
    ]
}
```

### A1.5 - Example for a CIM file

```
<?xml version="1.0" encoding="utf-8"?>
<rdf:RDF xmlns:rdf="http://www.w3.org/1999/02/22-rdf-syntax-ns#"
    xmlns:cim="http://iec.ch/TC57/2012/CIM-schema-cim16#"
    xmlns:md="http://iec.ch/TC57/61970-552/ModelDescription/1#"
    xmlns:entsoe="http://entsoe.eu/Secretariat/ProfileExtension/2#"
    xmlns:neplan="http://www.neplan.ch#">
    <md:FullModel rdf:about="urn:uuid:f2ff6631-14b2-42d2-8fdb-a2edc910aefe">
        <md:Model.created>2018-11-06T16:34:52</md:Model.created>
        <neplan:Model.createdBy>NEPLAN by Busarello + Cott + Partner AG,
Switzerland</neplan:Model.createdBy>
        <md:Model.scenarioTime>2018-11-06T16:34:50</md:Model.scenarioTime>
        <md:Model.version>7</md:Model.version>
        <md:Model.DependentOn rdf:resource="urn:uuid:25276efc-54c7-450a-87d6-6f58ae3470a9"/>
        <md:Model.description>NEPLAN</md:Model.description>
        <md:Model.modelingAuthoritySet>FULL</md:Model.modelingAuthoritySet>
        <md:Model.profile>http://iec.ch/TC57/61970-456/Topology/3</md:Model.profile>
    </md:FullModel>
    <cim:NameType rdf:ID="_180dea0a-f4a7-4fec-90f4-fbb189409882">
        <cim:NameType.name>description</cim:NameType.name>
    </cim:NameType>
    <cim:TopologicalNode rdf:ID="N0">
        <cim:IdentifiedObject.name>N0</cim:IdentifiedObject.name>
        <cim:TopologicalNode.BaseVoltage rdf:resource="#_fd4aebc6-81ee-42dd-bea2-
e3368f769175"/>
        <cim:TopologicalNode.ConnectivityNodeContainer rdf:resource="#_53a66d62-e48c-4548-
bdb0-8d46f596c259"/>
    </cim:TopologicalNode>

    <cim:Terminal rdf:about="#E-132">
        <cim:Terminal.connected>true</cim:Terminal.connected>
        <cim:Terminal.TopologicalNode rdf:resource="#N4"/>
    </cim:Terminal>

    <cim:NameType rdf:ID="_3e875c98-dd64-4d7d-af2b-be41ca499dd6">
        <cim:NameType.name>description</cim:NameType.name>
    </cim:NameType>
    <cim:BaseVoltage rdf:ID="_0a92d9bb-71b6-4256-aa94-54fde8700496">
        <cim:BaseVoltage.nominalVoltage>20.00</cim:BaseVoltage.nominalVoltage>
    </cim:BaseVoltage>

    <cim:VoltageLevel rdf:ID="_c9026ac7-114f-42db-ad42-c62d5f6dd04e">
        <cim:IdentifiedObject.name>98</cim:IdentifiedObject.name>
        <cim:VoltageLevel.Substation rdf:resource="#_3FA2-2E-F1-0000000000000003938"/>
        <cim:VoltageLevel.BaseVoltage rdf:resource="#_0a92d9bb-71b6-4256-aa94-54fde8700496"/>
    </cim:VoltageLevel>
```

```
    <cim:Substation rdf:ID="_3FA2-2E-F1-00000000000000323130">
        <cim:IdentifiedObject.name>N2</cim:IdentifiedObject.name>
        <cim:Substation.Region rdf:resource="#_f86cebef-3021-4a41-895e-b0d480beee45"/>
    </cim:Substation>

    <cim:GeographicalRegion rdf:ID="_452d9bf4-88a4-497a-93ce-cf500fc681e5">
        <cim:IdentifiedObject.name>Area 1</cim:IdentifiedObject.name>
    </cim:GeographicalRegion>

    <cim:SubGeographicalRegion rdf:ID="_f86cebef-3021-4a41-895e-b0d480beee45">
        <cim:IdentifiedObject.name>Zone 1</cim:IdentifiedObject.name>
        <cim:SubGeographicalRegion.Region             rdf:resource="#_452d9bf4-88a4-497a-93ce-
cf500fc681e5"/>
    </cim:SubGeographicalRegion>

    <cim:OperationalLimitType rdf:ID="_bcae0a62-8109-4523-b661-4bc89de7c05c">
        <cim:IdentifiedObject.name>PATL</cim:IdentifiedObject.name>

<cim:OperationalLimitType.acceptableDuration>45000</cim:OperationalLimitType.acceptableDuratio
n>
        <cim:OperationalLimitType.direction  rdf:resource="http://iec.ch/TC57/2012/CIM-schema-
cim16#OperationalLimitDirectionKind.absoluteValue"/>
    </cim:OperationalLimitType>

    <cim:EnergyConsumer rdf:ID="LOAD-I-7">
        <cim:IdentifiedObject.name>LOAD-I-7</cim:IdentifiedObject.name>
        <cim:EnergyConsumer.p>0.076500</cim:EnergyConsumer.p>
        <cim:EnergyConsumer.q>0.047410</cim:EnergyConsumer.q>
        <cim:Equipment.aggregate>false</cim:Equipment.aggregate>
        <cim:Equipment.EquipmentContainer             rdf:resource="#_bad2e7c9-5aa8-4017-af2c-
5ef5dcf65cf9"/>
    </cim:EnergyConsumer>
    <cim:Terminal rdf:ID="E-337">
        <cim:IdentifiedObject.name>LOAD-I-7_0</cim:IdentifiedObject.name>
        <cim:Terminal.sequenceNumber>1</cim:Terminal.sequenceNumber>
        <cim:Terminal.ConductingEquipment rdf:resource="#LOAD-I-7"/>
    </cim:Terminal>

    <cim:SvVoltage rdf:ID="N0_5B20">
        <cim:SvVoltage.v>110.000000</cim:SvVoltage.v>
        <cim:SvVoltage.angle>-0e+000</cim:SvVoltage.angle>
        <cim:SvVoltage.TopologicalNode rdf:resource="#N0"/>
    </cim:SvVoltage>

    <cim:SvPowerFlow rdf:ID="LOAD-I-7-sv">
        <cim:SvPowerFlow.p>0.076500</cim:SvPowerFlow.p>
        <cim:SvPowerFlow.q>0.047410</cim:SvPowerFlow.q>
        <cim:SvPowerFlow.Terminal rdf:resource="#E-337"/>
    </cim:SvPowerFlow>

    <cim:Diagram rdf:ID="_9a844459-cf44-48c4-b5ae-e56d7446f017">
        <cim:IdentifiedObject.name>Diagram 0</cim:IdentifiedObject.name>
        <cim:Diagram.orientation             rdf:resource="http://iec.ch/TC57/2010/CIM-schema-
cim16#OrientationKind.negative"/>
    </cim:Diagram>

    <cim:DiagramObject rdf:ID="_450e8d17-a49d-476b-ae6e-ef263e5e02b5">
        <cim:DiagramObject.rotation>0</cim:DiagramObject.rotation>
        <cim:DiagramObject.IdentifiedObject rdf:resource="#E-1229744368"/>
        <cim:DiagramObject.Diagram rdf:resource="#_9a844459-cf44-48c4-b5ae-e56d7446f017"/>
    </cim:DiagramObject>
    <cim:DiagramObjectPoint rdf:ID="_b5988043-8ea2-42e5-a9af-0c5400027158">
        <cim:DiagramObjectPoint.sequenceNumber>1</cim:DiagramObjectPoint.sequenceNumber>
        <cim:DiagramObjectPoint.DiagramObject         rdf:resource="#_450e8d17-a49d-476b-ae6e-
ef263e5e02b5"/>
        <cim:DiagramObjectPoint.xPosition>120.000000</cim:DiagramObjectPoint.xPosition>
        <cim:DiagramObjectPoint.yPosition>80.000000</cim:DiagramObjectPoint.yPosition>
    </cim:DiagramObjectPoint>
</rdf:RDF>
```

## A2 – SE Validation grid data

**Table A-6 Topology of the test network**

| | | | | | | | | | | |
|---|---|---|---|---|---|---|---|---|---|---|
| Line | 1 | 2 | 3 | 4 | 5 | 6 | 7 | 8 | 9 | 10 |
| Node 1 | 1 | 2 | 3 | 4 | 5 | 3 | 7 | 8 | 9 | 10 |
| Node 2 | 2 | 3 | 4 | 5 | 6 | 8 | 8 | 9 | 10 | 11 |

**Table A-7 Line parameters of the test network**

| | | | | | | | | | | |
|---|---|---|---|---|---|---|---|---|---|---|
| Line | 1 | 2 | 3 | 4 | 5 | 6 | 7 | 8 | 9 | 10 |
| Length (km) | 2.82 | 4.42 | 0.61 | 0.56 | 1.54 | 1.30 | 1.67 | 0.32 | 0.77 | 0.33 |

**Table A-8 Power injection of the test network**

| | | | | | | | | | | |
|---|---|---|---|---|---|---|---|---|---|---|
| Node | 2 | 3 | 4 | 5 | 6 | 7 | 8 | 9 | 10 | 11 |
| Active Power [kW] | 661.3 | 0.0 | 16.7 | 14.4 | 24.3 | 18.3 | 2.6 | 19.6 | 19.1 | 18.1 |
| Reactive Power [kVAr] | 154.6 | 0.0 | 7.0 | 3.6 | 6.1 | 4.6 | 1.6 | 4.9 | 11.9 | 5.4 |
| Apparent Power [kVA] | 679,1 | 0,0 | 18,1 | 14,8 | 25,0 | 18,8 | 3,0 | 20,2 | 22,5 | 18,9 |
| Power Factor [-] | 0,97 | 0,00 | 0,92 | 0,97 | 0,97 | 0,97 | 0,85 | 0,97 | 0,85 | 0,96 |

## A3 – Power Quality Evaluation service outputs

### A3.1 – PQE outputs

**Table A-4: PQE output fields of each APMU**

| | NAME | Feeder N[5] | Phase 1 | Phase 2 | Phase 3 | Neutral |
|---|---|---|---|---|---|---|
| FOR EACH CONNECTE | Device ID | | | | | |
| | Timestamp | | | | | |
| | Voltage Magnitude (V) | | | | | |

[5] Currently each APMU reports on up to 4 Feeders, i.e. N =1,2,3,4

| | | | | | | |
|---|---|---|---|---|---|---|
| | Current Magnitude (A) | | | | | |
| | Active Power Flow Direction (+/- Kw) | | | | | |
| | Reactive Power (VAr) | | | | | |
| | Apparent Power (VA) | | | | | |
| | Power Factor | | | | | |
| | Power Frequency | | | | | |
| | Voltage THD[6] (V) | | | | | |
| | Current THD (A) | | | | | |
| | Voltage 3rd Harmonic (V) | | | | | |
| | Voltage 5th Harmonic (V) | | | | | |
| | Voltage 7th Harmonic (V) | | | | | |
| | Current 3rd Harmonic (A) | | | | | |
| | Current 5th Harmonic (A) | | | | | |
| | Current 7th Harmonic (A) | | | | | |
| | EVENT | Notification Message when EVENT occurs e.g. "Voltage Unbalance : [*value*]%" [7]. | | | | |

## A3.2 – APMU sample script example

The following APMU JSON script implements an algorithm to detect an MV open circuit phase fault as specified by a DSO for a particular part of their network: .

```
{
   "MV Open Circuit Phase": {
     "Name": "MV Open Circuit Phase",
     "Version": "1.0",
     "Constants": {
       "vmaxless": "200",
       "vmaxgrt": "280",
       "maxperc": "1.1",
       "vminless": "137",
       "vdiv": "1.9",
       "minperc": "0.9"
     },
     "Functions": {
       "lmed": "lmed(l1,l2,l3) = med(l1,l2,l3)",
       "Vmin": "Vmin(v1,v2,v3) = min(v1,v2,v3)",
       "lmin": "lmin(l1,l2,l3) = min(l1,l2,l3)",
```

[6] If THD > 20% then all Voltage Harmonics up to the 50th are also returned.
[7] The EVENT Notification Messages can be defined by the DSO using the APMU grid-edge algorithms, as discussed in section 2.3.

```
        "Vmax": "Vmax(v1,v2,v3) = max(v1,v2,v3)",
        "Imax": "Imax(I1,I2,I3) = max(I1,I2,I3)",
        "Vmed": "Vmed(v1,v2,v3) = med(v1,v2,v3)"
      },
      "Expression": "if((([Vmin] < [Vmax] / [vdiv] )&([Vmin] < [vminless]))&(([Vmax] > [vmaxless])&([Vmax] < [vmaxgrt]))&(([Vmed] + [Vmin]) < ([maxperc] * [Vmax]))&(([Imin] > [minperc] * [Imed])&([Imed] < [maxperc] * [Imin])),[Imin]/[Imed],0)",
      "Actions": {},
      "NotifyMessage": "Possible MV Open Circuit Phase with confidence : [&Ans]",
      "IsEnabled": false,
      "Notified": false,
      "lockMax": 60,
      "lockCount": 1,
      "logenabled":false
    }
  }
```

### A3.3 – LV AMPU Test Results

Each test condition is indicated in first column in red text.

For each test condition, the parameters set on the calibrator are reported in columns A, B, C (red background).

For each test condition, the parameters visualized on the APMU Gridwatch interface are reported in columns F to AC (cyan background). All cells filled with measurements have a conditional format to check their accuracy class based on the reference values indicated by the calibrator.

For THD and harmonics, the error of the APMU with respect to the reference calibrator is reported below the corresponding measurement.

*f = 50 Hz; V range; C range*

| Voltage (V) | Current (A) | Phi (°) | V1 | V2 | V3 | C1 | C2 | C3 | S1 | S2 | S3 | P1 | P2 | P3 |
|---|---|---|---|---|---|---|---|---|---|---|---|---|---|---|
| 230.00 | 50.00 | 0 | 230.149 | 230.118 | 230.000 | 50.200 | 50.340 | 50.070 | 11.558 | 11.583 | 11.523 | 11.556 | 11.588 | 11.521 |
| 207.00 | 50.00 | 0 | 207.137 | 207.095 | 207.009 | 50.198 | 50.322 | 50.063 | 10.402 | 10.428 | 10.365 | 10.402 | 10.428 | 10.368 |
| 218.50 | 50.00 | 0 | 218.634 | 218.600 | 218.509 | 50.209 | 50.327 | 50.058 | 10.997 | 11.004 | 10.944 | 10.978 | 11.005 | 10.942 |
| 241.50 | 50.00 | 0 | 241.657 | 241.603 | 241.505 | 50.219 | 50.326 | 50.068 | 12.135 | 12.164 | 12.091 | 12.135 | 12.163 | 12.090 |
| 253.00 | 50.00 | 0 | 253.153 | 253.092 | 252.993 | 50.216 | 50.327 | 50.052 | 12.713 | 12.742 | 12.668 | 12.713 | 12.743 | 12.669 |
| 230.00 | 2.50 | 0 | 230.155 | 230.093 | 230.004 | 2.504 | 2.516 | 2.499 | 0.578 | 0.579 | 0.579 | 0.578 | 0.580 | 0.575 |
| 230.00 | 10.00 | 0 | 230.148 | 230.103 | 229.995 | 10.049 | 10.053 | 10.007 | 2.310 | 2.316 | 2.303 | 2.311 | 2.316 | 2.305 |
| 230.00 | 40.00 | 0 | 230.164 | 230.083 | 230.010 | 40.177 | 40.264 | 40.033 | 9.249 | 9.267 | 9.213 | 9.246 | 9.265 | 9.212 |
| 230.00 | 60.00 | 0 | 230.149 | 230.084 | 230.013 | 60.266 | 60.383 | 60.076 | 13.869 | 13.900 | 13.821 | 13.870 | 13.900 | 13.820 |

*f = 49 Hz*

| Voltage (V) | Current (A) | Phi (°) | V1 | V2 | V3 | C1 | C2 | C3 | S1 | S2 | S3 | P1 | P2 | P3 |
|---|---|---|---|---|---|---|---|---|---|---|---|---|---|---|
| 230.00 | 50.00 | 0.00 | 230.165 | 230.091 | 230.011 | 50.200 | 50.323 | 50.041 | 11.557 | 11.580 | 11.512 | 11.558 | 11.582 | 11.516 |

*f = 51 Hz*

| Voltage (V) | Current (A) | Phi (°) | V1 | V2 | V3 | C1 | C2 | C3 | S1 | S2 | S3 | P1 | P2 | P3 |
|---|---|---|---|---|---|---|---|---|---|---|---|---|---|---|
| 230.00 | 50.00 | 0.00 | 230.145 | 230.084 | 230.019 | 50.224 | 50.332 | 50.049 | 11.564 | 11.583 | 11.516 | 11.563 | 11.586 | 11.517 |

*Voltage Harmonics: $V_3$ = 11.5 V (5%)*

| Voltage (V) | Current (A) | Phi (°) | V1 | V2 | V3 | C1 | C2 | C3 | S1 | S2 | S3 | P1 | P2 | P3 |
|---|---|---|---|---|---|---|---|---|---|---|---|---|---|---|
| 230.287 | 50.00 | 0.00 | 230.445 | 230.386 | 230.299 | 50.193 | 50.240 | 50.013 | 11.566 | 11.580 | 11.523 | 11.551 | 11.565 | 11.507 |

*Voltage Harmonics: $V_5$ = 13.8 V (6%)*

| Voltage (V) | Current (A) | Phi (°) | V1 | V2 | V3 | C1 | C2 | C3 | S1 | S2 | S3 | P1 | P2 | P3 |
|---|---|---|---|---|---|---|---|---|---|---|---|---|---|---|
| 230.4136 | 50.00 | 0.00 | 230.568 | 230.495 | 230.414 | 50.202 | 50.228 | 50.014 | 11.573 | 11.588 | 11.526 | 11.553 | 11.561 | 11.506 |

*Voltage Harmonics: $V_7$ = 11.5 V (5%)*

| Voltage (V) | Current (A) | Phi (°) | V1 | V2 | V3 | C1 | C2 | C3 | S1 | S2 | S3 | P1 | P2 | P3 |
|---|---|---|---|---|---|---|---|---|---|---|---|---|---|---|
| 230.2873 | 50.00 | 0.00 | 230.441 | 230.378 | 230.289 | 50.204 | 50.240 | 50.021 | 11.566 | 11.579 | 11.519 | 11.552 | 11.564 | 11.507 |

*Voltage Harmonics: $THD_V$ = 7.5% ($V_3$, $V_5$, $V_7$ = 10 V)*

| Voltage (V) | Current (A) | Phi (°) | V1 | V2 | V3 | C1 | C2 | C3 | S1 | S2 | S3 | P1 | P2 | P3 |
|---|---|---|---|---|---|---|---|---|---|---|---|---|---|---|
| 230.6513 | 50.00 | 0.00 | 230.807 | 230.729 | 230.66 | 50.198 | 50.246 | 50.015 | 11.585 | 11.596 | 11.540 | 11.553 | 11.565 | 11.508 |

*Current Harmonics: C3 = 2.5 A (5%)*

| Voltage (V) | Current (A) | Phi (°) | V1 | V2 | V3 | C1 | C2 | C3 | S1 | S2 | S3 | P1 | P2 | P3 |
|---|---|---|---|---|---|---|---|---|---|---|---|---|---|---|
| 230.00 | 50.0625 | 0.00 | 230.15 | 230.076 | 230.014 | 50.243 | 50.298 | 50.083 | 11.571 | 11.576 | 11.522 | 11.553 | 11.566 | 11.509 |

*Current Harmonics: C5 = 3 A (6%)*

| Voltage (V) | Current (A) | Phi (°) | V1 | V2 | V3 | C1 | C2 | C3 | S1 | S2 | S3 | P1 | P2 | P3 |
|---|---|---|---|---|---|---|---|---|---|---|---|---|---|---|
| 230.00 | 50.0899 | 0.00 | 230.143 | 230.084 | 230.002 | 50.283 | 50.329 | 50.101 | 11.573 | 11.584 | 11.527 | 11.552 | 11.565 | 11.507 |

*Current Harmonics: C7 = 2.5 A (5%)*

| Voltage (V) | Current (A) | Phi (°) | V1 | V2 | V3 | C1 | C2 | C3 | S1 | S2 | S3 | P1 | P2 | P3 |
|---|---|---|---|---|---|---|---|---|---|---|---|---|---|---|
| 230.00 | 50.0625 | 0.00 | 230.151 | 230.091 | 229.994 | 50.260 | 50.310 | 50.077 | 11.565 | 11.580 | 11.523 | 11.552 | 11.564 | 11.506 |

*Current Harmonics: $THD_C$ = 7.5% ($C_3$, $C_5$ = 2A; $C_7$ = 2.5 A)*

| Voltage (V) | Current (A) | Phi (°) | V1 | V2 | V3 | C1 | C2 | C3 | S1 | S2 | S3 | P1 | P2 | P3 |
|---|---|---|---|---|---|---|---|---|---|---|---|---|---|---|
| 230.00 | 50.1423 | 0.00 | 230.142 | 230.083 | 230.012 | 50.338 | 50.389 | 50.157 | 11.584 | 11.596 | 11.542 | 11.553 | 11.563 | 11.507 |

*Reactive Loads*

| Voltage (V) | Current (A) | Phi (°) | S1 | S2 | S3 | P1 | P2 | P3 |
|---|---|---|---|---|---|---|---|---|
| 230.00 | 50.00 | -20.00 | 11.551 | 11.563 | 11.510 | 10.841 | 10.853 | 10.801 |
| 230.00 | 50.00 | -10.00 | 11.550 | 11.564 | 11.507 | 11.372 | 11.386 | 11.325 |
| 230.00 | 50.00 | -5.00 | 11.553 | 11.561 | 11.510 | 11.503 | 11.517 | 11.46 |
| 230.00 | 50.00 | 5.00 | 11.553 | 11.564 | 11.506 | 11.512 | 11.523 | 11.467 |
| 230.00 | 50.00 | 10.00 | 11.552 | 11.562 | 11.505 | 11.384 | 11.394 | 11.339 |
| 230.00 | 50.00 | 20.00 | 11.555 | 11.562 | 11.507 | 10.869 | 10.877 | 10.825 |

# A4 – Medium Voltage Test Results

## A4.1 - Accuracy Vs Test Voltage, Test Frequency 50 Hz

Results were reported as error between the magnitudes of the two acquired signals (in percentage) in function of the Test Voltage.

| CHANNEL | VOLTAGE (kV) ACU-01 | VOLTAGE (KV) APMU | ERROR (%) |
|---|---|---|---|
| 1 | 3544 | 3535 | -0.25 |
| 1 | 1058 | 1056 | -0.187 |
| 1 | 7100 | 7082 | -0.25 |
| 1 | 10657 | 10630 | -0.25 |
| 1 | 11720 | 11692 | -0.26 |
| 1 | 14200 | 14168 | -0.22 |
| 1 | 11800 | 11768 | -0.27 |
| 2 | 3544 | 3543 | -0.03 |
| 2 | 11800 | 11793 | -0.06 |
| 3 | 3544 | 3541 | -0.08 |
| 3 | 11800 | 11788 | -0.10 |

## A4.2 - Accuracy Vs Test Current, Test Frequency 50 Hz

Results were reported as error between the magnitudes of the two acquired signals (in percentage) in function of the Test Current.

| CURRENT [ARMS] CH1 | ERROR [%] | CURRENT [ARMS] CH2 | ERROR [%] | CURRENT [ARMS] CH3 | ERROR [%] | ACU-01 CURRENT [ARMS] |
|---|---|---|---|---|---|---|
| 13.602 | 0.31 | 13.613 | 0.39 | 13.514 | -0.34 | 13.56 |
| 43.666 | 0.29 | 43.689 | 0.34 | 43.38 | -0.37 | 43.54 |
| 87.264 | 0.25 | 87.313 | 0.30 | 86.708 | -0.39 | 87.05 |
| 126.203 | 0.31 | 126.132 | 0.25 | 125.367 | -0.36 | 125.82 |

## A4.3 - Overcurrent response, Test Frequency 50 Hz

Results were reported as error between the magnitudes of the two acquired signals (in percentage) in function of the Test Current.

| CURRENT [ARMS] CH1 | ERROR [%] | CURRENT [ARMS] CH2 | ERROR [%] | CURRENT [ARMS] CH3 | ERROR [%] |
|---|---|---|---|---|---|
| 124.1 | 0.16 | 124.2 | 0.24 | 124.2 | 0.24 |
| 248.1 | 0.26 | 247.8 | 0.14 | 248 | 0.22 |
| 372.2 | 0.32 | 372 | 0.27 | 372.1 | 0.30 |
| 420.2 | 0.05 | 420.3 | 0.07 | 420.5 | 0.12 |
| 265 | -46.42 | 253 | -48.84 | 260.9 | -47.24 |

## A4.4 - Overvoltage response, Test Frequency 50 Hz

Results were reported as error between the magnitudes of the two acquired signals (in percentage) in function of the Test Current.

| VOLTAGE [VRMS] CH1 | ERROR [%] | VOLTAGE [VRMS] CH2 | ERROR [%] | VOLTAGE [VRMS] CH3 | ERROR [%] |
|---|---|---|---|---|---|
| 1192 | -0.20 | 1218 | -0.03 | 1232 | -0.12 |
| 3506 | -0.18 | 3584 | 0.03 | 3622 | -0.14 |
| 10520 | -0.16 | 10754 | 0.05 | 10867 | -0.13 |
| 21033 | -0.19 | 21508 | 0.05 | 21733 | -0.13 |
| 42072 | -0.17 | 43013 | 0.05 | 43462 | -0.14 |
| 58195 | -0.26 | 59484 | -0.06 | 60118 | -0.23 |
| 52240 | -25.66 | 53710 | -25.08 | 54300 | -25.18 |

### A4.5 - Apparent and Active Power (Resistive Load)

| | CH1 | CH1 REF | CH2 | CH2 REF | CH3 | CH3 REF |
|---|---|---|---|---|---|---|
| ACTIVE POWER (KW) | 344.611 | 345.440 | 354.646 | 355.790 | 353.232 | 355.65 |
| APPARENT POWER (KVA) | 345.802 | 345.443 | 355.743 | 355.790 | 354.222 | 355.65 |

The following quantities were derived from the upper measurements. Their accuracy could not be determined, without the algorithm for active and apparent power calculation.

| | CH1 | CH1 REF | CH2 | CH2 REF | CH3 | CH3 REF |
|---|---|---|---|---|---|---|
| COS(Φ) | 0.997 | 1.000 | 0.997 | 1.000 | 0.997 | 1.000 |
| Φ (°) | 4.757 | 0.081 | 4.513 | 0.000 | 4.289 | 0.000 |
| Φ ERROR (°) | 4.676 | - | 4.513 | - | 4.289 | - |

### A4.6 - Accuracy Vs Temperature (Current)

Results were reported as error between the magnitudes of the two acquired signals (in percentage) in function of the Temperature.

| CHANNEL | MEASURED CURRENT [ARMS] | EXPECTED CURRENT [ARMS] | ERROR [%] | TEMPERATURE [°C] |
|---|---|---|---|---|
| I1 | 101.4 | 101.44 | 0.04 | 25 |
| I1 | 101.5 | 101.68 | 0.18 | 50 |
| I1 | 101.5 | 101.26 | -0.24 | -5 |
| I1 | 101.3 | 101.26 | -0.04 | 25 |
| I2 | 101.6 | 101.74 | 0.14 | 25 |
| I2 | 101.4 | 101.74 | 0.33 | 50 |
| I2 | 101.6 | 101.67 | 0.07 | -5 |
| I2 | 101.6 | 101.67 | 0.07 | 25 |
| I3 | 100 | 100.16 | 0.16 | 25 |
| I3 | 99.6 | 99.99 | 0.39 | 50 |
| I3 | 101.1 | 101.04 | -0.06 | -5 |
| I3 | 99.8 | 99.99 | 0.19 | 25 |

### A4.7 - Accuracy Vs Temperature (Voltage)

Results were reported as error between the magnitudes of the two acquired signals (in percentage) in function of the Temperature.

| CHANNEL | MEASURED VOLTAGE [VRMS] | EXPECTED VOLTAGE [VRMS] | ERROR [%] | TEMPERATURE [°C] |
|---|---|---|---|---|
| V1 | 10722 | 10748 | 0.25 | 25 |
| V1 | 10960 | 10997 | 0.33 | 50 |
| V1 | 10702 | 10699 | -0.03 | -5 |
| V1 | 10650 | 10670 | 0.18 | 25 |
| V2 | 10958 | 10939 | -0.17 | 25 |
| V2 | 11005 | 11038 | 0.30 | 50 |
| V2 | 10966 | 10980 | 0.13 | -5 |
| V2 | 10969 | 10949 | -0.18 | 25 |
| V3 | 11050 | 11038 | -0.11 | 25 |
| V3 | 10995 | 11038 | 0.39 | 50 |
| V3 | 10966 | 10987 | 0.19 | -5 |